Doctor of Philosophy

Functionality Assessment of the Seismic-Damaged Lifeline Systems under Cascading Failures

February 2019

Department of Architecture & Architectural Engineering
The Graduate School
Seoul National University

Seulbi Lee

Abstract

Functionality Assessment of the Seismic-Damaged Lifeline Systems under Cascading Failures

Seulbi Lee
Department of Architecture & Architectural Engineering
The Graduate School
Seoul National University

Lifeline system is a highly complex network consisting of diverse components that are spatially distributed and interconnected each other. As such, during an earthquake, it is common that the system encountered problems in maintaining reliable operation. Moreover, damage at a single-site component readily propagates to other interdependent components in same and different lifeline systems. In this context, many researchers have continued their efforts to offer useful indices to measure the degraded performance and to ensure the constant service supply of the lifeline systems. The essential research perspective, thus, shifts to understanding the secondary disruptions in the lifeline systems and how malfunctions arise. However, complex inter-dependency is still made challenges in estimating the lifeline system performance under abnormal conditions.

Therefore, this research develops a comprehensive framework for functionality assessment of the seismic-damaged lifeline systems to solve the problems: (a) destruction due to ground shaking, (b) reduction of inflow due to internal/external dependency, and (c) demand fluctuation due to environment changes. In detail, target of estimation is divided into ground motion at particular site, common-cause failure, cascading failure (in terms of internal and external dependency), and escalating failure. In particular, this research use inoperability input-output model incorporating Bayesian network (BN) and System dynamics (SD). To be specific, BN can facilitate prediction of the probability of the unknown event base on the input information or spatial path analysis in situations of data scarcity. On the other hand, SD can be handled demand fluctuation during an earthquake. Due to the inherent uncertainty in earthquake occurrences, this research conducts scenario-based performance assessment using the data from the 2011 Tohoku earthquake and the 2016 Gyeongju earthquake. The analysis results show that the operational state of a component is even dependent through the availability of input inflow from adjacent components rather than its physical damage. Moreover, since the actions taken immediately following an earthquake can play a significant role on the extent of cascading failures, this research provides useful information for those with a concern in the community resilience maintaining.

Keywords: Lifeline System; Functionality; Earthquake; Common-cause Failure; Cascading Failure; Resilience; Robustness; Rapidity.

Student Number: 2012-23127

Contents

Chapter 1 Introduction 1

1.1 Research Background..... 1
1.2 Problem Description 3
1.3 Research Objectives and Scope 9
1.4 Dissertation Outline 14

Chapter 2 Theoretical Backgrounds.....19

2.1 Types of Failures after an Earthquake..... 20
2.2 Lifeline System Performance Metric 24
2.2.1 Static Functionality 24
2.2.2 Dynamic Functionality.....25
2.3 Researches on Interdependent Lifelines..... 28
2.3.1 Economic Theory based Approaches 28
2.3.2 Network based Approaches 32
2.3.3 Simulation / Modeling based Approaches.....35
2.4 Summary 39

Chapter 3 Configuration of the Lifeline Network 42

3.1 Component Definitions 43
3.1.1 Power Supply System 43
3.1.2 Potable Water Supply System.....49

3.2 Seismic Fragility of a Component 55
3.3 Dependency between Components 61
3.4 Summary 66

Chapter 4 Functionality Assessment Framework.....68

4.1 Common-cause Failure Assessment 69
4.1.1 Ground Motion Prediction 69
4.1.2 Functionality of a Single Component 77
4.2 Internal Cascading Failure Assessment 80
4.2.1 Dependency in a Single Lifeline 80
4.2.2 Sub-Model using Inoperability Input-Output Model 81
4.3 External Cascading Failure Assessment 87
4.3.1 Dependency between Different Lifelines 87
4.3.2 Sub-Model using Bayesian Network 88
4.4 Impact of Demand on the Lifelines' Functionality 93
4.4.1 Demand Fluctuation due to Environmental Changes 93
4.4.2 Sub-Model using System Dynamics 93
4.5 Summary 102

Chapter 5 Case Simulations and Experiments 108

5.1 Power Network at Tohoku in Japan 109
5.1.1 Case Outline 109
5.1.2 Comparison with the Simulation Results 111
5.1.3 Additional Experiments 114

5.2 Power and Water Network at Daegu in South Korea..... 121
5.2.1 Case Outline 121
5.2.2 Comparison with the Simulation Results 125
5.2.3 Additional Experiments 127
5.3 Summary 141

Chapter 6 Applications for Improved Resilience.....145

6.1 Identifying a Critical Component 146
6.2 Suggestions of Restoration Management 153
6.3 Summary 157

Chapter 7 Conclusions 158

7.1 Research Results 158
7.2 Research Contributions 162
7.3 Future Research 163

References 167

List of Tables

Table 2-1 Examples of failures caused by actual disaster events 22
Table 2-2 Comparison of research approaches for lifeline system 38

Table 3-1 Attributes of each component in power system 44
Table 3-2 Description of each damage state for power plants..... 45
Table 3-3 Description of each damage state for substations 48
Table 3-4 Description of each damage state for water system 52
Table 3-5 Attributes of each component in potable water system..... 54
Table 3-6 Classification of the lifeline components..... 55
Table 3-7 Fragility functions for lifeline components 56

Table 4-1 Ground predictions for the low-moderate seismic region . 72
Table 4-2 Comparisons between observed and estimated PGA 77
Table 4-3 Inoperability with 10% degraded functionality..... 83
Table 4-4 Description and state of the BN variables 89
Table 4-5 Scale and functionality of the evidence variables 90
Table 4-6 Target of estimation, consideration, methodology 102

Table 5-1 Nodes in the Tohoku electric network..... 110
Table 5-2 Links in the Tohoku electric network.....111
Table 5-3 Functionality after the 2011 Tohoku earthquake..... 114
Table 5-4 Changes in electricity usage..... 118
Table 5-5 Nodes in the Daegu electric network..... 123

Table 5-6 Nodes in the Daegu potable water network 124
Table 5-7 Extreme condition test of the BN model 126
Table 5-8 Conditional probability table for the childe node WDD . 129
Table 5-9 Summary of two case studies 143

Table 6-1 Correlation matrix of Tohoku electric network..... 146
Table 6-2 Damage propagation of a first node 147
Table 6-3 Damage propagation and component criticality..... 148
Table 6-4 The posterior probability given evidence 151
Table 6-5 Restoration functions for lifeline components 153

Table 7-1 System failure rate caused by link outage 163

List of Figures

Figure 1-1 Lifeline system supply chain in normal operation 4
Figure 1-2 Lifeline system supply chain in case of an earthquake 6
Figure 1-3 The concept of resilience, robustness, and rapidity 11
Figure 1-4 Schematic diagram to illustrate service supply chain 12
Figure 1-5 Overview of the dissertation 17

Figure 2-1 Three types of failures in lifeline system 21
Figure 2-2 Reliability block diagram example 33
Figure 2-3 Basic CLD of lifeline system performance 37

Figure 3-1 Fault tree of a transmission and distribution substation ... 47
Figure 3-2 Behavior of each component 49
Figure 3-3 Fragility curves for the power plant 57
Figure 3-4 Fragility curves for the transmission substation 58
Figure 3-5 Fragility curves for the distribution substation 58
Figure 3-6 Fragility curves for the water treatment plant 59
Figure 3-7 Fragility curves for the storage tank 59
Figure 3-8 Fragility curves for the pumping station 60
Figure 3-9 Comparison of internal and external dependency 62
Figure 3-10 Example network for determining the dependency 62
Figure 3-11 Shortest link sets in the second example network 65

Figure 4-1 Hypocentral and epicentral distance 72

Figure 4-2 Peak ground accelerations for Magnitude 5.4 75
Figure 4-3 Functionality curves of lifeline system components..... 79
Figure 4-4 A set of example networks – line, star, tree, and mesh 81
Figure 4-5 Matrix function code for example networks 83
Figure 4-6 Inoperability considering the network topologies 84
Figure 4-7 Inoperability considering the network arrangement 86
Figure 4-8 BN diagram of the power and water system failure 91
Figure 4-9 Supply chain of power system during an earthquake 95
Figure 4-10 Loop for cascading failure in a power system..... 98
Figure 4-11 Loops for escalating failure in a power system 100
Figure 4-12 Entire SD model for seismic-damaged power system . 101
Figure 4-13 Summary of the functionality assessment framework . 106

Figure 5-1 Simplified Tohoku electric power network..... 109
Figure 5-2 Schematic diagrams of blackout households..... 113
Figure 5-3 Comparative analysis of simulation results..... 113
Figure 5-4 Relationship between two types of functionality..... 117
Figure 5-5 Changes in the expression of damage propagation..... 120
Figure 5-6 Layout of the case lifeline systems in Daegu city 122
Figure 5-7 Common-cause failure of each component types..... 128
Figure 5-8 The prior probability distribution of the BN model..... 132
Figure 5-9 The extent of cascading failure..... 133
Figure 5-10 Comparison of three types of failures effects..... 135
Figure 5-11 Comparison of two mitigation strategies..... 137

Figure 5-12 Sensitivity analysis with customer and supplier-side .. 140

Figure 6-1 Identifying a critical component for power and water... 152
Figure 6-2 Comparison of restoration plan 155

Chapter 1. Introduction

1. Research Background

Civil infrastructure systems produce and provide public services such as electricity, potable water, and fuel to local residents. Since such infrastructures consist of diverse components that are spatially distributed and physically interconnected each other, the systems are often encountered problems in maintaining reliable operation (O'Rourke 2007; Whitson and Ramirez-Marquez 2009). When an earthquake occurs, in particular, each of the components can be regarded as multiple hazard sources (Dueñas-Osorio and Kwasinski 2012) and seismic-damaged infrastructures can cause functional losses such as blackout (Barker and Haimes 1994). Moreover, damage at a single-site component readily propagates to other interdependent components in same and different infrastructures (McDaniels et al. 2007; Johansson and Hassel 2010; Dobson 2012). For example, in the wake of the 2010 Chile earthquake, the electric power system which serves electricity to 93% of the Chilean population was significantly destroyed on part of its distribution substations. This event resulted in the power supply delay for a week and simultaneously shutdown of telecommunication networks and water treatment plants that depends heavily on electricity (De la Llera et al. 2017). As such, a

component-damage-induced system disturbance commonly happens in the infrastructures after earthquake events. In this context, the concept of the lifeline system has been proposed to evaluate the performance of critical infrastructures during a natural disaster (O'Rourke 2007). In general, lifelines are grouped into six primary systems: electric power supply, transportation, potable water supply, sewage disposal, gas supply, and telecommunication. As the name implies, all of these play a key role in maintaining the daily lives of residents in the communities that they served. Thus, this calls for a thorough understanding of the seismic-behavior of the lifeline systems, including how a damage of individual component would propagate and how to quantify its effect on the whole system performance.

1.2 Problem Description

Lifeline services are supplied via several intermediate phase to end-user as shown in Fig. 1-1. For example, at the water treatment plant, raw-water is purified into a potable level and distributed to individual customers through a pumping station. In addition, because both a water treatment plant and a pumping station need electricity to operate their equipment, an electric power supply system is linked with a potable water system. In this case, terms in Fig. 1-1 are matched as follows:

- Lifeline system A and lifeline system B: a potable water system and an electric power system.
- Component α and component β: a water treatment plant and a pumping station.
- Intermediary product, final product, and a material: raw-water, potable-water, and electricity.

In the pre-disaster period, all components are in normal operation, thus demand for final product equals supply (i.e., delivered final product). However, under a post-disaster scenario, the equilibrium of demand and supply is a challenging task because of the following reasons:

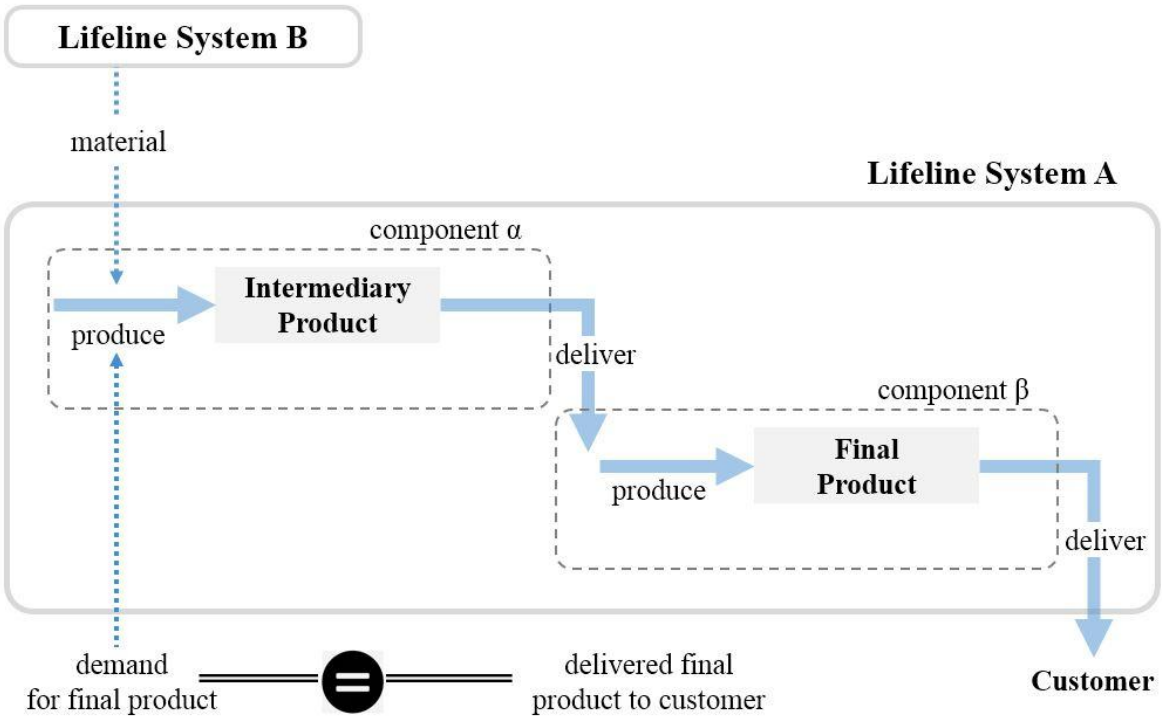

Figure 1-1. Lifeline system supply chain in normal operation

(a) Destruction due to ground shaking – each component may sustain different levels of damage when subjected to the same earthquake event according to its spatial and structural heterogeneity (Adachi and Ellingwood 2008; Zio and Golea 2012).

(b) Reduction of inflow due to internal/external dependency – Since resources for the operation of a component come through another interdependent component, failures of lifeline systems are not instantaneous, but take place in a cascade until the systems get restored (Barker and Haimes 2009). In other words, the ability of the system to withstand an earthquake have to assess as the time-varying performance indicator (Saydam and Dan 2011).

(c) Demand fluctuation due to environment changes – A demand for lifeline services varies (e.g., electricity demand increase due to the excessive usage of construction machinery for recovery, and simultaneously electricity demand decrease due to mandatory restriction) compared under normal conditions (Mori and Wakiyama 2012; Egawa et al. 2013).

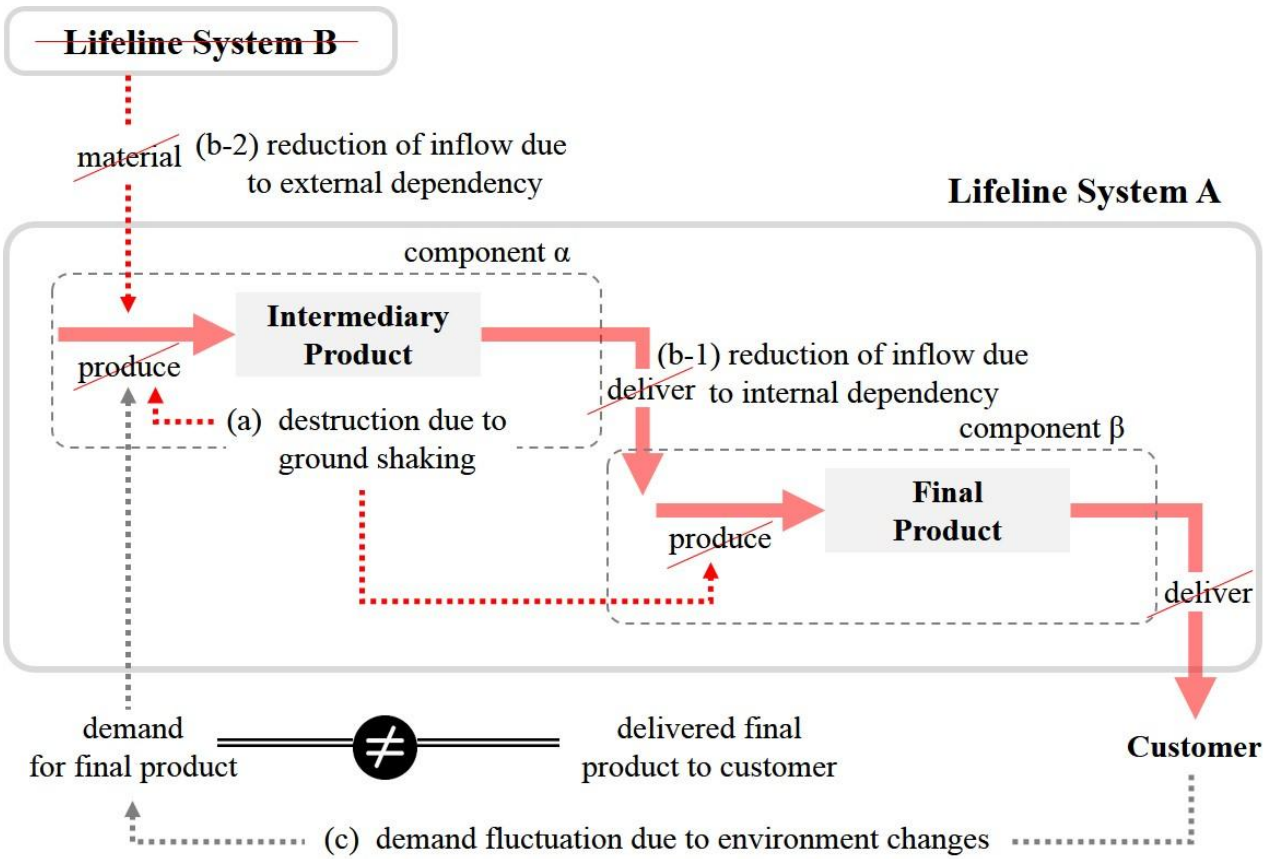

Figure 1-2. Lifeline system supply chain in case of an earthquake

In this context, many researchers have continued their efforts to estimate the degraded performance and to ensure the constant service supply of the lifeline systems in the post-earthquake phase. Fragility analysis of the structures given ground motion is typical methods to describe the probability of exceeding certain damage states (American Lifelines Alliance 2001; Federal Emergency Management Agency 2003; Korea atomic energy research institute 2008). Even though these works have contributed to predict the component seismic behavior, in reality, cascading failure plays a decisive role on the system performance (Nojima and Sugito 2000).

In this regard, the research perspective shifts from physical destruction to the secondary functional disruptions in the lifeline systems. For example, some researchers (Nedic et al. 2006; Qi et al. 2015) studied the patterns of cascading blackout in line with the electricity load growth. The standard procedure of these approaches are as follows: (a) particular components are intentionally removed in a power system, (b) once there is no power flow through the removed component, then a second component take over its tasks, (c) the power flow is self-re-routed to bypass overloads, and (d) performance of the system after the re-routed is evaluated. However, during an earthquake event, it is difficult to determine power flow directions that because multiple components at different origins go out of service concurrently (Dobson et al.

2008).

Furthermore, an operation mode of a component cannot represent binary state: success (100% operate) or complete failure (0% operate). Therefore, assessing the performance of complex lifeline system under seismic conditions needs to consider multiple failure states (e.g., slight, moderate, extensive, and complete suggested by the FEMA).

To summarize, a real-world lifeline system does not operate as an isolated facility and most of them are multi-state. Thus, performance estimation researches in the aftermath of an earthquake face the need to solve various uncertainty problems that come from component differences of structural behavior, vulnerability, and its impact on the whole system. In addition, certain cascade failure can be fed back into the initiating system in a form of the reduced inflow of production materials or demand fluctuation.

1.3 Research Objectives and Scope

To address the above-mentioned problems, the goal of this research is to examine how failures in the lifeline system propagate and what should be considered for maintaining the system performance. In particular, this research develops a comprehensive framework for functionality assessment of the seismic-damaged lifeline systems. The framework includes:

(a) Seismic ground motion prediction of a structurally specified component at single-site and estimation of its functionality degradation due to the physical destruction (i.e., common-cause failure).

(b) Internal (1^{st}) cascading failure analysis caused by common-cause failures of certain components within the same lifeline system.

(c) External (2^{nd}) cascading failure analysis caused by common-cause and internal cascading failures between different lifeline systems.

(d) Assessing the impact of the demand-side response that refers to the changes in lifeline services usage on the system performance.

Fig. 1-3 shows lifeline systems performance after an earthquake where F_0 is the original system performance, F_1 is the system performance withstand a given level of earthquake, t_0 is the time at an earthquake occurred, t_1 is the

time to start restoration, and t_2 is the time at a new equilibrium state. In general, resilience of a systems (hatched area in Fig. 1-3) can be measured in terms of the robustness (F_1 in Fig. 1-3) defined the ability to withstand a given level of stress without loss of performance at certain time (Norris et al. 2008) and the rapidity (t_2 - t_1 in Fig. 1-3) defined the ability to rapidly recover with adequate resources in a timely manner (Orabi et al. 2010). Because it is both important to sustain less damage and to recover in the shortest possible time, this research pays attention to the estimation of the robustness and the comparison restoration strategies effect on the rapidity. In addition, due to the inherent uncertainty in earthquake occurrences, this research conducts scenario-based damage assessment with a given magnitude and epicenter location.

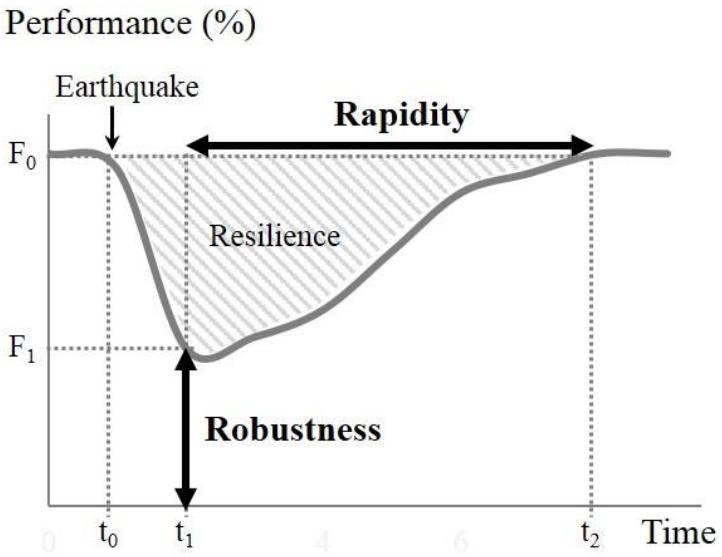

Figure 1-3. The concept of resilience, robustness, and rapidity

Meanwhile, some empirical researches (Krimgold et al. 2006; Holguín-Veras and Jaller 2011) demonstrated that the requirements of lifeline service after a disaster were frequent in the following order: transportation, electricity, and drink water. Because the transportation system is a link-oriented network that distance to epicenter may be ambiguous, the types of lifeline systems considered in this research are a power supply system and a potable water supply system.

This research also assumed that each of three types of components in power and potable water system can affect the public service supply process as described in Fig. 1-4. Regarding this figure, electricity is generated in a

power plant ((a) in Fig.1-4) and transformed to utilization voltage for final customers through a transmission substation ((b) in Fig.1-4) and a distribution substation ((c) in Fig.1-4) sequentially. On the other hand, since water from a reservoir such as a lake is purified to potable level in water treatment plant ((d) in Fig.1-4), storage tank ((e) in Fig. 1-4) and pumping station ((f) in Fig.1-4) just distributes potable water to customers. Thus, some pumping station is connected to a water treatment plant directly. In practice, it is necessary to analyze the additional components such as water pipeline and transmission/distribution lines; however, these will be used as supportive variables for determining the network topological attributes.

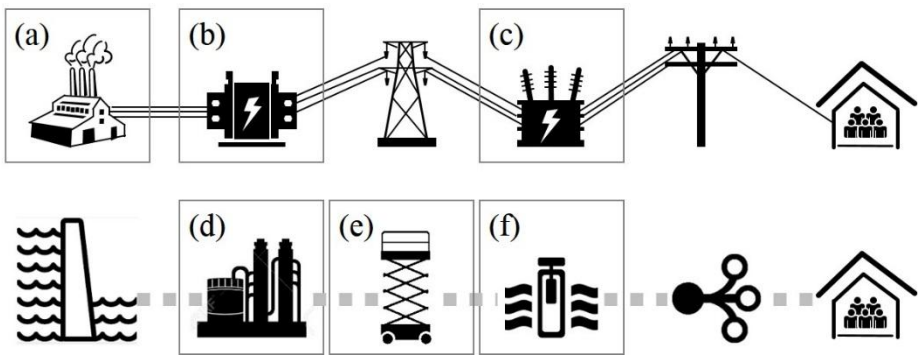

Figure 1-4. Schematic diagram to illustrate service supply chain

In addition, in case of the power supply system, there are two typical causes of flow problem that leads to system failure: (a) physical destruction attributed to the external forces and (b) power imbalance that occurs when

electric load exceeds the internal permissible limit (Dialynas et al. 1988; Mosleh 1991). However, the scope of system failure analysis in this research is limited to physical destruction; and the outage due to over/under load is not discussed here. Instead, the authors assume that the electric load of each node must remain within their capacity to minimize load imbalance problem.

1.4 Dissertation Outline

This dissertation is organized into seven chapters – including this chapter for the introduction – that deal with issues on the performance of the seismic-damaged lifeline systems. A brief description of chapters in the rest of the dissertation is as follows:

Chapter 2, theoretical backgrounds, examines relevant issues of the lifeline systems including what types of failures occur after an earthquake and what kinds of metrics are used to measure its performance. In-depth reviews on current researches focused interdependent lifeline systems is also conducted including economic theory based approaches, network based approaches, and simulation modeling based approaches.

Chapter 3, a configuration of the lifeline network, explains the definition and several attributes of the power and the potable water supply component that discussed in this research. In sequence, the concept of the fragility of single component and dependencies between components is presented regarding both the functional and spatial relationship.

Chapter 4, functionality assessment framework, introduces step-by-step procedures for: (a) the ground motion prediction at single-site component

under earthquake scenarios and common-cause failure analysis for each lifeline component given ground motions; (b) internal cascading failure analysis caused by dependency within a lifeline system using inoperability input-output model; (c) external cascading failure analysis caused by dependency between two different lifeline systems using Bayesian network; (d) impact analysis depending on the changes of the final demand using system dynamics.

Chapter 5, case simulation and experiment, applies the proposed functionality assessment framework to real-world lifeline systems. The power network at Tohoku region in Japan and the power and the potable water network at Daegu in South Korea are selected as representative events for the high seismicity regions and low-moderate region respectively.

Chapter 6, applications for improved resilience, proposes expected uses of the research results with two applications related to maintain original performance. In particular, identifying a critical component for operation after an earthquake and suggestions for restoration management are discussed.

Chapter 7, conclusions, summarizes the overall findings, implications for infrastructures safety management, contributions, and limitations of this research and presents possible directions of the future works.

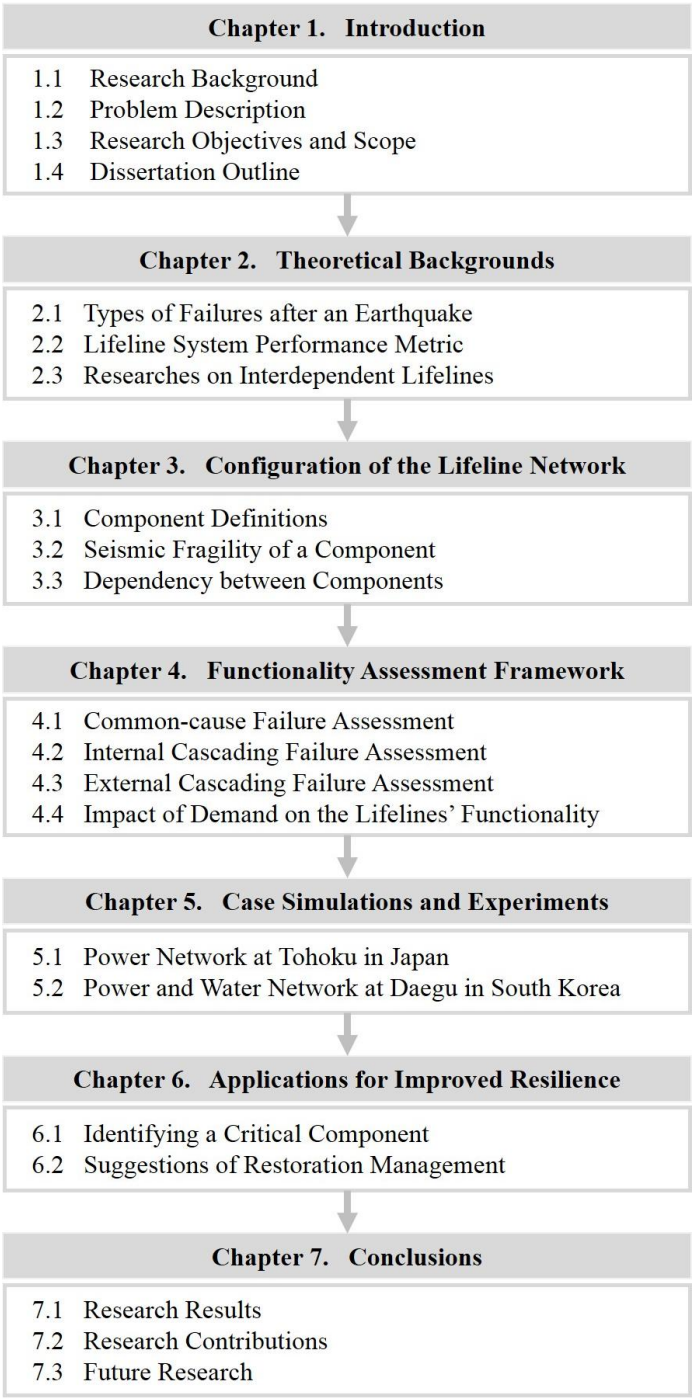

Figure 1-5. Overview of the dissertation

Chapter 2. Theoretical Backgrounds

Lifeline systems are interdependent in multiple ways, and thus many researchers took into account the identification, understanding, and assessment of the risk factors of system performance. In this chapter, three types of failures that commonly occur during an earthquake is addressed. In addition, this research presents the similarity and distinction of these failures based on examples of historical disaster events. On the basis of failure classifications, several system performance measurements are examined. In particular, this research describes the static functionality (e.g., reliability) which is the immediately degraded performance in consequence of an earthquake and the dynamic functionality (e.g., robustness), the primary analysis target, which progressively deteriorates performance until the restoration phase. The last part of this chapter is literature reviews on both the traditional theory and the recent advance methodologies. In detail, the outcome of previous research can be divided into three criteria: economic theory based approaches, network based approaches, and simulation/modeling based approaches. From comparing the viewpoint of such reviews, this research determines considerations and methodology for the functionality assessment regarding each type of failure.

2.1 Types of Failures after an Earthquake

As the lifeline systems becoming more interdependent in modern society, they have been vulnerable to human error, natural disaster, and intentional physical attack although operational efficiency has been improved (Ouyang 2010; Johansson et al. 2013; Wu et al. 2016). The 2003 North American blackout, the 2005 Hurricane Katrina in New Orleans, the 2010 Chile earthquake, and the 2011 Tohoku earthquake in Japan are the example events that demonstrated the vulnerability of lifeline systems (Araneda et al. 2010; Holguín-Veras and Jaller 2011; Cimellaro 2014). As such, the failures of components in the lifeline system generally have diverse aspects and can be exacerbated than the failures of isolated facilities. Therefore, from the perspective of a cause and development, the failures in seismic-damaged lifeline systems are classified into the following three types (Rinaldi et al. 2001) and it also presented in Fig.2-1:

- A common-cause failure – it is defined as the concurrent primary disruptions of two or more components in lifeline systems at the same time because of the root problem such as an earthquake.
- A cascading failure – it is defined as the secondary disruptions of a component in certain lifeline system that immediately caused by the disruptions of another components in same or different lifeline system.

- An escalating failure – it is defined as the secondary disruptions of a component in certain lifeline system that is aggravated by the prolonged disruptions of another components in same or different lifeline system.

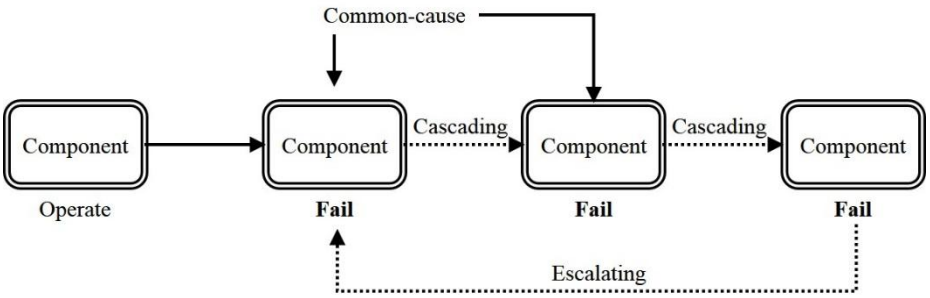

Figure 2-1. Three types of failures in lifeline system

Destruction of the power plant through earthquake ground shaking is a typical common-cause failure and temporarily shutdown of power substations, water treatment plants, and telecommunication networks caused by electricity outage are cascading failures. On the other hand, escalating failures represent in the form of the delay in repair activities or the demand changes. Table 2-1 presents the examples of above categorized failures when actual disaster event occurred. In any case, such failures are interdependent and make challenges to estimating lifeline system performance under abnormal conditions.

Table 2-1. Examples of failures caused by actual disaster events

Failure	Lifeline System	Descriptions
Common-cause failure	Power	• Meltdown of the Fukushima Daiichi nuclear power plant – 2011 Tohoku Earthquake (Kazama and Noda 2012).
	Potable water and wastewater	• Severe collapse of main water and sewage pipeline; and it took several weeks to re-establish services – 1985 Mexico City Earthquake (Juarez Garcia 2010).
	Transportation	• Tilting of the bridge beam supports – 2011 Tohoku Earthquake (Kazama and Noda 2012).
Cascading failure	Power	• Shuttering of all 46 of Japan's nuclear reactors due to the meltdown of the Fukushima Daiichi nuclear power plant – 2011 Tohoku Earthquake (Kazama and Noda 2012).
	Potable water and wastewater	• The closing of the 600 lift stations that pumped raw sewage in Orange County due to electricity distribution failure – 2004 Hurricane Charley (ALA 2006).
	Telecommunications	• Malfunctions of 285,000 telephone subscribers' lines due to loss of power at some telephone exchange centers – 1995 Kobe earthquake (Nojima and Kameda 1996).
	Transportation	• Flickering of traffic signals due to the power outage – 1995 Kobe earthquake (Nojima and Kameda 1996).
Escalating failure	Power	• Coal-fired power plants in Florida stopped their operation after 7 days of the hurricane due to the shortage of coal supply in a timely manner – 2005 Hurricane Katrina (ALA 2006).

	Potable water and wastewater	• The SCADA system for operation of water treatment plants was cut off due to the loss of telephone services – 2010 Chile Earthquake (Araneda et al. 2010).
	Telecommunications	• Delay in telecommunication service repair due to the destruction of roads for carrying restoration crews – 2005 Hurricane Katrina (ALA 2006).

Although all of them, common-cause, cascading and escalating failures, essentially have the same root-causes[1], they have distinctive characteristics regarding initiation and mitigation (Xie et al. 2018). To be specific, the major initiating reason of common-cause failures are similar in several components (e.g., exceeding a threshold of displacement); while cascading and escalating failures have inconsistent reasons accordance with the components' properties (e.g., overload, blackout, and shortage of production resources). For this reason, mitigation plans also have to establish with different considerations. Defense of common-cause failures, for example, is related to seismic reinforcement of each structure since the failures are direct consequences of a ground shaking. However, cascading and escalating failures can be reduced by redundancy resolution such as adding substitutable elements, the capacity expansion of backup resources, and topological optimization.

[1] In this paper, the root cause is an earthquake.

2.2 Lifeline System Performance Metric

2.2.1 Static Functionality

The set of measures which are constant or slowly varying with time are called static variables. In the previous literature on the lifeline systems, the general notion of static functionality refers to an inherent ability of a system to maintain performance immediately after a shock (Pant et al. 2013) and it is in accordance with its structure types (Rose and Liao 2005).

Reliability (the opposite word of fragility or vulnerability) defined the ability to perform the desired function under given environments (Johansson et al. 2013), is primarily studied static concept in the research fields of system engineering. Since a reliability is interested in a structural behavior, it is estimated by seismic response analysis software such as HAZUS-MH (NIBS 1999) and OpenSees (McKenna et al. 2000). In detail, a reliability measures the frequency of satisfaction that the system is considered as the normal state by counting the number of non-damaged components through a number of simulations with above software. Thus, a reliability is more appropriate for analyzing common-cause failure and reliability does not consider extreme events besides physical damage issues.

Because the reliability for estimating the common-cause failure has been widely discussed in the literature, it can be relatively easier to obtain. In this research, fragility functions provided by Federal Emergency Management Agency (FEMA 2003) and Korea atomic energy research institute (KAERI 2008) were considered. In particular, the functions of FEMA are developed based upon over 30 case studies of regional earthquake loss estimation in the United States. As is inherent to any estimation method, there are some uncertainties due to simplifications and geological characteristics; however, they have been calibrated by many researchers located in diverse regions such as Turkey (Ansal et al. 2008), China (Sai-ni et al. 2012) and Japan (Lai et al. 2013). These functions have thus been widely used in seismic-damage assessment for pre-defined 6 different lifeline systems including potable water supply system. On the other hand, the functions of KAERI are specialized for the power system and modified for South Korea based on FEMA's functions. Detailed descriptions of two functions will be discussed in Chapter 3.

2.2.2 Dynamic Functionality

The set of measures which are changes over time are called dynamic variables and the resilience is a representative of dynamic functionality for the lifeline systems. As described in Fig. 1-3, dimensions of the resilience can be divided into robustness and rapidity (Bruneau et al. 2003).

Robustness (the opposite word of inoperability) is referred the ability to withstand a given level of stress without loss of performance at certain time (Norris et al. 2008). Although, definitions of the reliability and the robustness seem to be similar, these two concepts are quite differently accepted to researchers (Saydam and Dan 2011; Asefa et al. 2014). Firstly, unchanged control variables for estimation is distinguished; the former is operation conditions while the latter is disaster intensity. Secondly, the robustness-based performance measure is interested in a change of the final output not only structural displacement but also various supply chain uncertainty. For this reasons, whereas the reliability enables to measure degraded performance due to the common-cause failure, another two types of failures as mentioned above, cascading and escalating failure are the matter of the robustness.

Since the volatile characteristics of robustness, it is generally evaluated after the disaster with observation or statistical data (Tsuruta et al. 2008) despite the need of such information in the pre-disaster phase (Cats et al. 2017). Although some of the literature (Maes et al. 2006; Koc et al. 3013) defined the system robustness as the minimum ratio of failure probability between under normal and abnormal conditions, little attention has been paid to quantifying the robustness with respect to cascading failures (Ferrario et al. 2016).

However, it is commonly seen in the literature that the robustness is a function of supply and demand. In this context, this research defined the robustness as follows:

$$\text{Robustness} = \frac{f(t)}{F_0} \qquad (1)$$

where, F_0 is original system performance level and $f(t)$ is system performance level at time *t*.

In case of the power supply system, for example, F_0 means the amount of desired electricity generation to meet demand (MW/day) and $f(t)$ means the amount of available electricity distribution after a seismic event (MW/day). Thus, for the lifeline systems, the robustness may be the percentage of customers with water or electric power after an earthquake.

2.3 Researches on Interdependent Lifelines

2.3.1 Economic Theory based Approaches

In the early stage of an earthquake engineering, lifeline system damage was determined in terms of repair cost (Rose et al. 1997). In this context, the economic theory based approach was mainstream for evaluating the regional impact of a catastrophic disaster event. To simplify the modeling, the main focus of such methods is cascading failure emerge after an interruption to the lifeline service supply from adjacent components.

A notable researches in this field, for example, is inoperability input-output model (IIM) proposed by Haimes and Jiang (2001). This IIM is based on the original Leontief input-output model (1951) that depicts how the output from one business sector becomes the input to another sector given that an economic system consists of several interconnected components. This IIM is based on Leontief's input-output model (1951) that quantifies the interdependencies between different business sectors. The major assumptions of the original Leontief's model includes: (a) an economy system consist of several interconnected business sectors, (b) an output produced by a business sector transfers to another business sector as an input, and (c) the final output is consumed by end-users.

In this regard, the formulation of the IIM of a system with n components as follows:

$$\mathbf{x} = \mathbf{A}\mathbf{x} + \mathbf{C} \Leftrightarrow \{x_i = \min(1, \sum_j a_{ij}x_j + c_j)\} \ \forall \ i, j \qquad (2)$$

Assuming $(\mathbf{E} - \mathbf{A})$ is nonsingular; Eq. 2 can be solved as follows:

$$\mathbf{x} = (\mathbf{E} - \mathbf{A})^{-1} \times \mathbf{C} \qquad (3)$$

where $\mathbf{x}$ is an inoperability (which is opposite to the robustness) matrix of a whole system, $\mathbf{A}$ is a component-by-component coefficient matrix, $\mathbf{C}$ is a common-cause failure matrix of the system, and $\mathbf{E}$ is a unit matrix.

In the Eq. 2 and 3, inoperability is expressed as a ratio of the reduced component's output compared to its initially intended output (e.g., $x_i = 0$ under normal conditions). In addition, component-by-component coefficients, the core concept of the IIM, is generally determined a ratio of the input from a component with respect to the total input requirements of another component. Such coefficients is generally required extensive data collecting derived from the historical earthquake records (McDaniels et al. 2007; Tsuruta et al. 2008), however, Haimes and Jiang also present guidelines for the determination of correlation between two components:

- Identify physical connections between the components. If there is no physical connections between them, then $a_{ji} = a_{ij} = 0$.

- If a complete failure of j^{th} component plays a decisive role of a complete failure of i^{th} component, then $a_{ij} = 1$. By the same way, if a complete failure of j^{th} component lead to a half failure of i^{th} component, then $a_{ij} = 0.5$.

- If a correlation between two components has stochastic features, then all possible failure scenarios must be statistically analyzed. If the empirical data is not sufficient, a simulation approaches may be helpful.

With pointing out the last phrase, many types of research for estimating extreme events derived such as the September 11 attack on the United States (Haimes et al. 2005), Hurricanes Katrina and Rita (Hallegatte 2008) and the Chile Earthquake (Dueñas-Osorio and Kwasinski 2012). For example, Holguín-Veras and Jaller (2012) collected information about resources requirements through three months after Hurricane Katrina. Then, they grouped the requests by industrial sectors and finally gave the insight that only 40 commodities (e.g., electricity, potable water, medical supports, and clothing) have a majority in requests, and these are supplied by an even smaller number of critical infrastructures. This finding is an important foundation of the impact of lifeline systems for maintaining the community resilience and a worthy example incorporating IIM with statistical analysis. However, this modeling method lacks the capability to capture the time-varying features such as how a temporal degradation affects the system and

how the system recovers.

To overcome such limitations, simulation methods have been integrated with IIM and these allow observing the complex changes within the system over time (Santos et al. 2009; Xu et al. 2012). Specifically, Agent-Based Model (ABM) has been successfully employed due to its ability to describe the topological, structural, and behavioral features of a component in a system as well as interactions among components, each of which is represented as an agent[2] (Santos et al. 2007; Olivia et al. 2010). In this context, it is suitable for observing the system that involves various interacting components and enables the examination of how system patterns emerge from the behaviors of agents in their given environment (Bulleit and Drewek 2012). Nevertheless, due to the economic origin of IIM, it still needs the collection of statistical data that have been gathered from the government or corresponding organizations to quantify the IIM coefficients.

To summarize, IIM facilitates estimation of the extent of cascading failures after a disaster. However, its effect is maximized when there are sufficient databases. Thus, this research combines the IIM with the network-based and the simulation-based approaches, will be discussed in the next

[2] Autonomous decision-making entities called agents such people, companies, and facilities (Barton et al. 2000).

section.

2.3.2 Network based Approaches

Lifeline system can be modeled can be modeled as a network G (V, E), where V represents the set of vertexes (also called nodes) and E represents the set of edges (also called links) (Zio and Piccinelli 2010). Each node is represented as a component that has several attributes, and each link is represented as a physical element to connect two components at different locations. In addition, such a link can be computed by Dijkstra's shortest path algorithms (1959), and an adjacency matrix that is a square matrix to define the topological structure of the network:

$$l_{ij} = \begin{cases} 1 & v_i \text{ and } v_j \text{ is phyiscally connected} \\ 0 & \text{otherwise} \end{cases} \quad (4)$$

Graph-theory including an above adjacency matrix is a useful background that helped understand topology of complex lifeline network. In particular, for the identifying the critical component to maintain system function, many researchers have been observed whether the system operates or fails, when certain node was disconnected from the system. For example, reliability block diagram (RBD) which create series and parallel configurations to show logical interactions between components is a basic

graphical analysis (Guo and Yang 2007). Fig. 2-2 is an example of RBD, in this case, both the elimination of "a4" and "c1" means complete failure of the sink node.

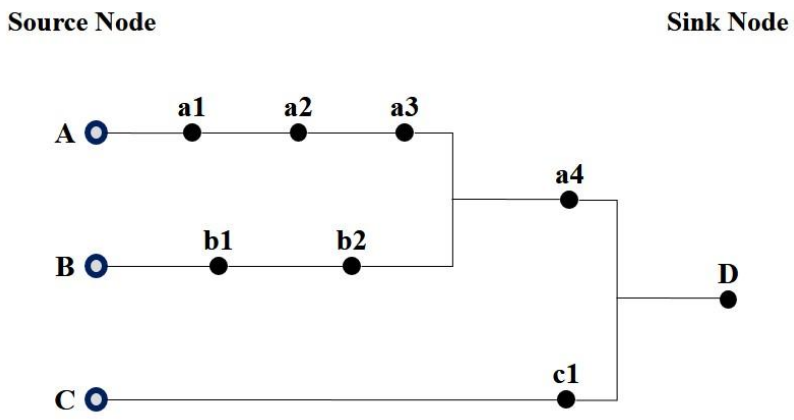

Figure 2-2. Reliability block diagram example

In general, such methods represent the system performance as a function of failure events that affect its overall state: success (100% operate) or complete failure. However, in the post-earthquake phase, it is obvious that lifeline systems' components have multiple failure states (e.g., slight, moderate, extensive, and complete suggested by the FEMA) not a binary state. For this reason, RBD has been transformed to other stochastic approaches such as fault tree analysis (FTA) and Bayesian network (BN). FTA has been proposed to identify which component is the main source of damage propagation through the analysis of all possible outcomes resulting from failure events. However, in accordance with the comparison research by

Khakzad et al. (2011), FTA is not suitable for handling redundant common-cause failures because it is assumed that each failure event is independent.

In the meantime, BN is a solution to predict the probability of the unknown event or to update the probability of the evidence event through the consideration of failure propagation. In addition, BN is useful in situations of data scarcity like earthquake engineering areas that historical observed data are rarely available. Due to the ability of BN to express uncertainty using the rules of conditional probability and to examine the extent of cascading failures, it has been applied to quantify the seismic risk at major infrastructures such as transportation (Bensi et al. 2009), power transmission (Di Giorgio and Liberati 2012) and waterway system (Wang and Yang 2018).

In detail, BN is directed acyclic graphs in which the nodes denote set of state variables and the arcs denote dependencies between the connected nodes (Pearl 1988). In the system reliability research, each node is generally represented as a single-site facility (e.g., substation in power system) or an event causing its failure (e.g., physical destruction of substation). Dependency is referred to as a directional relationship through which the state of a certain component is correlated to the state of the others (Rinaldi 2004). The inference approach in BN can be classified into two types: (a) forward analysis that is the step of computing the posterior probability based on prior

probabilities of the parent nodes and their conditional dependency; (b) backward analysis that is the step of computing the posterior probability based on observed evidence to find out the cause of an interest node.

This research firstly focuses on the forward analysis, thus, the conditional probability distribution of random variables $V = \{x_1, x_2, \ldots x_n\}$ is determined as follows (Bobbio et al. 2001):

$$\mathrm{P}(V) = \prod_i \mathrm{P}(x_i \left| \mathrm{Parent}(x_i) \right.) \qquad (5)$$

As such, most of the node in the BN is a stochastic variable that is probabilistically conditioned on its parent nodes, while some node can be a deterministic variable if it is functionally dependent on its corresponding parent nodes (VanDerHorn and Mahadevan 2018). Furthermore, if the probability prediction of an unobserved node is obtained by Eq. 5, the backward analysis will be accomplished with comparative ease via information updating.

2.3.3 Simulation / Modeling based Approaches

Even though previous works have contributed to better understanding of the lifeline system behavior, they mainly dealt the problems in supplier side.

These focused approaches may prevent practical estimation of the system performance because final demand is an important variables for the robustness estimation (see the Eq. 1). For example, Santos and Haimes (2003) confirmed that the inoperability of air-transport system was reduced around 10% as the consequence of demand reduction (e.g., travel) after the September 11 attacks in the United States. Thus, decision-making process for reliable operation of the lifeline system must include the systematic consideration of a demand-side response[3] (Albadi and El-Saadany 2008).

Simulation modeling is a complementary tools for estimating impact of such demand changes on system performance. In addition, since the inherent uncertainty and the data-scarcity in earthquake loss estimation, simulation modeling based approaches have been widely performed. They generally have been developed based on other theoretical researches such as agent-based IIM described above. Aspen Electricity Enhancement (ASPEN-EE) model provided by Barton et al. (2000) to simulate the agents' behavior (e.g., electricity usage of a household, commercial, and industry) given power outage scenarios is another example using ABM. However, this type of methodology needed too many assumptions to predetermine the agent behavior, in particular, when the relevant data is not sufficient.

[3] In this paper, demand-side response refers to the changes in lifeline services usage by end-user from their normal consumption patterns in response to changes in the external environment conditions over time.

Thus, this research use System dynamics (SD) specialized for capturing the evolutionary behavior of interconnected components by changes in supply and demand (Sterman 2000; Hwang et al. 2013; Hasan and Foliente 2015). In general, for the analysis of the lifeline systems, the stock represents quantities of the system output (e.g., electricity and potable water), flow represents the rate of productions and consumptions over time. In addition, causal-loop diagram (CLD) shows the cause-and-effect regarding the performance of lifeline system. Fig. 2-3 is a basic CLD including inoperability, functionality, production rate, demand, and amount of delivered as variables.

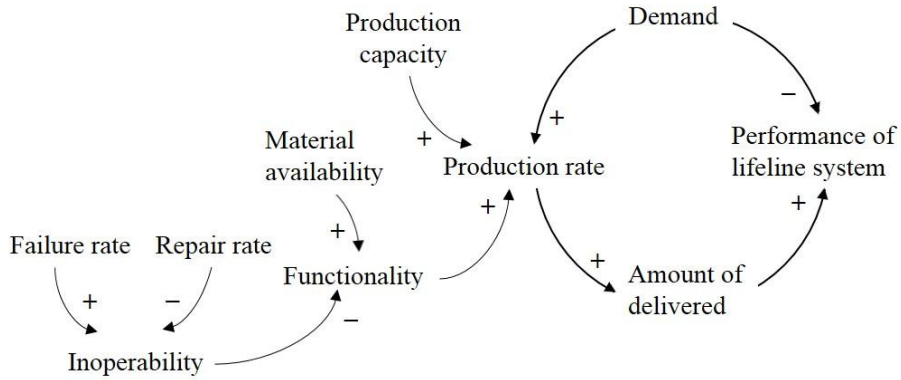

Figure 2-3. Basic CLD of lifeline system performance

Critical infrastructure protection decision support system (CIP/DSS) by Bush (2005) is widely known model using system dynamics to assist policy maker in comparing the effectiveness of alternative risk mitigation strategies.

However, since the model used too many variables (over 5000) related various infrastructures, feasibility is relatively low. In this context, this research develops SD model that re-establish the target subjects and levels of failure.

Table 2-2 summarizes the comparison of three types approaches used in this research regarding quantity of input data, quantification methods, target of analysis and time-varying features.

Table 2-2. Comparison of research approaches for lifeline system

Type	Quantity of input data	Quantification methods	Target of analysis	Time-varying
Input-output inoperability model	Large	Deterministic	Cascading failure	X
Bayesian network	Medium	Probabilistic	Cascading failure	O
System dynamics	Medium	Semi-quantification	Escalating failure	O

2.4 Summary

In this chapter, this research classified failures into (a) a common cause failure is a concurrent primary disruption after an event; (b) a cascading failure is an instantaneous secondary disruption, and (c) an escalating failure is a prolonged secondary disruption. Although the essential root-cause of such three types of failures is an earthquake, they are different from the perspective of initiation and mitigation. In particular, a common-cause failure occurs when structural displacement exceeds a threshold, while cascading/escalating failures happen when the upper-dependent component cannot operate adequately.

In this context, this research compared the current measurements for estimation of the lifeline system performance. In detail, the reliability is defined as the ability to perform the desired function immediately after an earthquake, and the robustness is defined as the ability to withstand a given level of stress without loss of performance until restoration starts. In other words, the reliability dealt with structural-behavior (i.e., common-cause failure) while the robustness is a matter of indirect and sequential damage (i.e., cascading and escalating failure).

Lastly, in order to solve the uncertainty problems regarding the

robustness estimation, this research conducted a comprehensive review on the traditional and current research on interdependent lifeline systems. Although some implication can be drawn by previous research outcomes, it is still difficult to explain how a disturbance affects the system performance. Specifically, internal dependency within a single infrastructure and the external dependency between two different infrastructures is generally evaluated after the disaster with empirical data or expert judgment despite the need for such information in the pre-disaster phase to prioritize decisions for inspection and replacements. In addition, as a result of reviews, it was noted that IIM is useful for analyzing how a common-cause failure at single-site component occurs cascading failure at another component. However, the extent of cascading is depended on extensive data collected by field observations, and IIM cannot capture time-varying robustness.

Thus this research use IIM incorporates with other research methods, in particular, BN to overcome the former limitation and SD for the latter. To be specific, BN facilitates prediction of the probability of the unknown event (e.g., cascading failure) base on the input information or spatial path analysis in situations of data scarcity. On the other hand, demand fluctuation during an earthquake is modeled based on SD, and it enables this research to understand truly by considering a consumer behavior as an important factor determining the lifeline system behavior.

Chapter 3. Configuration of the Lifeline Network

A lifeline system can be modeled as a network consist of a set of nodes and links. In Chapter 3, a definition and attributions of components (i.e. nodes) in a power supply system and a potable water supply system is defined. In particular, since the reliability of component is widely discussed in the previous literature and can be relatively easier to obtain, this chapter firstly presents common-cause failure estimation based fragility functions introduced by FEMA and KAERI. With such useful approach, this research assigns the operational state to each type of component to determine discrete functionality (i.e. the ability to supply the intended output, range 0 to 100%). This value is transformed to continuous variables in Chapter 4.

Meanwhile, a link represents dependency between two interdependent components and it is also discussed in terms of functional relationship and spatial relationship to build up the lifeline network.

3.1 Component Definitions

3.1.1 Power Supply System

As stated before, the components in the power supply system include electricity generators (i.e., power plant) and deliverers (i.e., transmission and distribution substation).

A power plant is the uppermost point of the whole electric power system and defined as facilities for the generation of electricity. From the viewpoint of seismic damage assessment, a power plant has its own static attributes such as types of fuels (i.e., fossil or nuclear), geographical coordinates (i.e., longitude and latitude) and connectivity (i.e., number of the connected transmission substations). As shown in Table 3-1, the "capacity" attribute value is also considered for the power generator in this research. This value indicates the maximum electric output that a power plant can produce under normal conditions; whereas the "generation" attribute value is the amount of electricity that a power plant produces over a specific period of time. In general, most power plants do not operate at their full capacity all the time. Moreover, in a post-earthquake situation, damaged power plants may completely shutdown for inspection and restoration (when the PGA value is over 0.1g in South Korea). In this context, this research assigned the

"operational states" of a power plant to the following four type: normal operation, emergency shutdown, emergency operation, and safety inspection. Table 3-2 shows the detailed descriptions of each state and how they match the states of fragility curves introduced by FEMA.

Table 3-1. Attributes of each component in power system

Component	Attributes	Units of Measure (or Possible Values)	Static / Dynamic
Generator	Index	given number for the node	Static
	Type	fossil or nuclear	Static
	Coordinate	(longitude, latitude)	Static
	Connectivity	No. of connected nodes	Static
	Capacity	MW	Static
	Generation	MWh	Dynamic
	State	See Figure 3-2	Dynamic
Deliverer	Index	given number for the node	Static
	Type	transmission or distribution	Static
	Coordinate	(longitude, latitude)	Static
	Connectivity	No. of connected nodes	Static
	Capacity	No. of customer	Static
	Sales	No. of customer	Dynamic
	Source Node	one of the generators	Dynamic
	State	See Figure 3-2	Dynamic
Customer	Type	Residential	Static
	Coordinate	(longitude, latitude)	Static
	Source Node	one of the deliverer node	Dynamic
	State	See Figure 3-2	Dynamic

Table 3-2. Description of each damage state for power plants

Damage State	Description	Functionality (%)
Normal operation	• PGA < 0.1g • Slight damage in FEMA	100
Emergency shutdown	• PGA $\geq 0.1g$ • Slight/Moderate/Extensive/Complete damage in FEMA	0
Emergency operation	• $0.1\text{g} \leq \text{PGA} \leq 0.2g$ • Moderate damage in FEMA	100
Safety inspection	• PGA $\geq 0.2g$ • Moderate/Extensive/Complete damage in FEMA	0

These states are determined by the extent of ground shaking (i.e., PGA); and the transition between certain states becomes enabled after the specified amount of time (i.e., inspection time or restoration time) elapses. In other words, a power plant's generation capability varies depending on its operational states, thus this research assumed that a power plant in slight or moderate state can fully generate its intended output, while the functionality of other states is 0%.

Power deliverers are facilities that play a role as intermediators between power generators and customers. Based on their functions, these can be classified into two types: transmission or distribution substations. Transmission substation takes electricity from generation plants, transform

and transfer it to the distribution substation; while distribution substation directly connects to the individual customers. These components also have several attribute values (details are described in Table 3-1) such as "source node." This value matches one of the power generator that contains the shortest path to the deliverers. However, this is important that the shortest path does not always mean minimum topological distance; rather, the lowest resistance. Thus, power deliverers take a source node as following steps.

(1) Find a generator which provides the shortest path.

(2) Check that following equation is satisfied for source node and sink node.

$$\sum x_i + x_{ij} \leq u_i \qquad (6)$$

where, x_i is present electricity transfer volume through a i^{th} node, x_{ij} is present electricity transfer volume from a i^{th} node to j^{th} node, and u_i is a capacity of i^{th} node.

(3) If it is false, check the equation again with the next nearest generator.

Electricity transfer volume here is in accordance with the number of customers (or deliverer nodes) that are connected to the deliverer nodes (or generator nodes) under normal conditions, and it is called "sales" (or "generation") value. The functionality of a deliverer, the ratio of "sales" to "capacity (which means intended sales)", is assigned by its own "damage state"

and the operational state of its source node.

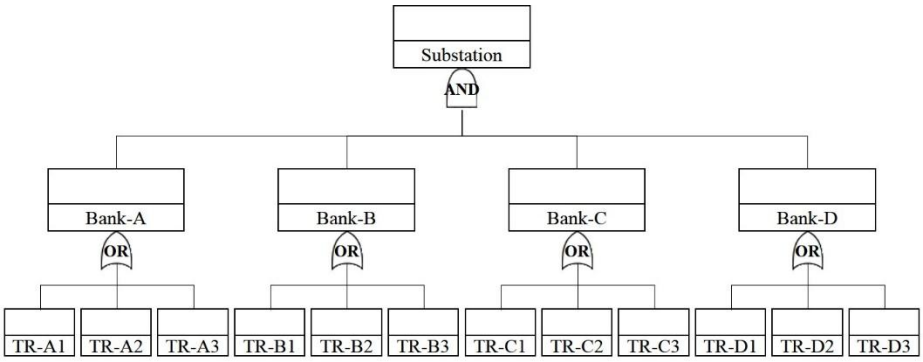

Figure 3-1. Fault tree of a transmission and distribution substation

For example, assuming that there is a low voltage (154kV) distribution substation in South Korea. In general, this type of substation consists of 4 Bank systems connected 3 single-phase transformers as shown in Fig. 3-1. Regarding this figure, if at least one of the transformers fails, a bank also fails (OR-gate); while since the relations of a substation and a bank is represented as AND-gate[4], complete failure of a substation occurs when all transformers fail. In addition, the capacity of a bank is 45MVA at normal and 60MVA at max. Thus, although one of the banks failed due to an earthquake, a substation can operate with 100% functionality using the rest of three banks. However, the functionality is reduced to 67% when two banks failed; and a substation stop to operate when three or four banks failed. Detailed descriptions of each

[4] OR-gate means logical disjunction of input events; while AND-gate means logical conjunction of input events in the fault-tree analysis.

damage state for 4 bank system including 345kV and 154kV substations is presented in Table 3-3

Table 3-3. Description of each damage state for substations

Damage State	Description	Functionality (%)
Slight	• Failure of 1Bank or • Failure of min.1 max.4 transformers	100
Moderate	• Failure of 2Bank or • Failure of min.2 max.6 transformers	100
Extensive	• Failure of 4Bank or • Failure of min.4 max.11 transformers	67
Complete	• Failure of all transformers	0

The last types of components, customers, represent the person or group of people who are the final users of electricity in the service area. In this research, customers are considered as non-vulnerable due to a lack of appropriate fragility curves related to their diverse building characteristics such as structures, materials, and height. Thus, a customer has only two states, in service or out of service; and these states are dependent on the damage state of its source node (one of the deliverer nodes) in their region.

Fig. 3-2 summarize the behavior of each component as described in this section. Power generators and deliverers are vulnerable to damage in the case of an earthquake, and they are in a certain state that can affect the customers'

state. Thus, the number of customers in the normal condition state ultimately determine the functionality of the whole power supply system network.

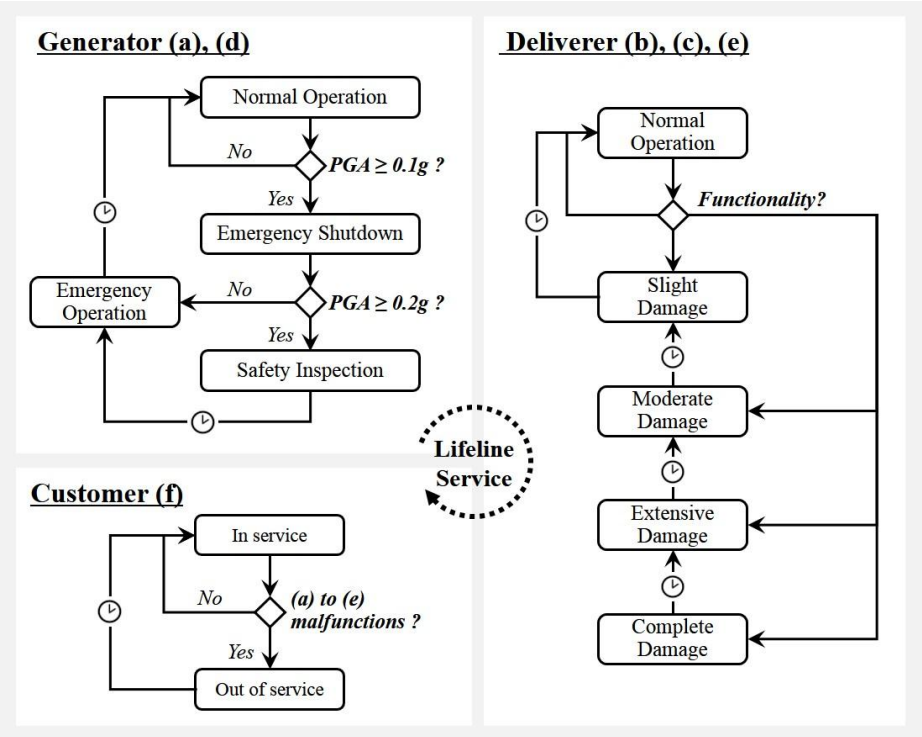

Figure 3-2. Behavior of each component

3.1.2 Potable Water Supply System

Similar to the power supply system, the potable water supply system also divided three categories: service generator, deliverer, and customer. However, while deliverers in the power system transform the electricity from high-voltage to low-voltage that can be used for customers, deliverers in the potable water supply system just let drinking water flows to customers.

In detail, a water treatment plant is defined as facilities for improving the quality of the raw-water up to potable level. While a potable water supply system includes terminal reservoirs for the intake raw-water (e.g., lake or dam), this research assumed that a water treatment plant is a source node of the whole system. A "type" of water treatment plants is in accordance with a type of raw-water such as groundwater and surface water. In addition, since the operational state of a water treatment plant depends on the electricity for operation, it has unique attributes such as the "power source", "power volume" and "power availability". The rest of attributes including "index", "coordinate", "connectivity", and "capacity" are shown in Table 3-4; and "state" is assumed that same as power plant since there is little knowledge on seismic-behavior of water treatment plants.

Storage tanks are built of steel, concrete, or wood and they hold the potable water. In this context, the damage of storage tanks means that there is a leakage of content due to cracks in their body. Another deliverers, pumping stations, generally consist one or more pumps that boost water pressure for transmission and distribution to customers in hillsides. Thus, a damaged-pumping station cannot supply the potable water to its point of destination.

Table 3-4. Attributes of each component in potable water system

Component	Attributes	Units of Measure (or Possible Values)	Static / Dynamic
Generator	Index	given number for the node	Static
	Type	ground water or surface water	Static
	Coordinate	(longitude, latitude)	Static
	Connectivity	No. of connected nodes	Static
	Capacity	Mgd	Static
	Power source	index of connected power distribution substation	Static
	Power volume	kW	Static
	Power availability	kW	Dynamic
	Generation	Mgd	Dynamic
	State	See Figure 3-2	Dynamic
Deliverer	Index	given number for the node	Static
	Type	storage tank or pumping station	Static
	Coordinate	(longitude, latitude)	Static
	Connectivity	No. of connected nodes	Static
	Capacity	No. of customer	Static
	Power source	index of connected power distribution substation	Static
	Power volume	kW	Static
	Power availability	kW	Dynamic
	Sales	No. of customer	Dynamic
	Source Node	one of the generators	Dynamic
	State	See Figure 3-2	Dynamic
Customer	Type	residential	Static
	Coordinate	(longitude, latitude)	Static
	Source Node	one of the deliverer node	Dynamic
	State	See Figure 3-2	Dynamic

In this research, the functionality of components in a potable water supply system was referred to the best estimate damage ratio introduced by FEMA (detail values are in Table 3-5).

Table 3-5. Description of each damage state for water system

Damage State	Water treatment plat	Storage tank	Pumping station
Slight	92%	80%	95%
Moderate	60%	60%	62%
Extensive	23%	20%	20%
Complete	0%	0%	0%

3.2 Seismic Fragility of a Component

Before using the fragility functions, class of a component (e.g., building type and operation capacity), seismic design level (e.g., anchored / unanchored), and seismic response spectrum (e.g. Peak ground acceleration, PGA) must be determined. Table 3-6 describes the classification of lifeline components that analyzed in this research (as same as shown in Fig. 1-4). For example, water treatment plant in this paper refers to medium water treatment plant with capacity ranging from 50mgd to 200mgd (millions of gallons per day).

Table 3-6. Classification of the lifeline components

Lifeline Component	Index	Descriptions
Power Plant (PP)	EPP3	• Medium/Large PP with anchored (>100 MW)
Transmission Substation (TS)	ESS3	• Medium voltage TS with anchored (345kV)
Distribution Substation (DS)	ESS1	• Low voltage DS with anchored (154kV)
Water Treatment Plant (WTP)	PWT3	• Medium WTP with anchored (50-200 mgd)
Storage Tank (ST)	PST2	• On ground unanchored ST
Pumping Station (PS)	PPP1	• Small PS with anchored (<10 mgd)

Meanwhile, each component has own damage state including normal (ds1), slight (ds2), moderate (ds3), extensive (ds4), and complete (ds5). The fragility curves represented lognormal distribution provides the probability of exceeding such damage states. Table 3-7 displays discrete damage state probabilities in the form of means and standard deviation of PGA (unit: g, acceleration of gravity, 9.8m/sec^2) for each component types.

Table 3-7. Fragility functions for lifeline components

Index	Damage State	PGA (g)		Index	PGA (g)	
		Median	β*		Median	β*
EPP3	Slight	0.1	0.6	PWT3	0.37	0.40
	Moderate	0.25	0.6		0.52	0.40
	Extensive	0.52	0.55		0.73	0.50
	Complete	0.92	0.55		1.28	0.50
ESS3	Slight	0.20	0.60	PST2	0.18	0.60
	Moderate	0.28	0.50		0.42	0.70
	Extensive	0.39	0.40		0.70	0.55
	Complete	0.71	0.40		1.04	0.60
ESS1	Slight	0.31	0.70	PPP1	0.15	0.75
	Moderate	0.37	0.55		0.36	0.65
	Extensive	0.46	0.45		0.66	0.65
	Complete	0.92	0.45		1.50	0.80

* β is the lognormal standard deviation

According to Table 3-7, all of the components are vulnerable to earthquake, for example, if the PGA equals 0.28g, transmission substations may be in the moderate state with high probability. However, some definitions of damage states in FEMA and KAERI are rather ambiguous (e.g., slight damage means a short time malfunction for water treatment plant). Thus, this research will be assigned the functionality (range 0 to 100%) to each state and convert the graphs, as shown through Fig.3-3 to Fig. 3-8, to functionality curves in the next chapter. In addition, the prediction approaches of PGA, the value of x-axis in the graphs, will be also proposed in Chapter 4.

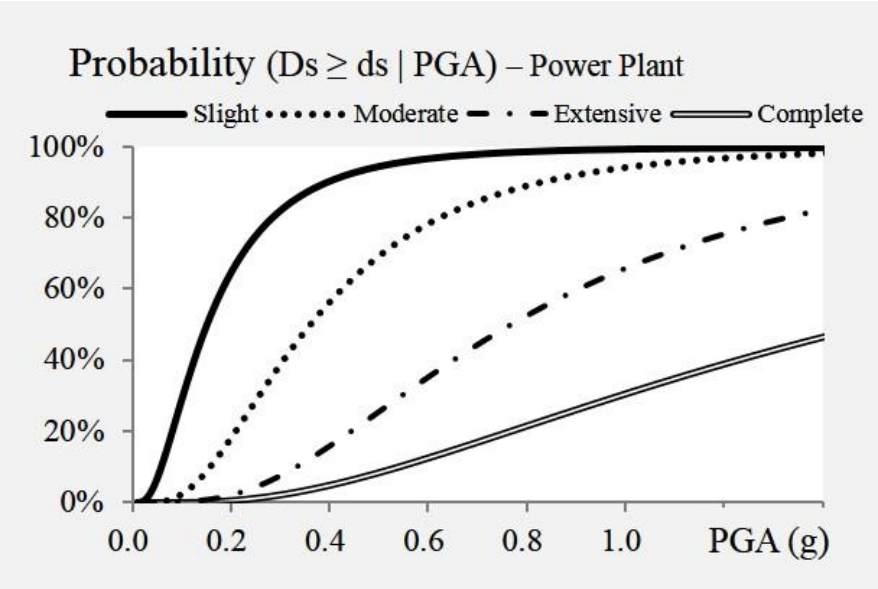

Figure 3-3. Fragility curves for the power plant (KAERI 2008)

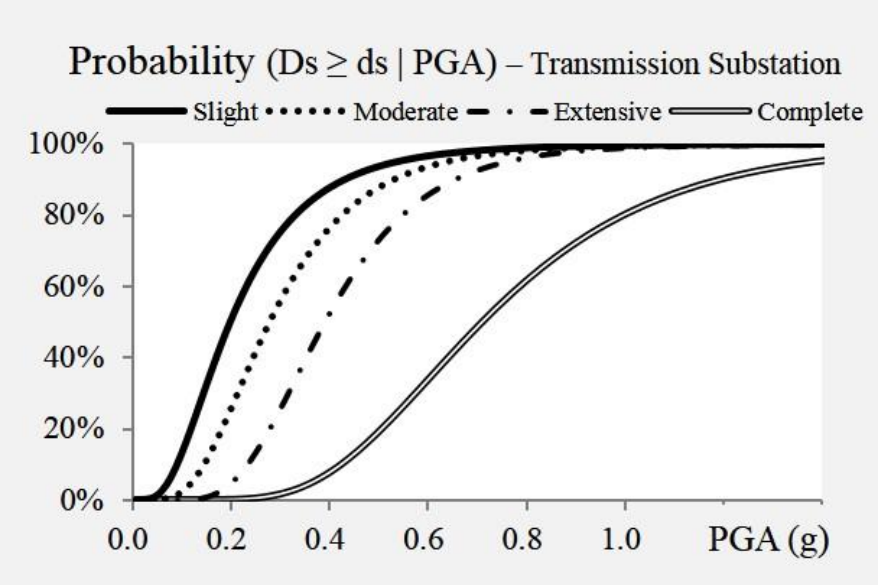

Figure 3-4. Fragility curves for the transmission substation (KAERI 2008)

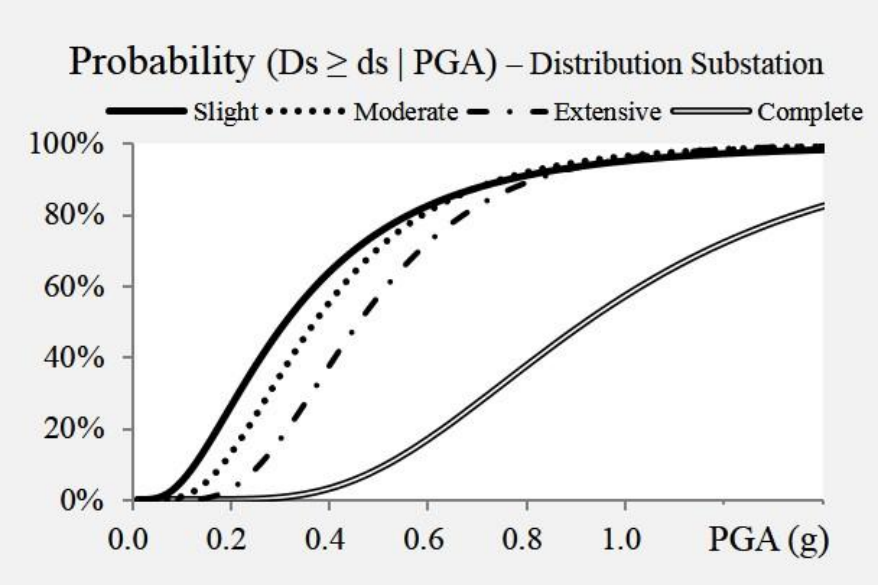

Figure 3-5. Fragility curves for the distribution substation (KAERI 2008)

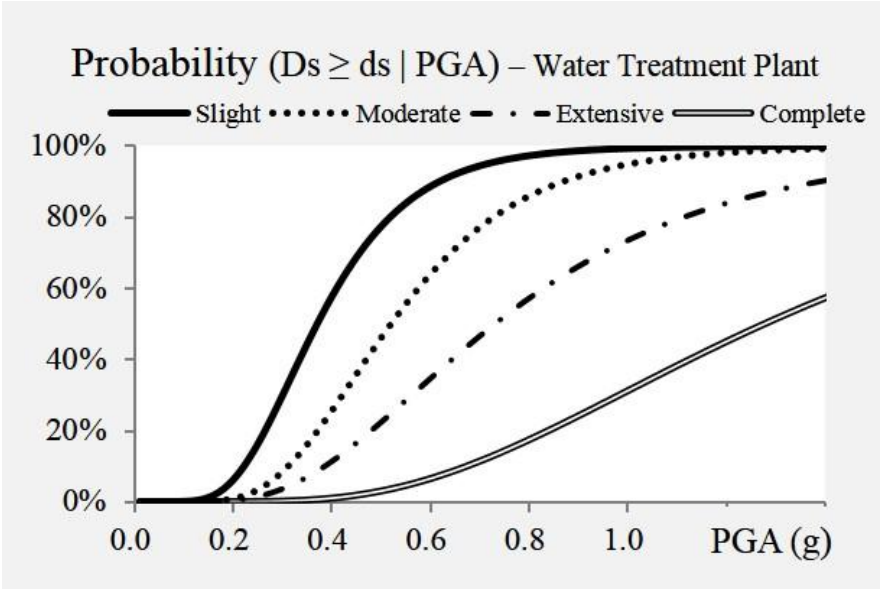

Figure 3-6. Fragility curves for the water treatment plant (FEMA 2003)

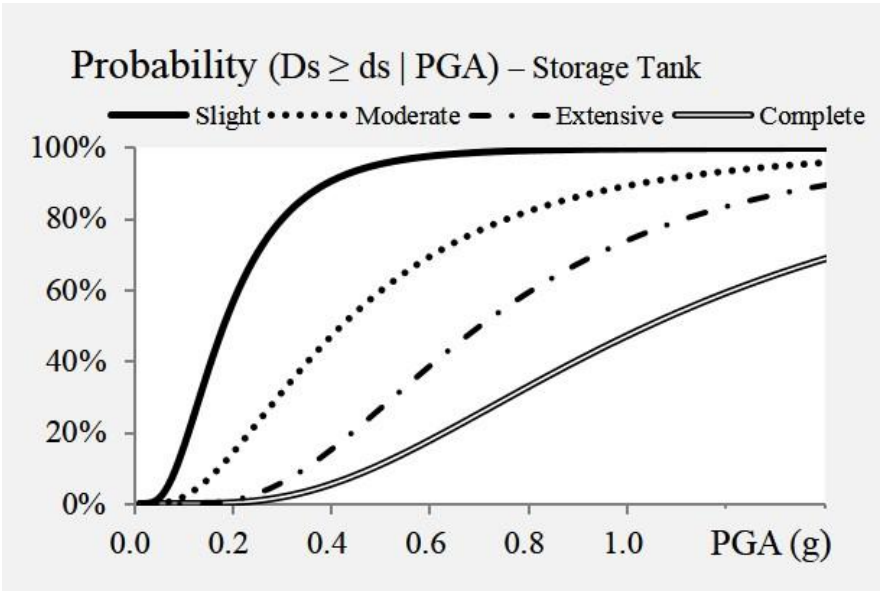

Figure 3-7. Fragility curves for the storage tank (FEMA 2003)

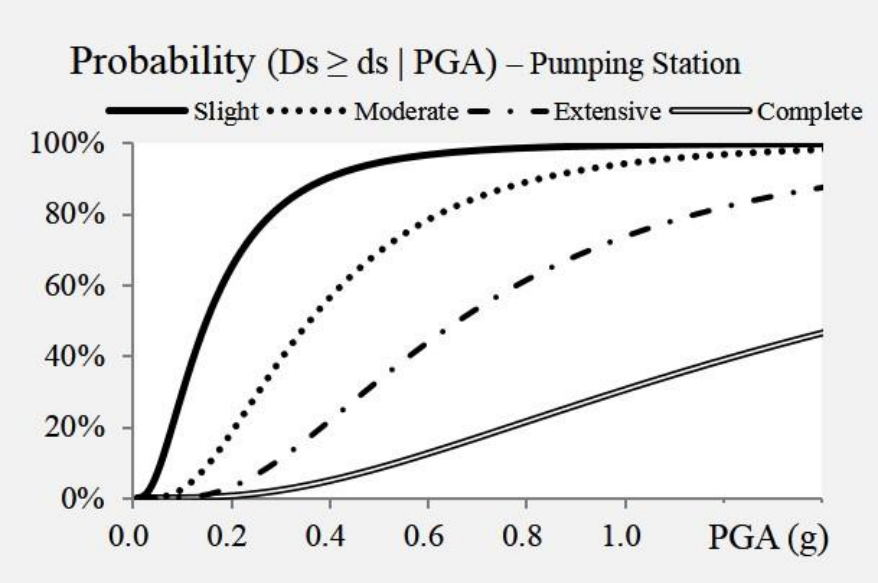

Figure 3-8. Fragility curves for the pumping station (FEMA 2003)

3.3 Dependency between the Components

Even if only a part of the lifeline system is damaged, its impact on the whole system can be catastrophic because the performance of the system depends not only on the physical damage of each component but also on the interactions among interdependent components (Frangopol and Saydam 2011).

As such, the dependency that causes cascading failures is mathematically defined whether there is a physical connections between components (i.e., if a link exists then 1, otherwise 0). However, in this research, the dependency between components is referred to as a directional functional relationship through which the state of a certain component is correlated to the state of the others (Rinaldi 2004). In detail, the dependency of a component ((B) in Fig. 3-9) to another component ((A) in Fig. 3-9) in lifeline network V is determined as a ratio of the input from (A) with respect to the total input requirements of (B).

$$\text{Dependency}_{BA} = \frac{\text{Input from A}}{\sum_{i} \text{Input from } i} \quad (i \in V) \qquad (7)$$

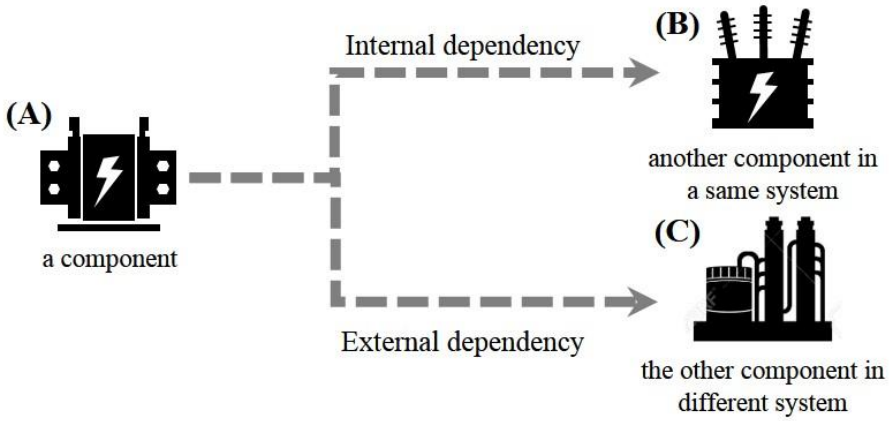

Figure 3-9. Comparison of internal and external dependency

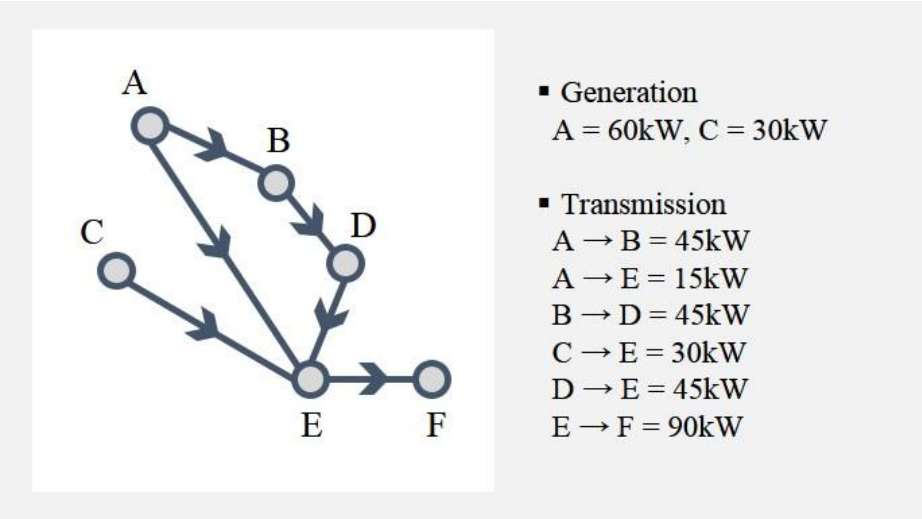

Figure 3-10. Example network for determining the dependency

For example, this research assumed that there is a power network consists of six components (A to F in Fig. 3-10). To be specific, A/C generates 60kW/ 30kW electricity per day respectively and it transmits to F through B,

D, and E. In this example network, the mathematical dependency can be presented as following an adjacency matrix:

$$A = \begin{pmatrix} 0 & 0 & 0 & 0 & 0 & 0 \\ 1 & 0 & 0 & 0 & 0 & 0 \\ 0 & 0 & 0 & 0 & 0 & 0 \\ 0 & 1 & 0 & 0 & 0 & 0 \\ 1 & 0 & 1 & 1 & 0 & 0 \\ 0 & 0 & 0 & 0 & 1 & 0 \end{pmatrix} \qquad (8)$$

Such an adjacency matrix is useful for construct the network topology and calculating the paths, however, it cannot represent which one is the most important subject to components with multiple paths.

On the other hand, the functional dependency based on Eq. 7, can prioritize the impact of connected components:

$$A = \begin{pmatrix} 0 & 0 & 0 & 0 & 0 & 0 \\ 1 & 0 & 0 & 0 & 0 & 0 \\ 0 & 0 & 0 & 0 & 0 & 0 \\ 0 & 1 & 0 & 0 & 0 & 0 \\ 0.17 & 0 & 0.33 & 0.5 & 0 & 0 \\ 0 & 0 & 0 & 0 & 1 & 0 \end{pmatrix} \qquad (9)$$

Therefore, it is expected that the operational state of component E in above example network is highly influenced by that of component D rather than others. However, in most real-world network case, the data sets of input and output are not published to the public for security reasons. This research, thus, proposed following equations based on Dijkstra's shortest path algorithms (1959):

$$a_{ij} = \frac{\sum_{k} (1 / d_{ki}(j))}{\sum_{k} (1 / d_{ki})} \quad \forall\ i, j \qquad (10)$$

where, d_{ki} denotes the length of the shortest path from source node k and sink node i, $d_{ki}(j)$ denotes the length of the shortest path from source node k and sink node i which contains intermediate node j.

In Equation 6, a dependency corresponds with the path distance and connectivity between components in a network, and this value is determined to be a continuous variable ranged from 0 to 1. This statement is based on the following assumptions: (a) a sink node can take all paths in the network; however, the majority will take the path of the least resistance in a normal situation; (b) resistance is in inverse proportion to the length of the path between nodes; (c) a sink node can change their path when a source node suffers overload or a cascade outage is triggered.

For example, by using the original shortest path algorithm, the following

three link sets {1, 7, 4}, {2, 9, 6, 7, 4}, and {3, 11, 6, 7, 4} are identified for the component 4 as described in Fig. 3-11; and this research assumed that the path length of each link set is about 86,145m, 187,186m, and 220,394m respectively. Then, component 4 is more likely to take the path from source node 1 because this path, {1, 7, 4}, is shorter than the other two paths. However, if a cascading failure is triggered by the shutdown of component 1, it may change the route to sub-optimal path, {2, 9, 6, 7, and 4}. At the same time, destruction of the component 7 will lead to a complete malfunction of the component 4 because all of three paths from source nodes contain component 7. Thus, from the definitions of dependency, the correlation coefficients from component 7 to component 4 equals one ($a_{47} = 1$).

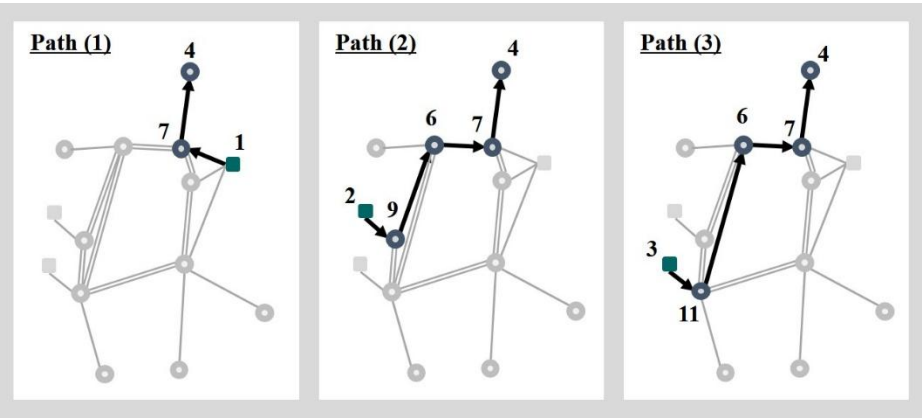

Figure 3-11. Shortest link sets in the second example network

3.4 Summary

In this chapter, this research described the component in a power supply system and a potable water supply system. There were two types of components, generators defined the service generation facilities, and deliverers defined service transforming or transferring facilities. In detail, a power plant is the uppermost point of power supply chain, and "generation" was considered key attributes of this type of component [Mwh]. It refers to the amount of electricity that can be produced by a power plant. Therefore, "generation" can be zero when a power plant stop to operate. Regarding the "generation", this research divided "operational states" of a power plant such as normal operation (F =100%), emergency shutdown (F=0%), emergency operation (F=100%), and safety inspection (F=0%).

Another generator is water treatment plant for improving the quality of raw-water up to potable level. Although terminal reservoirs to intake raw-water are, this research assumed that a water treatment plant is a source node of a potable water supply system. In this context, it also has "generation" attributes [Mgd] and the same behavior as that of a power plant. Whereas since a water plant needs electricity for operation, "power availability" was assigned and it can also affect "operational states." Meanwhile, this research

assumed that transmission and distribution substation, two power deliverers, take their source node regarding low resistance and capacity. In addition, electricity "sales" was assumed the number of customers in service and this value in accordance with "damage state" including slight (F=100%), moderate (F=100%), extensive (F=67%), and complete (F=0%). Storage tanks and pumping stations also assigned this "damage state"; while the functionality value of each state is some different.

Furthermore, this research develops common-cause failure estimation method based on the six fragility functions – for the medium/ large power plants, the medium voltage transmission substations, the low voltage distribution substations, the medium water treatment plant, on ground unanchored storage tank, and the small pumping stations – introduced by FEMA and KAERI (details in Chapter 4). A dependency that causes cascading failure in the lifeline systems was also discussed in this chapter. Firstly, the dependency between component A and B (D_{BA}) was defined as the ratio of the input from A with respect to the total input requirements of B. In particular, for the real-world lifeline network that the input data is not published, this research proposed the dependency calculation equation based on spatial path analysis. With several network examples, this research also examined the process of damage propagation.

Chapter 4. Functionality Assessment Framework

Determining an actual performance compared to desire level is uncertain because various problems, such as physical destruction, disruptions of a supply chain, and demand fluctuation, can arise. In this chapter, a step-by-step procedures for constructing the functionality assessment framework of seismic-damaged lifeline system is introduced. To be specific, this framework includes four sub-models: (a) the ground motion prediction at single-site component under earthquake scenarios and common-cause failure analysis for each lifeline component given ground motions; (b) internal cascading failure analysis caused by dependency within a lifeline system using inoperability input-output model; (c) external cascading failure analysis caused by dependency between two different lifeline systems using Bayesian network; and (d) impact analysis depending on the changes of the final demand using system dynamics.

4.1 Common-cause Failure Estimation

4.1.1 Ground Motion Prediction

Ground motions recorded at particular sites increases with earthquake intensity and is usually attenuated accordance with a distance from the epicenter. Site conditions also affect the seismic wave amplification (e.g., motions on the soil are greater than on the rock). Therefore, a basic ground motion (Y) prediction equation as follows (Boore and Atkinson 2008):

$$\ln Y = f_M(M) + f_D(R, M) + f_S(V_{S30}, R, M) \qquad (11)$$

where, f_M, f_D, f_S represented the magnitude scaling, distance attenuation and site amplification function, respectively. M is moment magnitude, R is the epicentral distance, and the V_{S30} is the inverse of the average shear-wave velocity from surface to a depth of 30m.

As stated above, this research conducts the deterministic calculations of ground shaking based on earthquake scenario given magnitude. In addition, this scenario also contains the information of a location of the epicenter and focal depth; and they used for determining epicenter distance as described Eq. 12 to Eq. 13.

$$\Delta lat = E_{lat} - P_{lat} \qquad (12)$$

$$\Delta long = E_{long} - P_{long} \qquad (13)$$

$$a = \sin^2\left(\frac{\Delta lat}{2}\right) + \cos(P_{lat}) \times \cos(E_{lat}) \times \sin^2\left(\frac{\Delta long}{2}\right) \quad (14)$$

$$X = 2R \times \tan^{-1}\left(\sqrt{a} \div \sqrt{1-a}\right) \quad (15)$$

where E_{lat} = the latitude of epicenter [degree]; E_{long} = the longitude of epicenter [degree]; P_{lat} = the latitude of observation point [degree]; P_{lat} = longitude of observation point [degree]; R = radius of the earth [approximately 6,370 km]; and X = epicentral distance [km]

In terms of ground motions (Y), there are various measures such as spectral acceleration (SA), peak ground velocity, (PGV), peak ground acceleration (PGA), and permanent Ground Deformation (PGD). Among these response spectrum, this research focused PGA of the single-site components. In order to assess the PGA value, many ground motion prediction equations have been provided for the high seismicity regions such as Japan, Western America, and Italy. The regression equation by Kanno et al. (2006) also for such regions and it can be expressed as follows:

$$\log(PGA) = a_1 M_w + b_1 X - \log\left(X + d_1 \cdot 10^{e_1 M_w}\right) + c_1 + \varepsilon_1 \ (\mathrm{D} > 30\mathrm{km}) \quad (16)$$

$$\log(PGA) = a_2 M_w + b_2 X - \log(X) + c_2 + \varepsilon_2 \ (\mathrm{D} \geq 30\mathrm{km}) \quad (17)$$

where PGA= predicted peak ground acceleration [cm/sec^2]; M_w= moment magnitude; D= focal depth [km]; a_1= 0.56; b_1= -0.0031; c_1= 0.26; d_1= 0.0055; ε_1= 0.37; e_1= 0.5; a_2= 0.41; b_2= -0.0039; c_2= 1.56; and ε_2= 0.40.

For the low to moderate seismic regions, however, this equation may not represent the ground motions because the available strong earthquake records are very limited (Han and Choi 2007). Thus, in this research considered several ground motion prediction equations as described in Table 4-1, specially developed for low to moderate seismic regions such as Eastern North America (Campbell 2003; Shahjouei and Pezeshk 2016) and South Korea (Park et al. 2001; Jo and Bagg 2003; Yun et al. 2009; Emolo et al. 2015).

Some equations include, *R*, hypo-central distance and it is derived from epicentral distance:

$$R^* = \sqrt{X^2 + D^2} \qquad (18)$$

where X = epicentral distance [km]; D = focal depth [km].

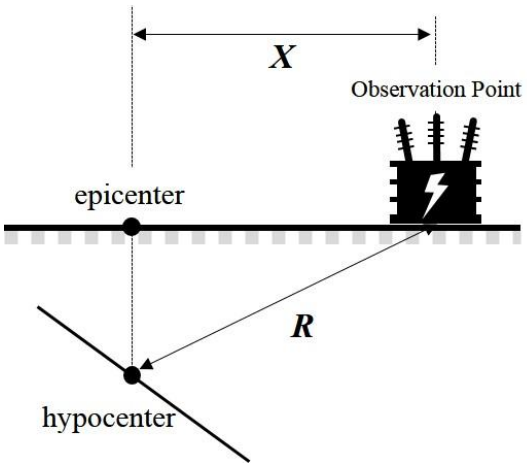

Figure 4-1. Hypocentral and epicentral distance

Table 4-1. Ground predictions for the low-moderate seismic region

Researcher	Equations
Campbell (2003)	$\mathrm{Y} = c_1 + c_2 M_w + c_3 (8.5 - M_w)^2 + c_4 \ln R^* + (c_5 + c_6 M_w) R$ $R^* = \sqrt{R^2 + (c_7 e^{c_8 M_w})^2}$ where Y = ln(*PGA*) [*g*]; M_w = moment magnitude; R = hypocentral distance [km]; c_1 = 0.907; c_2=0.983; c_3 = -0.066; c_4= -2.7; c_5 = 0.159; c_6= -2.8; c_7= 0.212; c_8= -0.301.
Emolo et al. (2015)	$\mathrm{Y} = a + bM_w + c \log R^* + dX + e$ $R^* = \sqrt{X^2 + h^2}$ where Y = log(*PGA*) [cm/sec2]; M_w = moment magnitude; X = epicentral distance [km]; a = -3.07; b =0.73; c = -0.76; d = -0.0029; e = 0.3260; h = 1.7.

Park et al. (2001)	$\mathrm{Y} = c_0 + c_1 R - \log R$ $c_0 = c_{00} + c_{01}(M_w - 6) + c_{02}(M_w - 6)^2 + c_{03}(M_w - 6)^3$ $c_1 = c_{10} + c_{11}(M_w - 6) + c_{12}(M_w - 6)^2 + c_{13}(M_w - 6)^3$ where Y = ln(*PGA*) [gal]; M_w = moment magnitude; R = hypocentral distance [km]; c_{00} = 3.391; c_{01}=0.3601; c_{02} = -0.0362; c_{03} = 0.0064; c_{10} = -0.0037; c_{11} = 0.0013; c_{12} = -0.0001; c_{13} = -0.000027.
Jo and Bagg (2003)	$\mathrm{Y} = c_0 + c_1 R + c_2 \ln R - \ln R^* - 0.5 \times \ln R^{**}$ $R^* = \min(R, 100)$ $R^{**} = \max(R, 100)$ $c_0 = c_{00} + c_{01}(M_w - 6) + c_{02}(M_w - 6)^2 + c_{03}(M_w - 6)^3$ $c_1 = c_{10} + c_{11}(M_w - 6) + c_{12}(M_w - 6)^2 + c_{13}(M_w - 6)^3$ $c_2 = c_{20} + c_{21}(M_w - 6) + c_{22}(M_w - 6)^2 + c_{23}(M_w - 6)^3$ where Y = ln(*PGA*) [gal]; M_w = moment magnitude; R = hypocentral distance [km]; c_{00} = 10.7383; c_{01}=0.5909; c_{02} = -0.0562; c_{03} = 0.0214; c_{10} = -0.0024; c_{11} = 0.0002; c_{12} = -0.00002; c_{13} = 0.00004; c_{20} = -0.2437; c_{21} = 0.095; c_{22} = -030088; c_{23} = -0.0033.

Shahjouei and Pezeshk (2016)	$$\mathrm{Y} = c_1 + c_2 M_w + c_3 {M_w}^2 + (c_4 + c_5 M_w) f_1(R^*) + (c_6 + c_7 M_w) f_2(R^*) + (c_8 + c_9 M_w) f_3(R^*) + c_{10} R^*$$ $$R^* = \sqrt{X^2 + {c_{11}}^2}$$ $$f_1(R^*) = \min(\log R^*, \log 60)$$ $$f_2(R^*) = \max[\min\{\log(R^*/60), \log(120/60)\}, 0]$$ $$f_3(R^*) = \max\{\log(R^*/120), 0\}$$ where Y = log(*PGA*) [*g*]; M_w = moment magnitude; R = hypocentral distance [km]; c_1 = -0.3002; c_2=0.5066; c_3 = -0.0453; c_4= -3.224; c_5 = 0.2998; c_6= -1.283; c_7= 0.1045; c_8= -3.0856; c_9 = 0.2778; c_{10} = -0.0008; c_{11} = 3.81.
Yun et al. (2009)	$$\mathrm{Y} = c_1 + c_2 M_w + (c_3 + c_4 M_w) f_1(X) + c_6 (M_w - 6)^2 + c_7 f_2(R) + c_8 f_3(R)$$ $$f_1(X) = \ln(X + e^{c5})$$ $$f_2(X) = \ln\{\min(R, 50)\}$$ $$f_3(X) = \ln\{\max(R, 50)\}$$ where Y = ln(*PGA*) [*g*]; M_w = moment magnitude; X = epicentral distance [km]; R = hypo-central distance [km]; c_1 = 35.768; c_2=-2.357; c_3 = -6.884; c_4= 0.579; c_5 = 5.237; c_6= -0.139; c_7= -1.1218; c_8= -0.488.

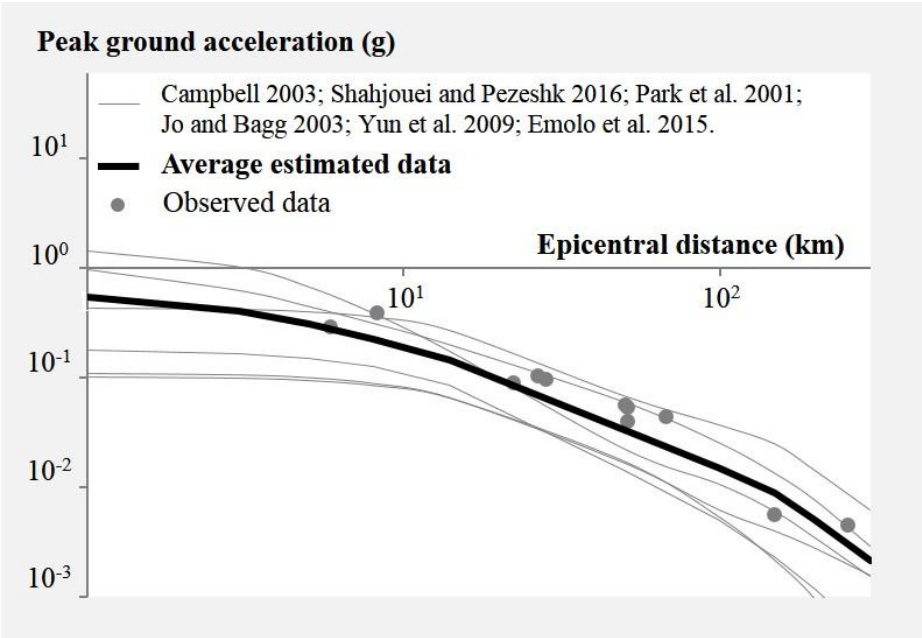

Figure 4-2. Peak ground accelerations for Magnitude 5.4

In order to examine the fitness of proposed prediction equations, this research compared the observed PGA data recorded when 2016 Gyeongju earthquake (detailed in Chapter 5.2) – moment magnitude 5.4, focal depth 13km and epicenter location (129.216E, 35.781N) – occurred in South Korea (Korea Meteorological Administration 2016; Lee 2017) and estimated PGA with the same conditions. Specifically, this research used the average of PGA (g) estimated from above equations as an index of how strongly the ground where power and water system components are located shakes.

Figure 4-2 and Table 4-2 shows the comparison result of observed data and estimated data. Because the objective of PGA prediction is to compute the probability of components' seismic destructions in fragility functions that will be discussed in next section, these results are regarded as acceptable representations of the real world. Hence, the authors used an equation highlighted in Fig. 4-2 across the research.

Table 4-2. Comparisons between observed and estimated PGA

Station code	Epicentral distance [km]	Observed PGA [g]	Estimated PGA [g]	Error rate [%]
MKL	5.9	0.291	0.279	4.0%
USN	8.2	0.396	0.222	43.9%
DKJ	22.2	0.090	0.084	6.8%
KNWA	28.0	0.098	0.064	34.6%
KNKA	51.0	0.054	0.032	40.4%
KNUA	148.0	0.006	0.009	55.0%
KNYA	254.0	0.005	0.005	11.7%
DAG2	26.5	0.105	0.068	34.7%
MIYA	50.1	0.057	0.033	42.1%
PHA2	50.8	0.040	0.032	20.3%
CHR	67.5	0.044	0.023	47.5%

4.1.2 Functionality of a Component

In Chapter 2, the author discussed the fragility functions by FEMA and KAERI (through Table 2-2 and Fig. 2-2 to 2-7). Then, in Chapter 3, each damage state (i.e., normal (ds1), slight (ds2), moderate (ds3), extensive (ds4), and complete (ds5)) was re-defined regarding own characteristics. Furthermore, these state was proposed in the form of the functionality. For example, if there is a low voltage distribution substation (same as described in Chapter 3.1) and the observed PGA at the place is 0.15g, the probability of each damage state is based on Table 2-2:

$$
\begin{aligned}
&P(D_S=ds1 \mid PGA=0.15g)=0.50\\
&P(D_S=ds2 \mid PGA=0.15g)=0.35\\
&P(D_S=ds3 \mid PGA=0.15g)=0.13\\
&P(D_S=ds4 \mid PGA=0.15g)=0.02\\
&P(D_S=ds5 \mid PGA=0.15g)=0.00
\end{aligned}
\qquad (19)
$$

In this example, the functionality would be:

$$\text{Functionality} = 0.5\times 100\% + 0.35\times 100\% + 0.13\times 67\% = 93.71\% \qquad (20)$$

Therefore, the functionality for the single-site component is estimated by the weighted combination:

$$\sum_i \{P(D_{DS} = ds_i) \times \text{Functionality at } ds_i\} \;\forall\; i \qquad (21)$$

Functionality of all other components was obtained the same approach and Fig. 4-3 summarize such functionality curves over PGA.

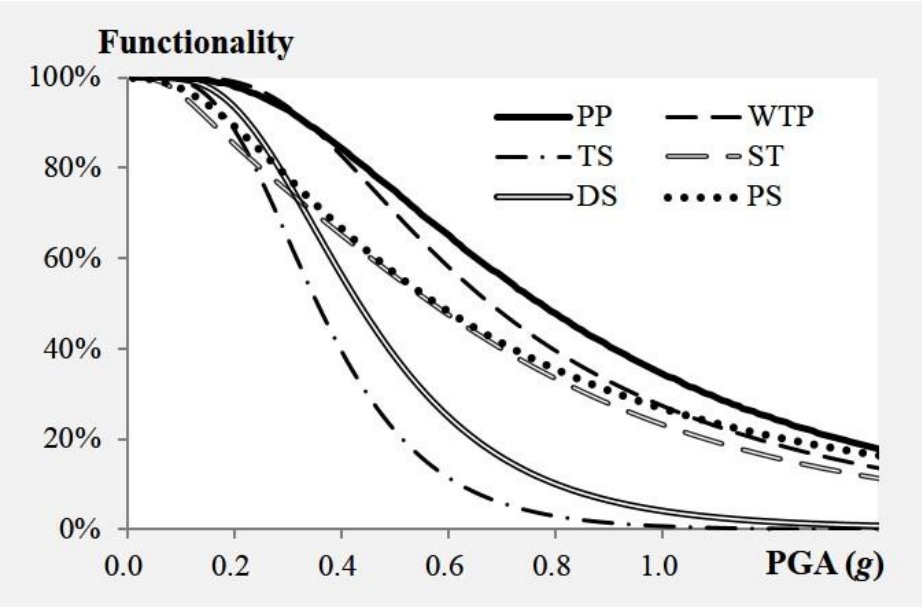

Figure 4-3. Functionality curves of lifeline system components

4.2 Internal Cascading Failure Estimation

4.2.1 Dependency in a Single Lifeline

The key challenge in seismic risk assessment of lifeline systems is dealing with the failure propagation emerge after an interruption of adjacent components. In this context, IIM examine the extent of cascading failure as the result of common-cause failures considering dependencies. In particular, this research herein focused internal dependency on a single system. Based on Eq. 3, component-by-component matrix is generally determined a ratio of the input from j^{th} component with respect to the total input requirements of i^{th} component. In detail, this research introduced the following probabilistic approach for the quantification of correlation coefficients between two connected nodes. This is a square matrix, where *n* equals the total number of nodes in the lifeline network and this is in accordance with Eq. 10.

$$a_{ij} = P(\text{failure of node } i \,|\, \text{failure of node } j) \quad (22)$$

Furthermore, to determine which components offer a greater contribution to the system performance, this research defines the damage propagation in a system as follows:

$$\frac{\sum(1 - CCF_i) \times S_i - \sum\{1 - (CCF_i + CF_i)\} \times S_i}{\sum S_i} \qquad (23)$$

where CCF_i is the common-cause failure of a i^{th} node [0 to 1]; CF_i is the cascading failure of a i^{th} node, S_i is the amount of intended services of i^{th} node in the normal operation.

Thus, the value of damage propagation in a component equals its cascading failure when S_i is constant; and this research assumed that dynamic functionality commonly falls short of the average static functionality in the lifeline system because the ability of each (i.e. $CCF > 0$).

4.2.2 Sub-Model using Inoperability Input-Output Model

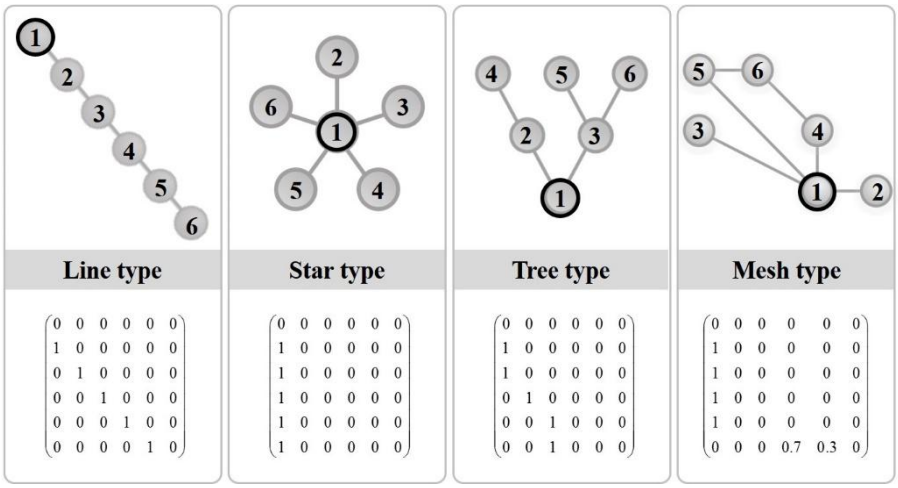

Figure 4-4. A set of example networks – line, star, tree, and mesh

For the ease of demonstrating the model applicability to quantifying internal dependency, this research proposes a set of example networks with respect to network topologies and arrangements of components. As shown in Fig. 4-4, there are four types of network and their component-by-component coefficient matrices are presented below the figure.

These topologies are detailed as follows: (1) line — all nodes are arranged in a line; (2) star — all nodes are connected to a central node; (3) tree — a root node connects to two or more sub-level nodes, forming a tree structure; and (4) mesh — each node is connected some or all the other nodes. An indexed number of a node indicates the rank of direction, and the service is delivered in only one direction from high to low (i.e., 1 is the highest and 6 is the lowest).

In addition, this research assumed all of the path lengths between two directly connected nodes are same in line, star, and tree type network; while the path (1→5→6) is longer than the path (1→4→6) in the ratio of 7: 3 in the mesh type network. As stated earlier, since IIM assumed the input/output data is deterministic variables observed at discrete-time, it is needed to integrate the approaches that can repetitively simulates the calculation process. Therefore, this research used AnyLogic 7.3.6 Personal Learning Edition, a

software that imports the network topological data from excel file and quantifies cascading failures. Fig. 4-5 shows the matrix function code for example networks based Eq. 23.

```
// common-cause failure matrix
 double [] C = new double[6];
 for (int i=0; i < 6; i++) {C[i] = nodes.get(i).Common-causeFailure;};

// (E-A)^(-1)
 double [][] E_A = new double[6][6];
 for (int i=0; i < 6; i++)
 {for (int j=0; j < 6; j++) {E_A[i][j] = Inverse_table(6*i+j+1);};};


// cascading failure matrix
 double[] X = new double[6];
  for(int i=0; i<6; i++)
  {for(int k=0; k<6; k++) {X[i] += E_A[i][k] * C[k];};};

for(int n=0; n<6; n++)
{nodes.get(n).CascadingFailure = min(100, C[n+3]*100);};


// total failure
TotalDamage =( nodes.get(0).CascadingFailure + nodes.get(1).CascadingFailure
             + nodes.get(2).CascadingFailure + nodes.get(3).CascadingFailure
             + nodes.get(4).CascadingFailure + nodes.get(5).CascadingFailure)/6 ;
```

Figure 4-5. Matrix function code for example networks

For example, this research assumed that all of the nodes sustain damage after an earthquake and their functionality to be reduced by 10%, (i.e., c_1 to c_5 = 0.1). Then, using the matrix function, the in operability vector (x) after the disruption can be determined as presented in Table 4-3.

Table 4-3. Inoperability with 10% degraded functionality

Type	Line	Star	Tree	Mesh

Inoperability	35%	18%	23%	20%

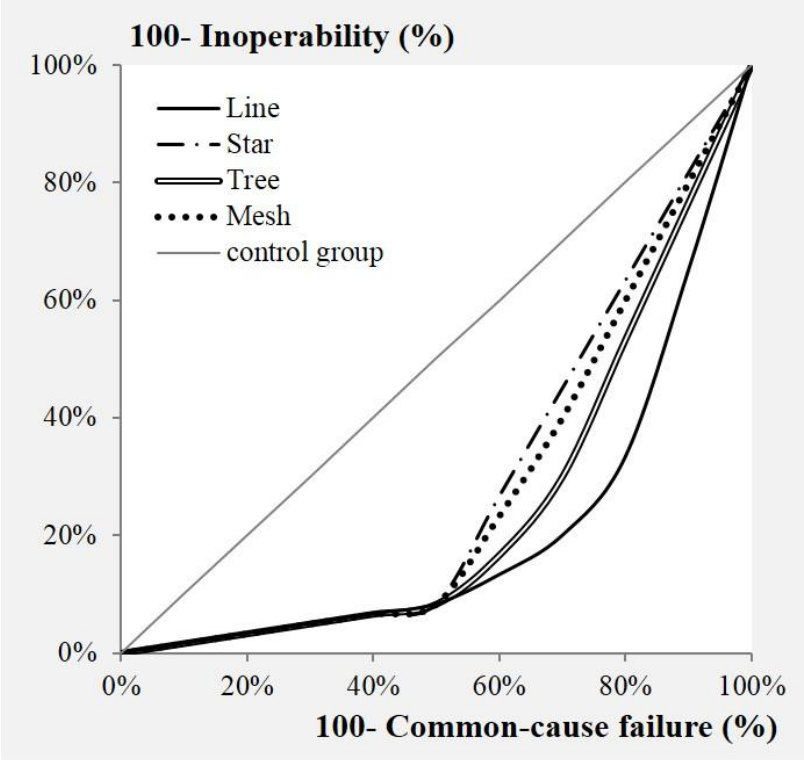

Figure 4-6. Inoperability considering the network topologies

On the basis of the inoperability with a scenario corresponding to a reduction of 10% in the functionality of all nodes, it can say that the network is vulnerable to the following order: line-type, tree-type, mesh-type, and star-type. This statement coincides with the results when the value of functionality reduction by 10% increments until all nodes are complete failures (i.e., c1 to c5 = 1.0) as can be seen in Fig. 4-6. This is because when a system has several

orders of nodes such as line-type network; the nodes have more chance to be propagated damage from upper-rank nodes. While a star-type network does not trigger the damage propagation except when the central node fails because each node is separately. However, since the central node is involved all other nodes operating in the star-type network, this is not appropriate for the system that has too many nodes. In this context, mesh type networks that some nodes have two or more paths are widely used for configuration of real-world lifeline system.

Thus, this research also design four kinds of mesh-type networks to analyze the effect of the network arrangements on the system performance. Fig. 4-8 display the example networks and simulation results using the IIM. For example, the inoperability of the first network (Mesh-1 in Fig. 4-7) is 60% when average common-cause failure is 20%; in contrast, that of second network (Mesh-2 in Fig. 4-7) is 47% at same conditions. Such results indicate that relocation of components, particularly for start node is helpful to manage and mitigate the lifeline system vulnerability in the post-earthquake phase.

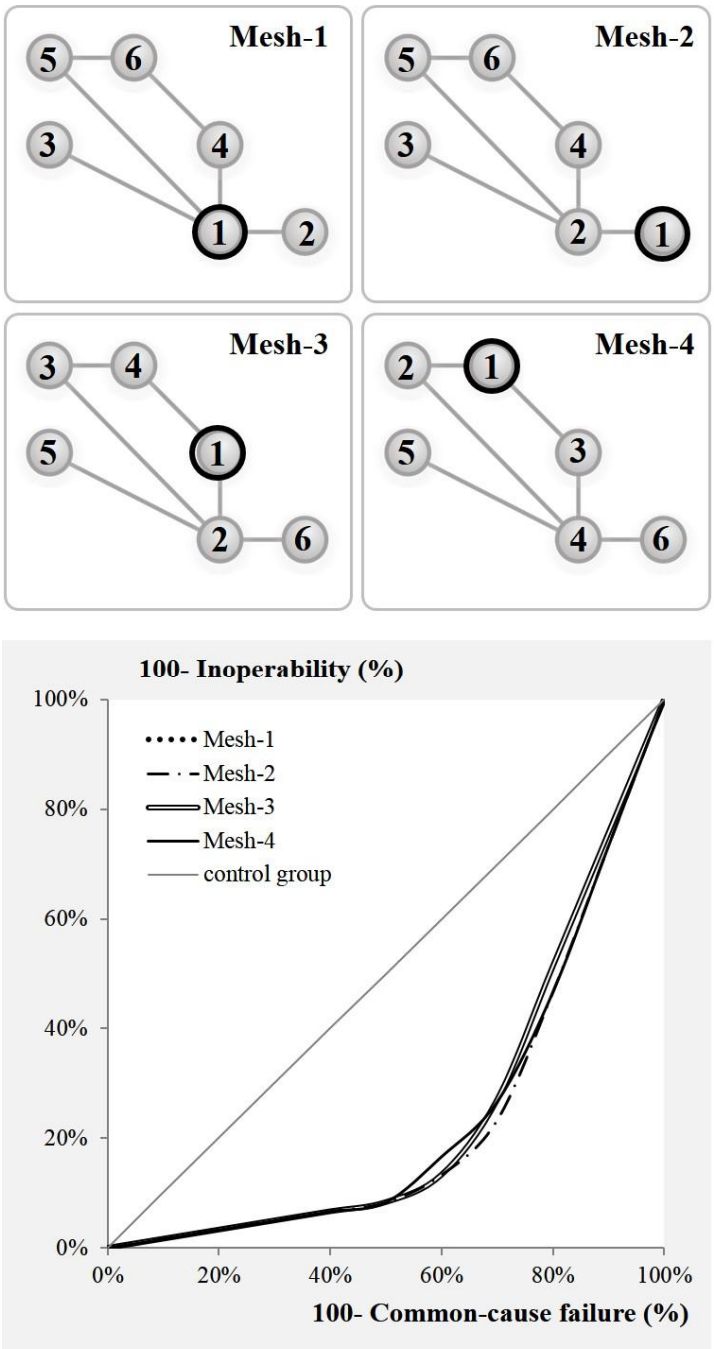

Figure 4-7. Inoperability considering the network arrangement

4.3 External Cascading Failure Estimation

4.3.1 Dependency between Different Lifelines

The aims of this BN model is to determine possible events driving uncertainty in cascading failures. In particular, this research assumed the dependency can exist between two sub-sectors from different lifeline system (Adachi and Ellingwood 2008). For example, electricity supply from distribution substation influencing the operation of the connected water treatment plant. Subsequently, a power plant may have to shut down if delivery of fuel is temporarily interrupted by transportation delays. In this regard, BN allows the prediction of the impact of possible failure event on the whole lifeline system performance.

The primary features of this BN model is that it integrates the IIM for compiling the conditional probability table (CPT). In addition, for the PGA-based damage assessment of a single-site component, lognormal fragility functions for the each component is applied. Then, based on the criteria of such functions, this research classified the scale of evidence variables at each failure state and transformed it to the functionality (i.e., the ability to supply the intended output). Details was already described in above section.

4.3.2 Sub-Model using Baeysian Network

BN variables and their sequences

In order to construct the BN diagram, the author firstly identified variables. In this research, the variables refer to the event causing seismic failure in power and potable water supply system including the following two types: a common-cause failure and a cascading failure. When an earthquake occurs, each component cannot perform their desired function by own destruction. For example, a power plant may not generate the required amount of electricity according to its original capacity or transmission substation may not transform the high-voltage electricity to lower level that can be used. Moreover, since each component needs diverse inputs to produce its objective output, they commonly suffer from cascading failure by a prolonged outage of input (e.g., power, water inflow from the upstream nodes and power distribution for operation). Thus, this research assumed that power and water supply system will fail if either the destruction of a component itself or the reduction of input for a component operation trigger. To summarize, in consequence of an earthquake, total 16 events given in Table 4-4 were identified as BN variables. Each variable has own state such as normal, slight, moderate, extensive and complete damage (detailed description in Table 4-5 and Chapter 3).

Table 4-4. Description and state of the BN variables

Variables		Description	State	Symbol
Earthquake intensity		Earthquake moment magnitude	Minor Major Critical	E_M
Power Supply	Common-cause failure	Destruction of power plant	ds1 to ds5	D_{PP}
		Destruction of transmission substation	ds1 to ds5	D_{TS}
		Destruction of distribution substation	ds1 to ds5	D_{DS}
	Cascading failure	Reduction of power inflow to transmission substation	True False	RPI_{TS}
		Reduction of power inflow to distribution substation	True False	RPI_{DS}
	Final failure event	Power distribution disruption	True False	PDD
Potable Water Supply	Common-cause failure	Destruction of water treatment plant	ds1 to ds5	D_{WTP}
		Destruction of storage tank	ds1 to ds5	D_{ST}
		Destruction of pumping station	ds1 to ds5	D_{PS}
	Cascading failure	Reduction of water inflow to storage tank	True False	RWI_{ST}
		Reduction of water inflow to pumping station	True False	RWI_{PS}
		Reduction of power distribution for water treatment plant operation	True False	RPO_{WTP}
		Reduction of power distribution for storage tank operation	True False	RPO_{ST}
		Reduction of power distribution for pumping station operation	True False	RPO_{PS}
	Final failure event	Water distribution disruption	True False	WDD

Table 4-5. Scale and functionality of the evidence variables

Variables	State	Median (g)	β	Scale	Functionality
D_{PP}	Slight	0.15	0.75	$D_{PP} < 0.15$	100%
	Moderate	0.36	0.65	$0.15 \leq D_{PP} < 0.4$	100%
	Extensive	0.77	0.65	$0.4 \leq D_{PP} < 0.8$	0%
	Complete	1.5	0.8	$0.8 \leq D_{PP}$	0%
D_{TS}	Slight	0.2	0.6	$D_{TS} < 0.33$	100%
	Moderate	0.28	0.5	$0.33 \leq D_{TS} < 0.67$	67%
	Extensive	0.39	0.4	$0.67 \leq D_{TS} < 1$	0%
	Complete	0.71	0.4	$D_{TS} = 1$	0%
D_{DS}	Slight	0.31	0.7	$D_{DS} < 0.33$	100%
	Moderate	0.37	0.55	$0.33 \leq D_{DS} < 0.67$	67%
	Extensive	0.46	0.45	$0.67 \leq D_{DS} < 1$	0%
	Complete	0.92	0.45	$D_{DS} = 1$	0%
D_{WTP}	Slight	0.37	0.4	$D_{WTP} < 0.08$	92%
	Moderate	0.52	0.4	$0.08 \leq D_{WTP} < 0.4$	60%
	Extensive	0.73	0.5	$0.4 \leq D_{WTP} < 0.77$	23%
	Complete	1.28	0.5	$0.77 \leq D_{WTP}$	0%
D_{ST}	Slight	0.18	0.6	$D_{ST} < 0.2$	80%
	Moderate	0.42	0.7	$0.2 \leq D_{ST} < 0.4$	60%
	Extensive	0.7	0.55	$0.4 \leq D_{ST} < 0.8$	20%
	Complete	1.04	0.6	$0.8 \leq D_{ST\,P}$	0%
D_{PS}	Slight	0.15	0.75	$D_{PS} < 0.05$	95%
	Moderate	0.36	0.65	$0.05 \leq D_{PS} < 0.38$	62%
	Extensive	0.66	0.65	$0.38 \leq D_{PS} < 0.8$	20%
	Complete	1.5	0.8	$0.8 \leq D_{PS}$	0%

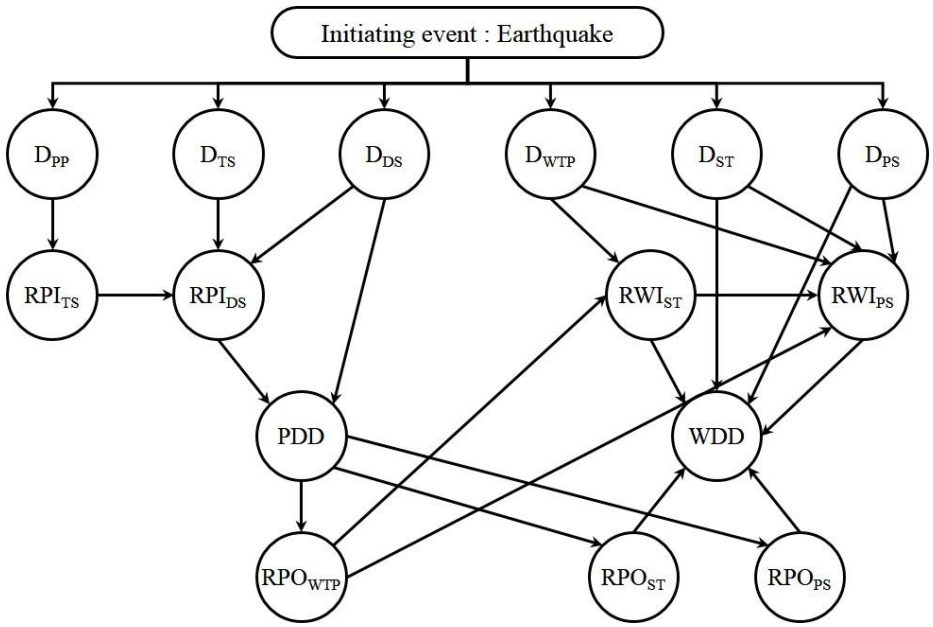

Figure 4-8. BN diagram of the power and water system failure

Fig. 4-8 shows a graphical diagram of the BN variables for this research. As mentioned above, an earthquake is an initiating event causing components' destruction (i.e., D_{PP} to D_{PS}). Such common-cause failure events become parent nodes of reduction of power or water inflow except the uppermost node of two systems (i.e., RPI_{TS}, RPI_{DS}, RWI_{ST}, and RWI_{PS}). In particular, destruction of some distribution node (i.e. D_{DS}, D_{ST}, and D_{PS}) can affect not only reduction of power inflow interconnected node (i.e., RPI_{DS}, and RWI_{PS}) but also service distribution disruption (i.e. PDD, and WDD). Power distribution disruption induces power shortage in water component operations. As this sequence, final water service disruptions depend on the state of six

different failure events.

4.4 Impact of Demand on the Lifelines' Performance

4.4.1 Demand Fluctuation due to Environmental Changes

Some researcher confirmed the effect of fear factors (Santos and Haimes 2003) that means psychological-induced irrational demand such as stocking up heavily food after disaster events. However, since the electricity and the potable water is not commodity, this research assumed that it cannot be stored for individual use. The proposed SD model is used to solve two main questions: (a) what kinds of failures occur during an earthquake? And how they propagate to a whole lifeline system? and (b) if each component reliability improves, can supply of the system meet demand? If not, how can a decision maker manage the imbalance between supply and demand?

4.4.2 Sub-Model using System Dynamics

Supply chain of lifeline system

To analyze the supply chain disruptions, this research considered two types of stocks: "*intermediary product*" and "*final product*". An intermediary product is the output from a component becoming the input to another component, while the final product is the last output of single lifeline system for delivering to end-user. One of the important variables in this model is "common-cause failure".

In the pre-disaster phase, the common-cause failure of all components equal zero (normal operation). In turn, since each component can operate properly to meet its designed capacity, there is the balance of expected output in supplier-side and usable output for customer-side (i.e., robustness also equals one). When an earthquake occurs, however, each component may have different common-cause failure as discussed in Chapter 4.1, the probability of exceeding thresholds for maintaining functions according to its location and structural properties. For this reasons, each component has a different level of available capacity, the amount of electricity generated (in power plant) or transmitted to lower-voltage (in transmission and distribution substation). This value is equal to the product of functionality (range 0 to 1) and designed capacity (megawatt per day). Moreover, if a component needs intermediate output from upper supply chain as its input, amount of delivery evaluates the production rate. For example, in the system consisting of two components A and B as shown in Fig. 4-9, the production rates in component B depends on its available capacity and delivery from component A. Thus, although the available capacity of component B is 50 unit per day, total daily production is lower than 50 unit if delivery from component A is not sufficient.

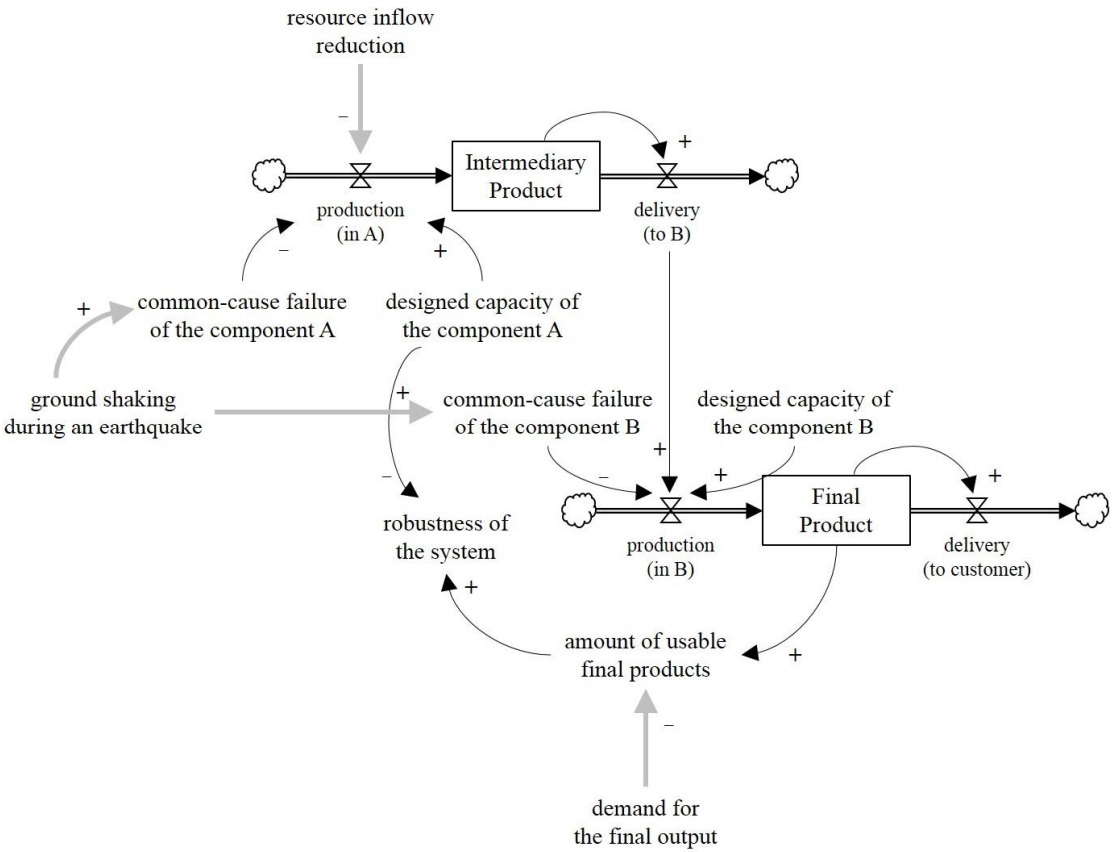

Figure 4-9. Supply chain of power system during an earthquake

Another two issues can arise in abnormal conditions is "*resource inflow reduction*" and change of "*demand for final output*." Resource inflow reduction is defined as the level of decrease in the number of materials for the system operation compared to normal condition with full resources. Since these materials come through others lifeline systems, this value is related to cascading failure. On the other hand, demand for final output is defined as the amount of service that would be used by customers. In general, lifeline service demand after an earthquake can be increased as a result of repair activities and decreased as a result of mandatory energy-saving policies. Thus it can be assured that this value relates to escalating failure. This paper assumes that there are full resources for normal operation and demand within the region is constant under pre-earthquake scenario.

Major causal loop diagrams

Before constructing an entire model for analyzing the robustness of seismic-damaged lifeline system, this research conducted a brief overview of two factors driving uncertainty robustness. Causal loop diagrams as shown in Fig. 4-10 and 4-11 show how they bring changes regarding the system behavior in the affected region.

(1) Resource inflow reduction

Each component needs diverse materials to produce its objective output. For example, thermal power plant produces electricity throughout burning a fossil fuel such as coal. In addition, since the plant converts heat energy into mechanical energy, cooling water that absorbs heat from the steam turbine is essential to maintain functions. Therefore, if the blackout during an earthquake event is prolonged, shortage of production factors may occur because such coal and cooling water are attained in consequence of the operation of other infrastructure systems and they required electricity to produce again (Krimgold et al. 2006). Moreover, despite a sufficient of coal and/or cooling water, delivery issues from transportation delays can lead power robustness decrease. In sum, reduction of the power robustness leads to malfunction of other infrastructure systems, and then it leads to an inability of supply for electricity production (reinforcing loop, “R1” in Fig. 4-10).

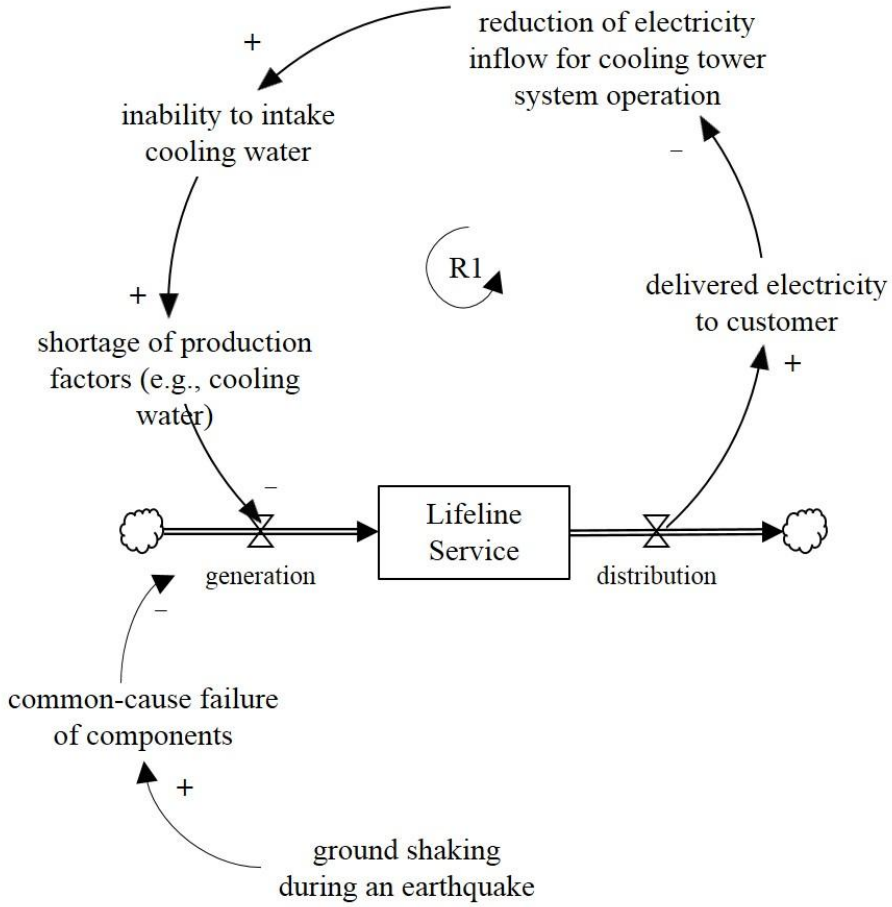

Figure 4-10. Loop for cascading failure in a power system

(2) Demand for final output

In the aftermath of an earthquake, repair activities are needed to restore the damaged lifeline systems including electric power system (Orabi et al. 2010). Subsequently, needs for the public services are provided by essential facilities for the safety of human lives such as medical station are commonly increased. In turn, much electronic equipment use and this will trigger an increase in the daily electricity usage (reinforcing loop, "R2" in Fig. 4-11).

However, the link between needs for repair and actual restoration actions is difficult to occur immediately because such works easily face resource constraints during a disaster phase. Meanwhile, in accordance with the Chida et al.'s works (2015), the daily maximum demand was reduced to a greater degree after 2011 Tohoku earthquake (e.g., average electricity usage during pre-earthquake phase is 14 GW while the after-earthquake phase is 12 GW).

This is because, when a reduction of supply enters into long-term problems, government implement power conservation policy at the public facilities. In Tohoku case, electric power company used rolling black-out strategy during two weeks in order to mitigate the imbalance between supply and demand. In addition, the campaign of "Setsuden" which is mandatory

energy saving movement at individual facilities to overcome power shortage leads to a decrease of daily electricity usage (balancing loops, "B1" in Fig. 4-11).

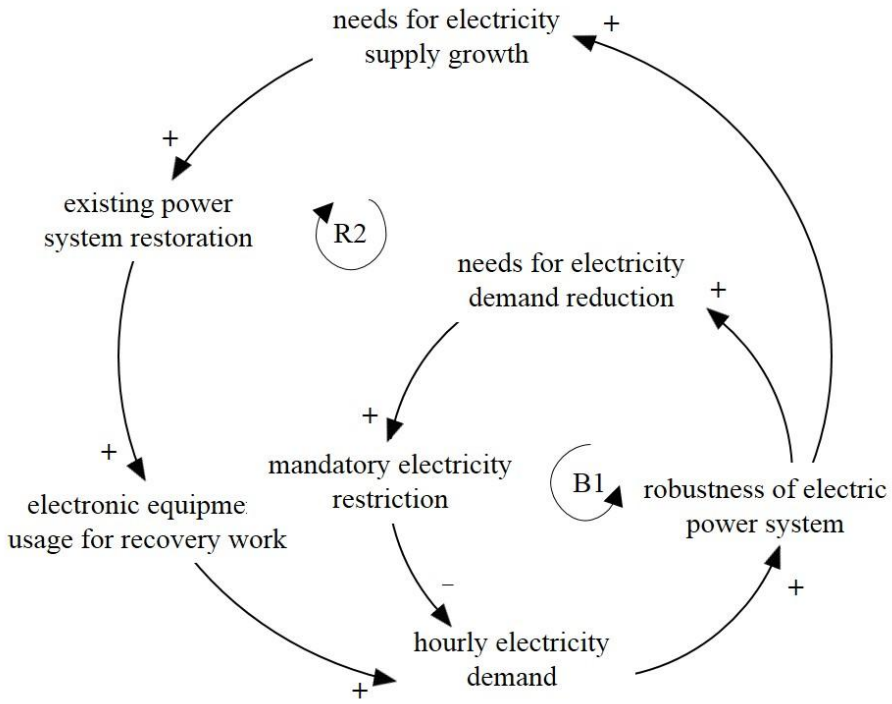

Figure 4-11. Loops for escalating failure in a power system

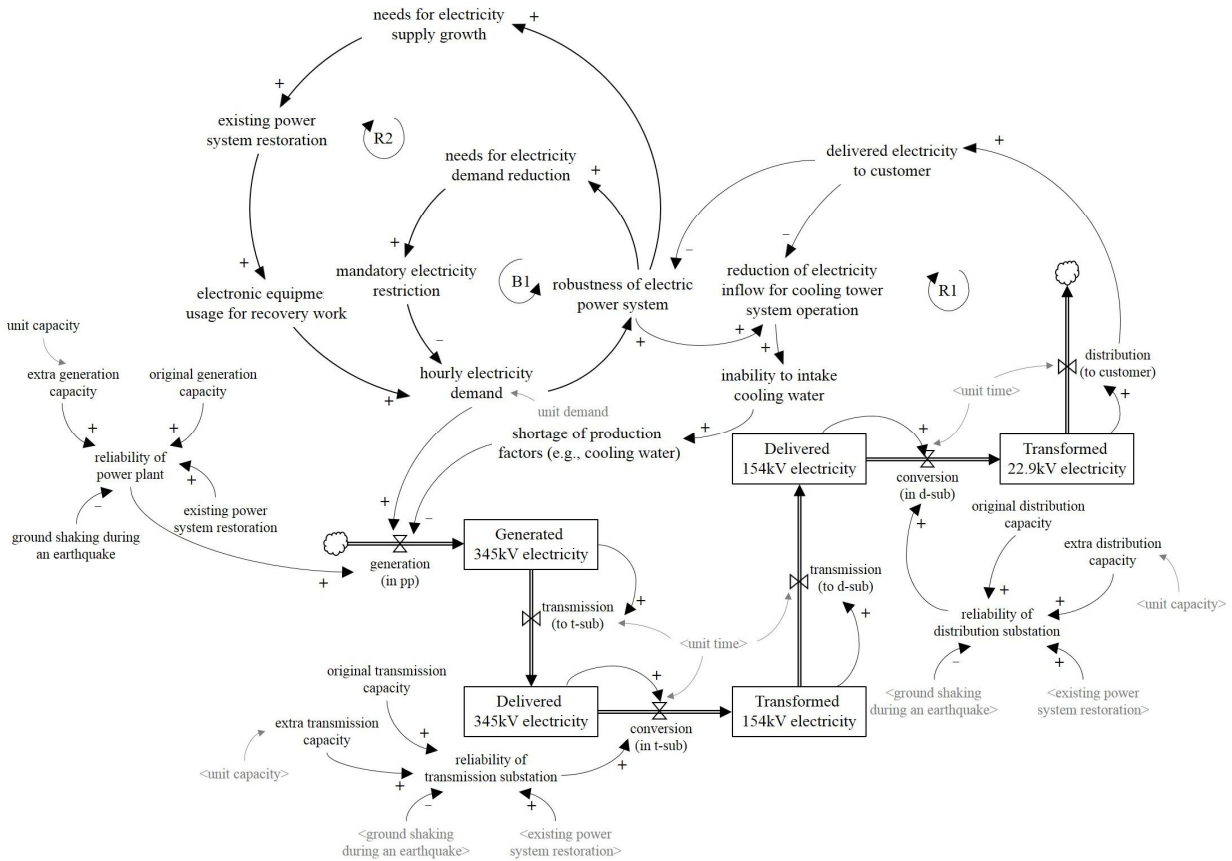

Figure 4-12. Entire SD model for seismic-damaged power system

4.5 Summary

In this chapter, this research developed robust estimation framework for the seismic-damaged lifeline system. Target of estimation was divided into ground motion, common-cause failure, cascading failure (in terms of internal and external dependency), and escalating failure. Table 4-6 summarized the consideration and methodologies for such estimating target.

Table 4-6. Target of estimation, consideration, and methodology

Target of estimation	Consideration	Methodology
Ground motion	• Attenuation according to distance	Empirical Model based on regression analysis of the historical earthquake (adaptation from previous research)
Common-cause failure	• Component type • Seismic fragility	
Cascading failure	• Internal dependency within a single lifeline system	Input-Output Inoperability Model
	• External dependency between different lifeline systems	Bayesian Network Model
Demand effect	• Supply chain of systems	System Dynamics Model

For example, ground motions recorded at particular site increases with earthquake intensity and is usually attenuated accordance with a distance from the epicenter. On the basis of these assumptions, this research selected the regression equation by Kanno et al (2006) as for the high seismicity regions such as Japan and Western America. Furthermore, for the low to moderate seismic regions including South Korea, this research presented the PGA estimation curves by averaging predicted data (Campbell 2003; Shahjouei and Pezeshk 2016; Park et al. 2001; Jo and Bagg 2003; Yun et al. 2009; Emolo et al. 2015). Then, this research applied the weight combination equation to transform the discrete functionality of each state as described in Chapter 3 to continuous variables. As a result, expected common-cause failure given PGA can be determined by functionality curves.

Dependency in a single system was regarded as the cause of internal cascading failure and was estimated using IIM. Specifically, a probabilistic approach for the quantification of correlation coefficients between two connected nodes was used. Furthermore, to determine which components offer a greater contribution to system performance, this research assumed the damage propagation in a system is same as the extent of internal cascading

failure[5].

A set of example networks with respect to network topologies: (a) line, (b) star, (c) tree, and (d) mesh was also analyzed and the results derived the network is vulnerable to the following order: (a)-(c)-(d)-(b). This is because a sequentially connected line network have more chance to damage propagation from upper-rank nodes. While a star network does not interconnect except the central node. However, since the star network is generally not used for the lifeline system, this research concludes that a mesh network is the most appropriate for configuration topologies. Moreover, this research also confirmed that relocation of components is helpful to manage and mitigate the lifeline system vulnerability in this chapter.

On the other hand, external dependency between two different systems was regarded as the cause of external cascading failure and was estimated using BN. In order to construct the BN diagram, this research assumed that power and water supply system will fail if either the destruction of a component itself or the reduction of input for a component operation trigger. Through the assumptions, total 16 events – (1) earthquake magnitude, (2) to (7) destruction of a component, (8) and (9) reduction of power inflow in a power supply system , (10) and (11) reduction of water inflow, (12) to (14)

[5] In general, this value is greater than zero after an earthquake.

reduction of power inflow in a water supply system, (15) power distribution disruption, and lastly (16) water distribution disruption. – were identified as BN variables.

In the final parts of this chapter, this research construct the SD model to analyze the impact of physical destruction, resource inflow reduction and, demand changes. For example, regarding the last variables, there were two types of CLD such as excessive demand (power system robustness reduction → requirements for supply growth → existing power system restoration → usage electronic equipment for recovery work → hourly electricity demand increasing → power system robustness reduction) and mandatory restriction (power system robustness reduction → necessity of demand reduction → mandatory electricity restriction → hourly electricity demand decreasing → power system robustness recovery).

The overall functionality assessment framework proposed in this research summarize in Fig. 4-13.

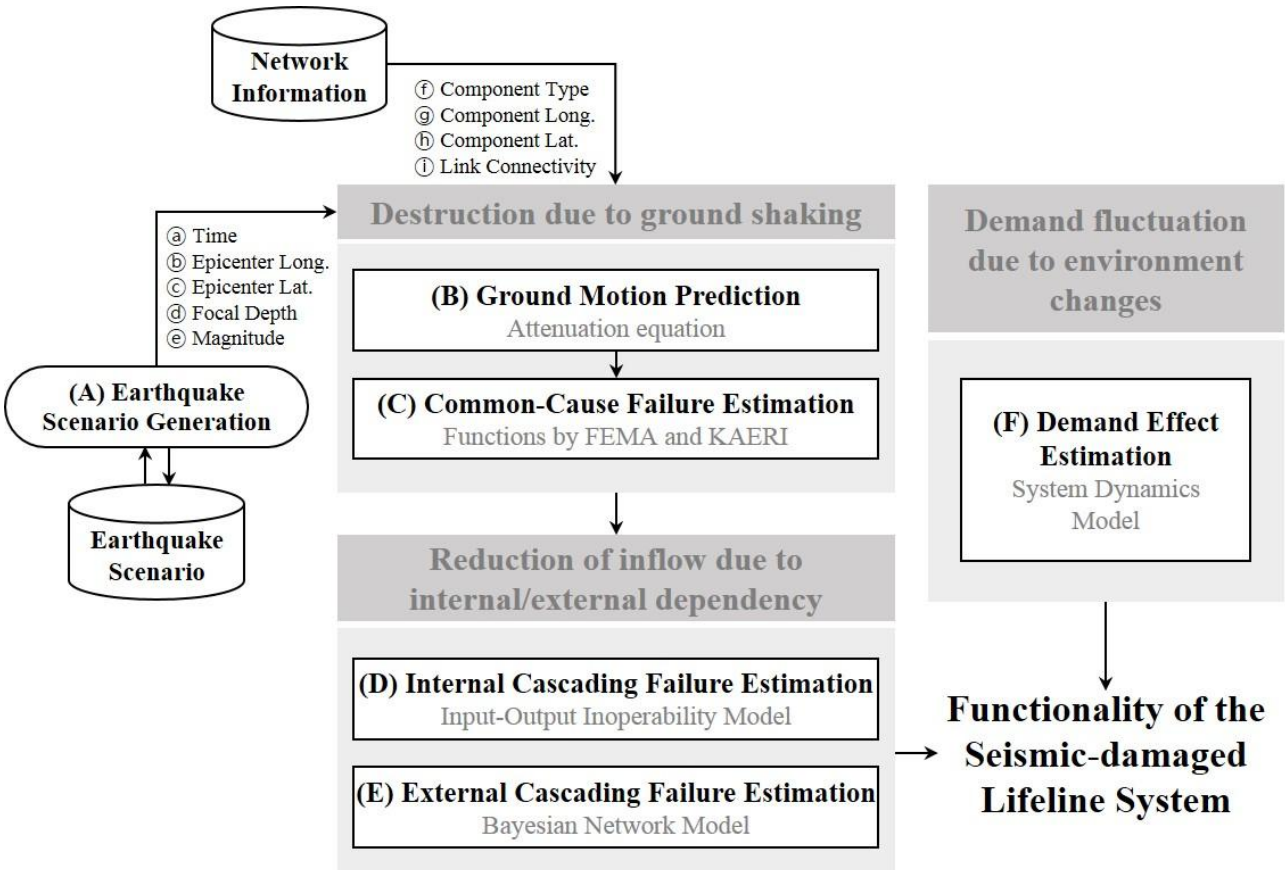

Figure 4-13. Summary of the functionality assessment framework

Chapter 5. Case Simulations

In order to examine the developed model's applicability in the real world setting, two historical events is selected as case networks: (a) the 2011 Tohoku earthquake in Japan for the high seismicity regions, and (b) the 2016 Gyeongju earthquake in South Korea for the low-moderate region. In this chapter, the comparison between the actual observed data and simulation results is conducted for validations of the proposed estimation approaches in Chapter 4.

Then, additional experiments are simulated for analyzing how the system withstands disruptions and how perturbation cascade to dependent components. In addition, from a perspective of the robustness, critical component indicates: (a) a component that highly covers supply itself or (b) a component that causes combinations of failures. The latter one, in particular, emerges when many components that complexly interdependent compose a network. Based on such assertions, this research identifies a critical component to maintain the original performance. In this chapter, analysis of demand changes is also discussed based on two cases.

5.1 Power Network at Tohoku in Japan

5.1.1 Case Outline

Description of the System

The electric power system in Tohoku region (Aomori, Akita and Iwate prefectures) in Japan is owned and managed by Tohoku electric power company (Tohoku-EPCO).

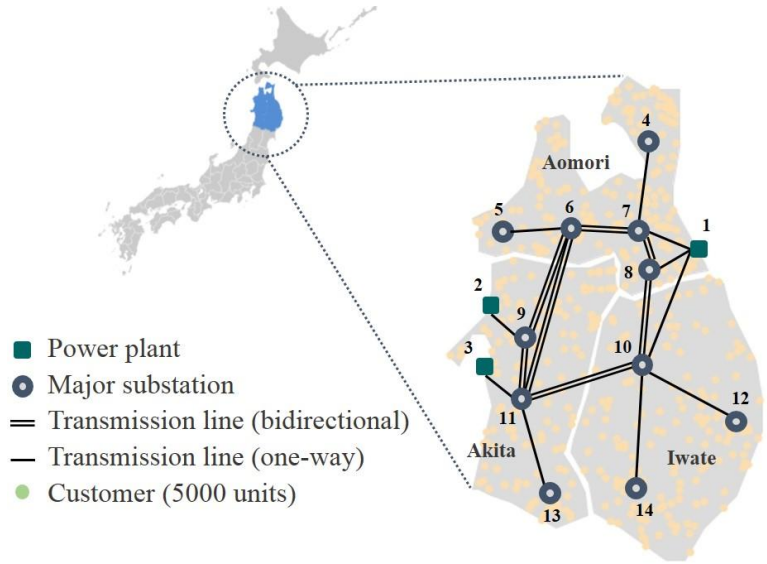

Figure 5-1. Simplified Tohoku electric power network

As shown in Fig. 5-1, this network, simplified from the Tohoku-EPCO annual report (2011), has 3 fossil power plants (indexed 1 to 3 in Fig.5-1). In addition, since the data of all substations in case region was cannot acquired,

this research handles only major 11 substations (indexed 4 to 14 in Fig.5-1) connected by 24 bidirectional or one-way transmission lines and assumes that some of the substation can transmit and distribute, while others can only perform distribution activities. Additional descriptions of the attribute values of the nodes and links in the network components are present in Table 5-1 and Table 5-2.

Table 5-1. Nodes in the Tohoku electric network

Index	Node	Type	Capacity	Coordinate	
				Longitude	Latitude
1	Power Generator	EPP3	1100MW	141.49	40.71
2			1200MW	139.99	40.19
3			1600MW	140.05	39.79
4	Power Deliverer	ESS3	270 households	141.19	41.31
5			150 households	140.14	40.78
6			245 households	140.71	40.77
7			165 households	141.17	40.78
8			210 households	141.36	40.53
9			210 households	140.04	40.20
10			225 households	141.18	39.90
11			115 households	140.08	39.81
12			230 households	141.88	39.62
13			265 households	140.53	39.21
14			250 households	141.14	39.14

* Each generator operates 7 hours a day
** Electricity use of a household is randomly distributed with mean value 10kWh/day

Table 5-2. Links in the Tohoku electric network

Link ID	Node		Length (m)	Link ID	Node		Length (m)
	Start	Finish			Start	Finish	
a	1	7	27,922	m	8	7	32,317
b	1	8	23,144	n	8	10	71,020
c	1	10	93,452	o	9	6	85,942
d	2	9	4,063	p	9	11	42,885
e	3	11	3,815	q	10	8	71,020
f	6	5	48,103	r	10	11	93,768
g	6	7	38,879	s	10	12	67,587
h	6	9	85,942	t	10	14	85,131
i	6	11	119,511	u	11	6	119,511
j	7	4	58,234	v	11	9	42,885
k	7	6	38,879	w	11	10	93,768
l	7	8	32,317	x	11	13	76,875

5.1.2 Comparison with the Simulation Result

Test of the Input-Output Inoperability Model

This research was considered the 2011 M 9.0 earthquake that occurred offshore on the Sanriku coast (142.37E, 38.82N), the coastal areas along the Tohoku region. When the simulation began on March 11, the model triggered a single seismic event with magnitude 9.0 and depth of earthquake center about 24km. Then operational/damage states of power generators and deliverers were immediately determined by the PGA value of the region where they reside under the earthquake scenario. Consequently, customers'

blackout started in the Iwate prefecture near the epicenter and rippled across the region to the part of the Tohoku region.

Tohoku-EPCO reported that about 2.04 million households (89.0% of total households) in Aomori, Akita and Iwate prefectures suffered from a temporary power blackout; and the electricity sector in these regions were restored within 7 days after the disaster event (97% restored) (Kazama and Noda 2012). To examine how well proposed IIM fits such reported data, this research compares estimated simulation results and actual observed data focused on the number of power outage households. Detailed model test results are summarized as schematic diagrams (a circle highlighted in red represents about 5,000 blackout households) in Fig. 5-2 and a comparison graph in Fig. 5-3. Due to the uncertainty from input data and the natural hazard itself, it is challenging to predict an exact amount of affected households for a given situation. However, general behavior patterns of a power outage ratio (calculated as the ratio of blackout households to total households) and restoration progress correspond to actual data patterns. For example, there are approximately 1.92 million households (82.3% of total households) subjected to blackout the day after earthquake, and the number of affected households decreased up to 0.304 million (87% restored) by three days after the earthquake and to 0.047 million (98% restored) by 8 days after the earthquake. Although these results are not perfect, this is an acceptable

representation of the real world from the perspective of the intended use of the model (i.e., component identification, system performance quantification, and damage propagation analysis).

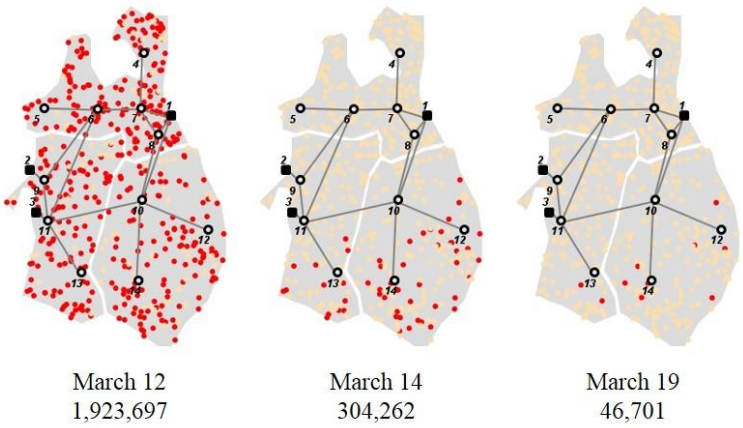

Figure 5-2. Schematic diagrams of blackout households

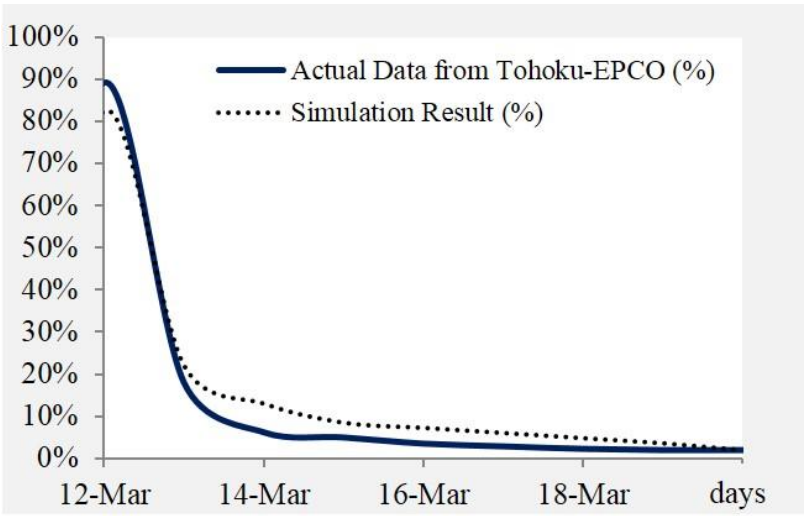

Figure 5-3. Comparative analysis of simulation results.

5.1.3 Additional Experiment

Robustness Estimation

Table 5-3 reports an estimated PGA and both the component and system level functionality of each component after the 2011 Tohoku Earthquake. In the case of a studied network, three of generator nodes automatically stopped operation right after the earthquake and restarted soon with about half of their original functionality.

Table 5-3. Functionality after the 2011 Tohoku earthquake

Node Index	PGA (g)	Static Functionality (%)	Dynamic Functionality (%)	State
1	0.144	56.1	56.1	Emergency Operation
2	0.125	62.7	62.7	Emergency Operation
3	0.171	48.4	48.4	Emergency Operation
4	0.075	93.3	12.9	Extensive Damage
5	0.085	90.7	0	Complete Damage
6	0.108	83.6	4.6	Extensive Damage
7	0.124	77.9	19.6	Extensive Damage
8	0.168	62.6	2.9	Extensive Damage
9	0.128	76.5	33.4	Moderate Damage
10	0.288	30.4	0	Complete Damage
11	0.172	60.9	6.3	Extensive Damage
12	0.487	9.9	0	Complete Damage
13	0.339	22.0	0	Complete Damage
14	0.547	7.5	0	Complete Damage

It should be noted that component and system level functionality of a generator node are the same values, while, regarding deliver nodes (indexed 4

to 14), system level functionality falls short of static functionality. This statement means that damage propagation occurs at several subordinated nodes. In particular, fifth node has a great deal of difference between two types of functionality. This is because: (a) it is far from the epicenter and thus its structural destruction is slight, however (b) supply reduction from upper-connected node (e.g., indexed 1, 7 and 6) simultaneously accumulate since it is located at the end of the network.

Then, this research quantifies the damage propagation in a case earthquake scenario through Eq. 23; and same quantification assessment is conducted at all ranges of static functionality as described in Fig. 5-4. This figure examines the relationship between two types of functionality in Tohoku network and the solid lines indicate the control group, which assumes that there is no damage propagation. In the control group, for example, 40% of the average Static functionality means 40% of that of the Dynamic. Thus, a difference of y-axis values between the control group and Tohoku region means correlation coefficients induced damage propagation. This gap gradually increases until the Static functionality reaches about 50% and then begins to decrease. In particular, there is 23.3% of unforeseen damage propagation in the whole network after the case earthquake (the average static functionality is about 53.9%, whereas the average dynamic functionality is about 30.6%).

These findings are useful information that the person (e.g., homeowner, service staff of the power station, and emergency management officer) who has a concern on the Tohoku electricity sector have to expect over 20% additional functional loss when the average component functionality shows from 40% to 66% (See the difference bar at bottom of Fig. 5-4).

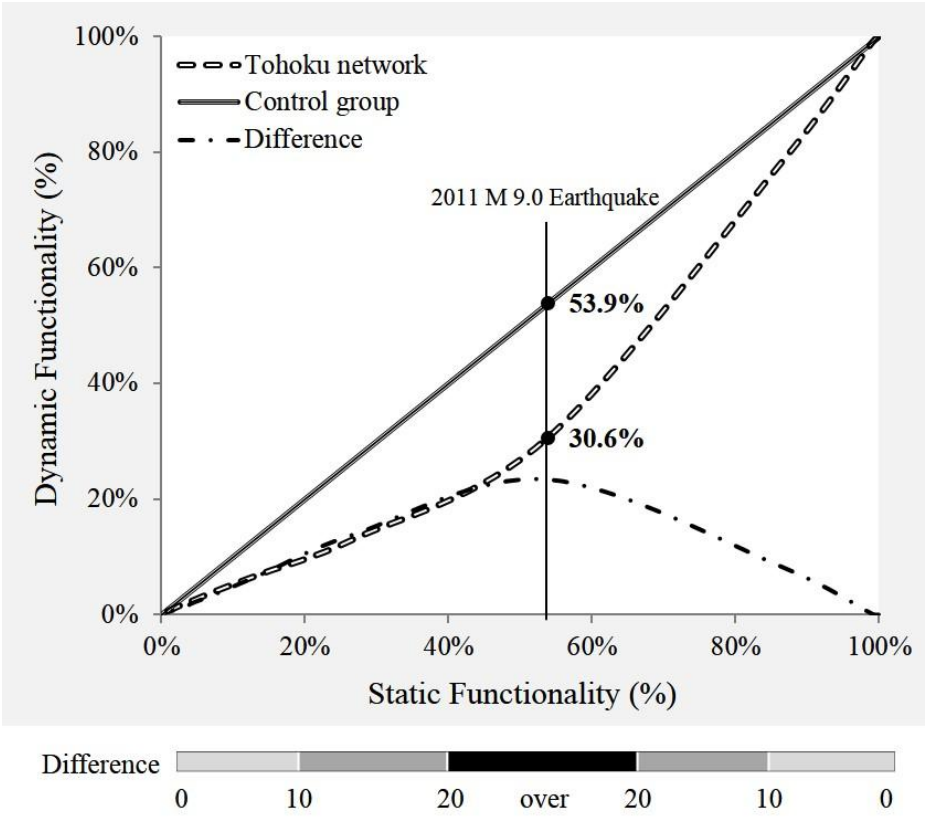

Figure 5-4. Relationship between two types of functionality

Impact of Demand Changes

Another feature that of the model presented here is its ability to observe the demand effect on network performance. In particular, to determine the impact of changes in electricity usage, this research considers the concept of "Setsuden" which is mandatory energy saving movement to overcome power shortage after the 2011 Tohoku earthquake. More specifically, the authors assume that daily electricity usage in Iwate region is reduced 10%, 25%, and 50% respectively when compared to original scenario (see Table 5-4). This, in turn, leads to change in the expression pattern of damage propagation at certain components that are in Iwate region (node 10, 12, 14) or near the region (node 8, 13).

Table 5-4. Changes in electricity usage

Simulation Cases	Electricity usage in a day (kWh)			
	Aomori	Akita	Iwate	Total
Original Scenario	8900	6700	7750	23,350
Setsuden 10%	8900	6700	6980	22,580
Setsuden 25%	8900	6700	5810	21,410
Setsuden 50%	8900	6700	3880	19,480

Figure 5-5 offers the result of sensitivity analysis to evaluate how reduced demand affect the damage propagation regarding two agents. The fact that the maximum value in each graph remains approximately constant indicates that degree of damage propagation varies over supply-side (e.g., network topological structure) not demand-side. On the other hand, initial points of propagation occurrence in two example node move to the right side as the Setsuden rate increase. This pattern change is more clarified in node 10 because it generally covers electricity demand in Iwate region and thus there is a surplus that can be used for the preparation of supply malfunction. Therefore, through the results of this sensitivity analysis, it is confirmed that the demand-side efforts to conserve electricity usage can be regarded as reinforcement of network robustness in post-disaster case.

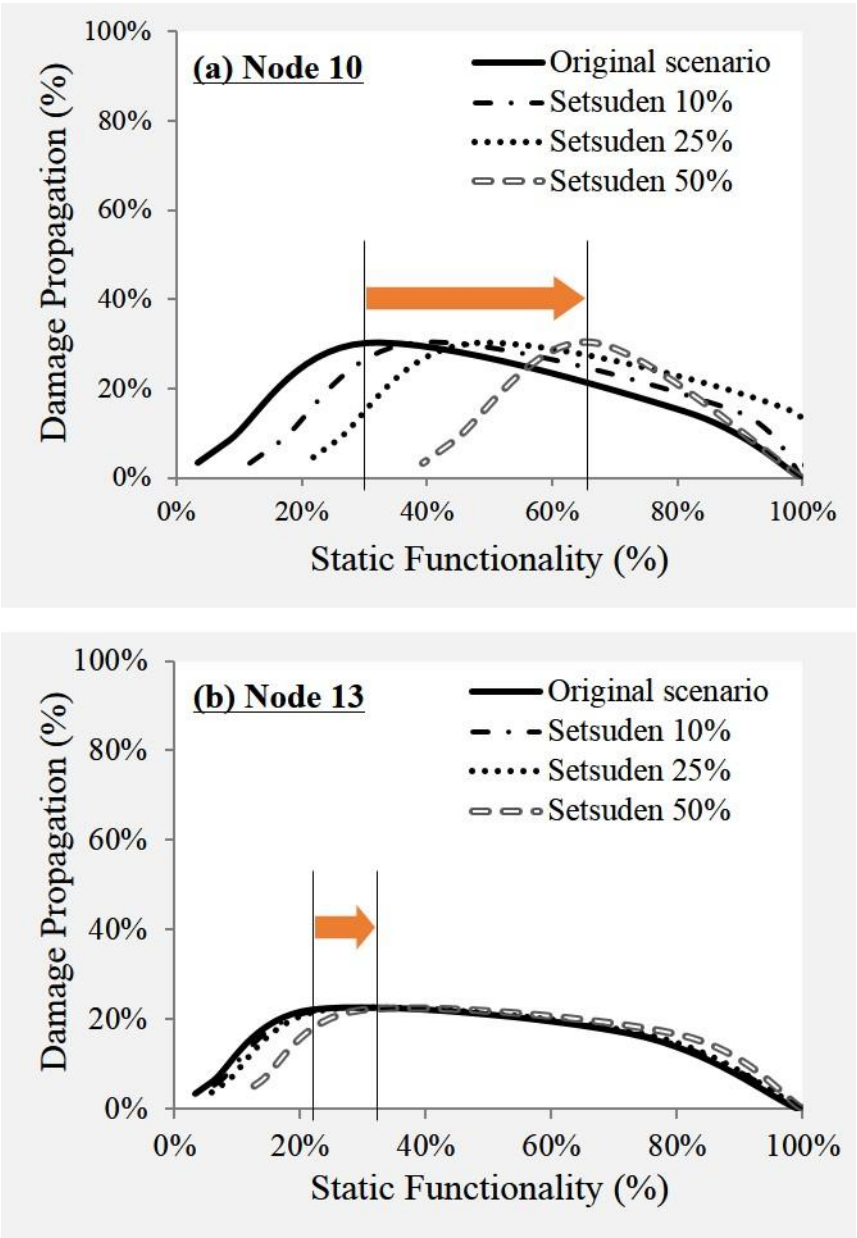

Figure 5-5. Changes in the expression of damage propagation

5.2 Power and Water Network at Daegu in South Korea

5.2.1 Case Outline

Description of the System

This research took the power and potable water supply system located Daegu city in South Korea as case network. Since the power system discussed here do not include power plants, this research assumed that four source nodes (transmission substations, namely P1 to P4 in Fig. 5-6) receive electricity from power plants at outside the city and transmit it to the rest 29 nodes (distribution substations, namely P5 to P33 in Fig. 5-6). Therefore, D_{PP} and RPI_{TS} in Fig.4-8 equal zero.

Analogously, the potable water system consist of 4 source nodes (water treatment plants, namely W1 to W4 in Fig. 5-6) and 20 distribution nodes (storage tanks and pumping stations, namely W5 to W24). This research also assumed that reduction of power inflow from adjacent distribution substations only influences the state of four water treatment plants, not other two types of components with relatively low electricity usage. In this regard, RPOST and RPOPS in Fig.4-9 also equal zero. Details of the nodes in the power and potable water supply network are present in Table 5-5 and Table 5-6.

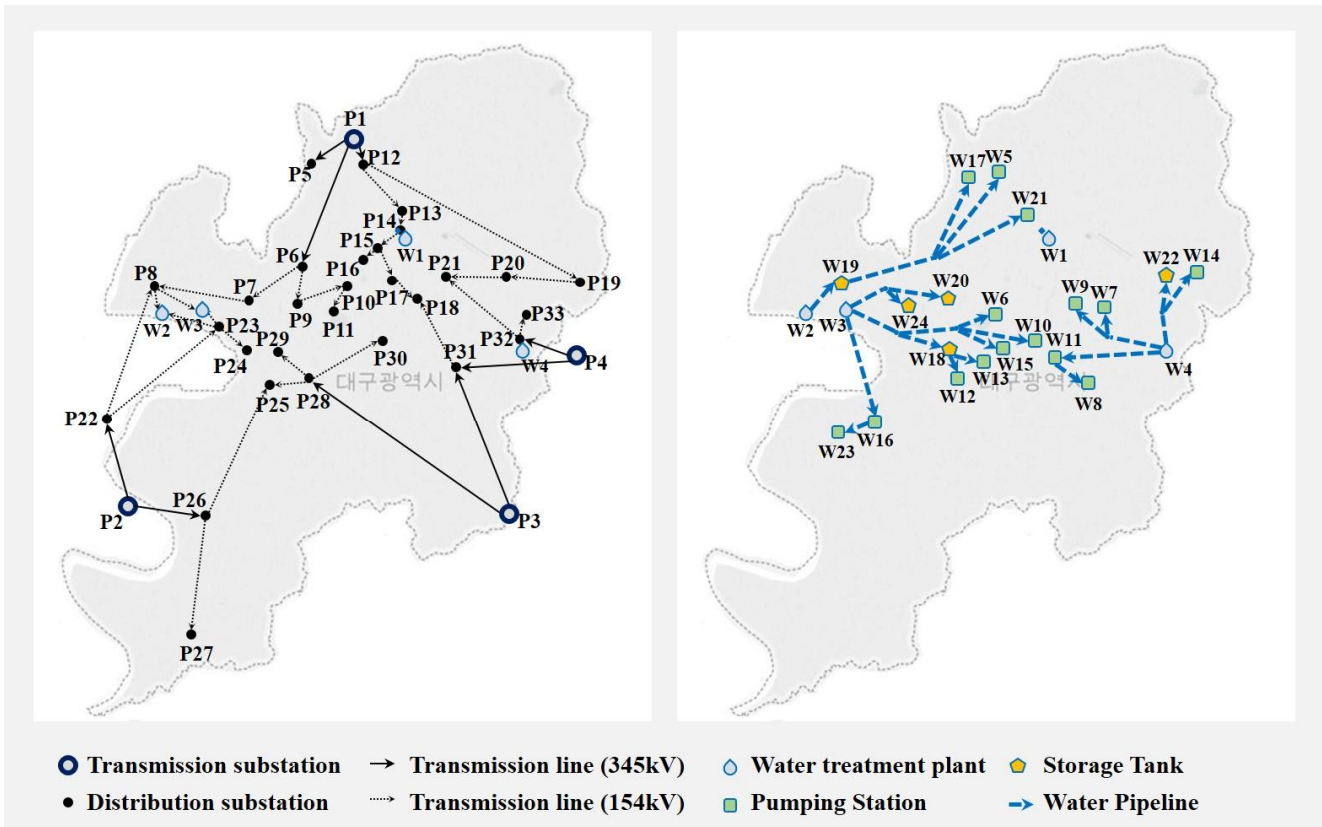

Figure 5-6. Layout of the case lifeline systems in Daegu city

Table 5-5. Nodes in the Daegu electric network

Index	Node	Type	Capacity (households)	Coordinate	
				Longitude	Latitude
1	Power Deliverer	ESS3	409,400	128.5741	35.9561
2			181,800	128.4049	35.7355
3			252,900	128.6889	35.7311
4			149,900	128.7387	35.8283
5			35,000	128.5419	35.9424
6		ESS1	47,000	128.5359	35.8806
7			28,000	128.4958	35.8607
8			16,000	128.4252	35.8703
9			24,000	128.5324	35.8586
10			19,000	128.5689	35.8694
11			19,000	128.5586	35.8540
12			52,000	128.5751	35.9454
13			49,000	128.6107	35.9141
14			11,000	128.6086	35.9034
15			6,000	128.5913	35.8925
16			15,000	128.5839	35.8869
17			20,000	128.6014	35.8728
18			21,000	128.6208	35.8617
19			26,000	128.7411	35.8717
20			36,000	128.6871	35.8747
21			29,000	128.6416	35.8751
22			14,000	128.3894	35.7883
23			46,000	128.4734	35.8452
24			38,000	128.4935	35.8312
25	Power Deliverer	ESS1	43,000	128.5105	35.8102
26			30,000	128.4626	35.7296
27			21,000	128.4532	35.6582
28			81,000	128.5404	35.8141
29			44,000	128.5177	35.8299
30			70,000	128.5950	35.8369
31			75,000	128.6497	35.8203
32			47,000	128.6975	35.8367
33			32,000	128.7007	35.8519
Total			994,000	-	-

Table 5-6. Nodes in the Daegu potable-water network

Index	Node	Type	Capacity (households)	Coordinate	
				Longitude	Latitude
1	Water Generator	PWT3	37,300	128.6042	35.9016
2			138,000	128.4249	35.8554
3			538,600	128.4503	35.8587
4			280,100	128.6968	35.8309
5	Water Deliverer	PPP1	45,600	128.5688	35.9390
6			66,800	128.5611	35.8540
7			63,600	128.6483	35.8566
8			49,500	128.6253	35.8244
9			60,700	128.6313	35.8613
10			45,700	128.5998	35.8414
11			60,000	128.6081	35.8288
12			106,700	128.5447	35.8184
13			75,000	128.5490	35.8305
14			16,900	128.7172	35.8830
15			69,100	128.5698	35.8385
16			28,300	128.4739	35.7884
17			44,500	128.5476	35.9340
18		PST2	29,500	128.5396	35.8312
19			108,500	128.4506	35.8731
20			92,100	128.5320	35.8649
21		PPP1	18,400	128.5917	35.9148
22		PST2	29,400	128.6985	35.8782
23		PPP1	28,300	128.4497	35.7815
24		PST2	26,600	128.5011	35.8608
Total			994,000	-	-

5.2.2 Comparison with the Simulation Result

Test of the Bayesian Network Model

In the case of the 2016 Gyeongju earthquake, there was not much seismic-damage in terms of common-cause failure. For this reason, this research considered an earthquake that occurred at the right side of the case region (128.882E, 35.78N) with magnitude 6.0 (minor), 6.4 (major) and 6.8 (critical). Then, to verify whether the behavior of the proposed BN model is consistent and intended, a set of test given two extreme-condition is conducted. First set of extreme-condition is "PDD=TRUE" and "WDD=TRUE" for representing the power-outage and the potable-water outage. On the other hand second set of extreme-condition is "PDD=FALSE" and "WDD=FALSE" for analysis of restoration efficiency.

Table 5-7 indicates that the consequence of entirely power-outage, most of the nodes also fails except the "RPI_{DS} =TRUE" that located the upper level of PDD. However, the probability of "RPI_{DS} =TRUE" increased, and it can be assured that distribution substations in extensive damage state. Whereas, the fully recover of water distribution lead to the probability of all other nodes to be zero, because WDD is an end node of the BN model.

Table 5-7. Extreme condition test of the BN model

Nodes (TRUE)	Extreme 1		Extreme 2	
	PDD=TRUE	WDD=TRUE	PDD=FALSE	WDD=FALSE
RPI_{DS}	74.3	53.6	0	0
RWI_{ST}	100	75.8	3.83	0
RWI_{PS}	100	90.1	18.4	0
RPO_{WTP}	100	72	0	0
PDD	100	72	0	0
WDD	100	100	24.2	0

Table 5-7 indicates that the consequence of entirely power-outage, most of the nodes also fails except the "RPI_{DS} =TRUE" that located the upper level of PDD. However, the probability of "RPI_{DS} =TRUE" increased, and it can be assured that distribution substations in extensive damage state. Whereas, the fully recover of water distribution lead to the probability of all other nodes to be zero, because WDD is an end node of the BN model.

5.2.3 Additional Experiment

Common-cause failure and dependency

Fig. 5-7 shows the average common-cause failure of five types of components (D_{TS}, D_{DS}, D_{WTP}, D_{ST} and D_{PS} in Fig. 4-9) for the simulated earthquake scenarios. Such average value was determined by each components' functionality (described in Eq. 19) and demand distribution. Regarding this result, there is around 10% physical destruction except transmission substations that includes P4 nearest the epicenter. However, as mentioned earlier, a destruction of transmission substations can trigger cascading failure of other components in both the power and the water system. In addition, the extent of cascading varies with the dependency between components. For example, as shown in Fig. 5-7, some components in the power system such as P8, P18, P21, P25 and P31 has two or more different electricity supply path from source nodes. In detail, P21 has two paths, $PATH_{1\text{-}21}$ = {1, 12, 19, 20, 21} and $PATH_{4\text{-}21}$ = {4, 32, 21}, that shortest length is 27,221km and 10,433km respectively. Thus, a malfunction of the P4 plays a vital role rather than other 3 source nodes in terms of the reduction of power inflow (RPI_{DS} in Fig. 4-9) to the P21. In the same way, because electricity for operation of W4 also depends P4, series of failure propagation P4 to W4 (RPO_{WTP} in Fig. 4-9) and W4 to its connected components (RWI_{ST} and RWI_{PS} in Fig. 4-9) can occur in the water system.

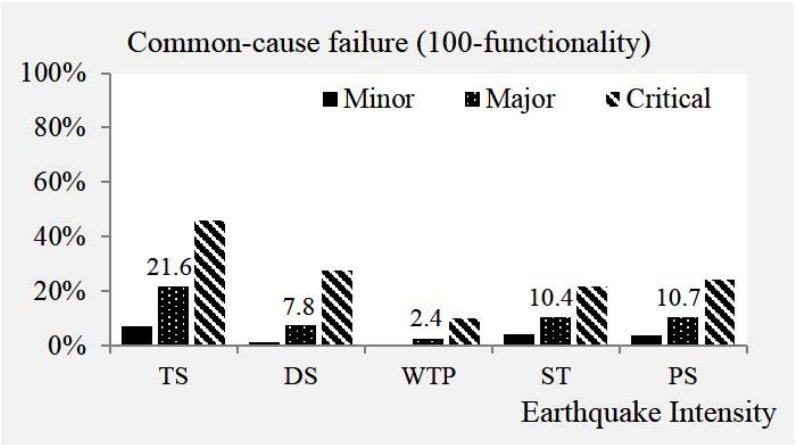

Figure 5-7. Common-cause failure of each component types

As such, the authors quantified the conditional probability of each BN variables given common-cause failure using IIM. Table 5-8, one of the example CPT, reports the probability distribution of WDD considered the states of RWIST, RWIPS, DST and DPS, {True, False} or {None, Slight, Moderate, Extensive, Complete}. This CPT for the multistate variables has total 100 rows. Firstly, if "RWIST = RWIPS = TRUE", there is no water inflow to storage tanks and pumping stations due to power outage at WTP or physical damage issues of water components. Thus, the probability of WDD is 100% regardless of the state of DST and DPS. In the case of "RWIST = TRUE" and "RWIPS = FALSE", all of storage tanks (e.g., W18 to W20, W22, W24 in Fig. 5-6) and some of pumping stations that is connected a storage tank (e.g., W5, W12, W13, W17, W21 in Fig. 5-6) cannot supply potable

water. For this reasons, the minimum value of WDD is 50.81% (the ratio of supply from the rest of 10 water distribution components) only for "DPS = NONE". On the other hand, if "RWIST = FALSE" and "RWIPS = TRUE", the minimum value of WDD is 78.38% (the ratio of supply from the storage tanks) only for "DST = NONE" because all of pumping stations are in trouble. When the last combinations, "RWIST = RWIPS = False", conditional probability of WDD varies 0% to 100% depending on the common-cause failure of storage tanks and pumping stations.

Table 5-8. Conditional probability table for the childe node WDD

RWI_{ST}	RWI_{PS}	D_{ST}	D_{PS}	WDD	
				True	False
True	True	None	None	100	0
True	True	None	Slight	100	0
True	True	None	Moderate	100	0
True	True	None	Extensive	100	0
True	True	None	Complete	100	0
⋮	⋮	⋮	⋮	⋮	⋮
True	False	None	None	50.81	49.19
True	False	None	Slight	53.27	46.73
⋮	⋮	⋮	⋮	⋮	⋮
False	True	None	None	78.38	21.62
False	True	None	Slight	78.38	21.62
⋮	⋮	⋮	⋮	⋮	⋮
False	False	None	None	0	100

⋮	⋮	⋮	⋮	⋮	⋮
False	False	Complete	Complete	100	0

Robustness Estimation

After the determining the probability distribution of parent nodes and CPT, the probability of power and water distribution disruptions can be derived as follows:

$$\begin{aligned} P(\mathrm{PDD}) &= P(\mathrm{E_M}, \mathrm{D_{TS}}, \mathrm{D_{DS}}, \mathrm{RPI_{DS}}) \\ &= P(\mathrm{D_{TS}}|\mathrm{E_M}) \times P(\mathrm{D_{DS}}|\mathrm{E_M}) \times P(\mathrm{RPI_{DS}}|\mathrm{D_{TS}}, \mathrm{D_{DS}}) \end{aligned} \quad (24)$$

$$\begin{aligned} P(\mathrm{WDD}) &= P(\mathrm{E_M}, \mathrm{D_{WTP}}, \mathrm{D_{ST}}, \mathrm{D_{PS}}, \mathrm{RPO_{WTP}}, \mathrm{RWI_{ST}}, \mathrm{RWI_{PS}}) \\ &= P(\mathrm{D_{WTP}}|\mathrm{E_M}) \times P(\mathrm{D_{ST}}|\mathrm{E_M}) \times P(\mathrm{D_{PS}}|\mathrm{E_M}) \\ &\quad \times P(\mathrm{RPO_{WTP}}|\mathrm{PDD}) \times P(\mathrm{RWI_{ST}}|\mathrm{D_{WTP}}, \mathrm{RPO_{WTP}}) \\ &\quad \times P(\mathrm{RWI_{PS}}|\mathrm{D_{WTP}}, \mathrm{D_{ST}}, \mathrm{D_{PS}}, \mathrm{RWI_{ST}}, \mathrm{RPO_{WTP}}) \end{aligned} \quad (25)$$

For the sake of convenience of calculations, the authors have been run the BN model in NETICA software and Fig. 5-8 presents the prior probability distribution of the BN variables for the case systems. As shown in the figure, transmission substations and pumping stations are relatively vulnerable to the earthquake. These results also demonstrate that the operational state of WTP in the Daegu city was impacted by the availability of electricity rather than its physical damage. In addition, with respect to the performance of the water

system, the reduction of water inflow to pumping stations is key variables.

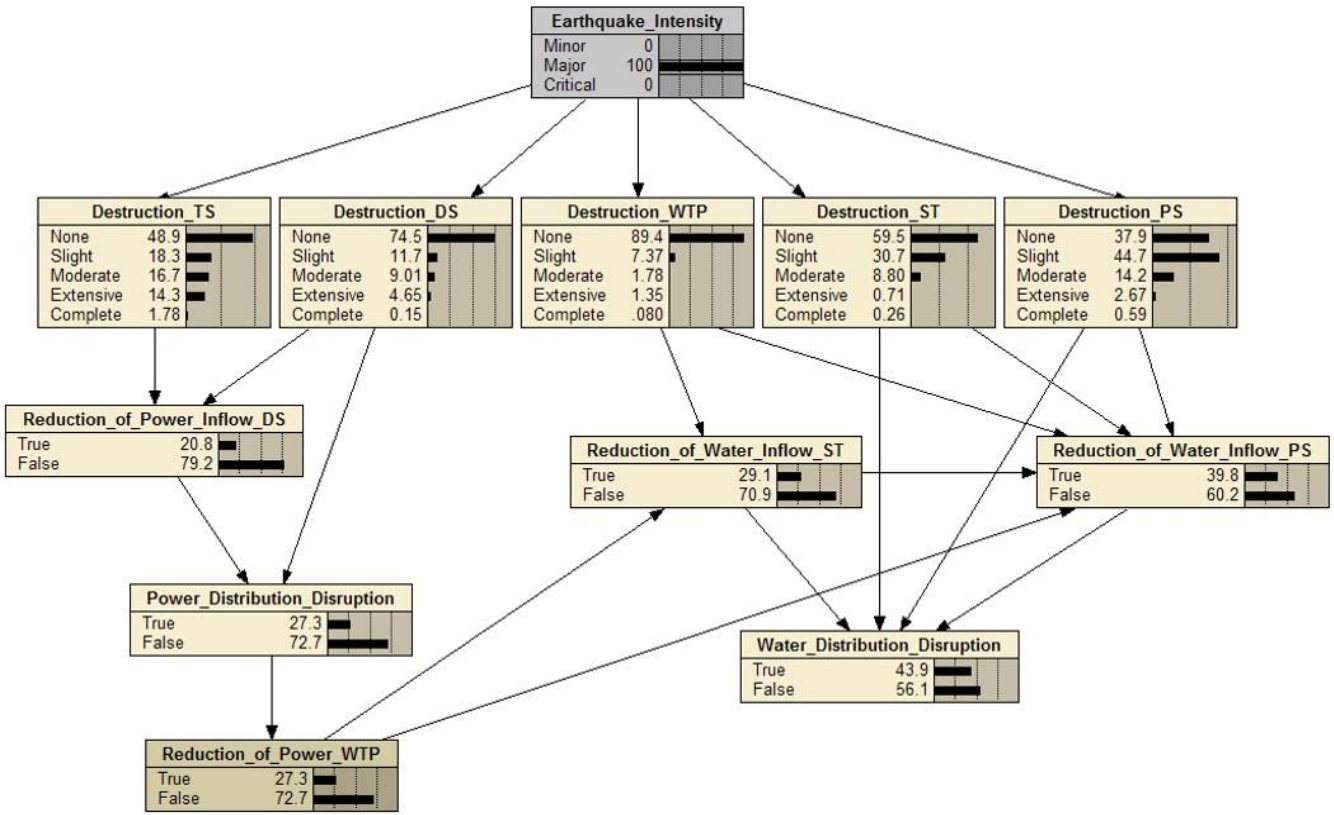

Figure 5-8. The prior probability distribution of the BN model

Fig. 5-9 summarizes the relationship between the common-cause failures and the final service distribution disruptions incorporating cascading failures with the earthquake of magnitude 6.0 to 7.0. For example, when the magnitude 6.4 earthquake occurred, power system expected functionality was about 90.3% if only considering destruction; however more practical functionality was 72.7% because the reduction of power inflow arouses. Similarly, water system functionality reduced up to 56.1% from 86.5% by the effect of the reduction of water inflow and reduction of power distribution. In other words, hatched areas in Fig. 5-9 indicated the extent of the cascading failure (in particular, (a) and (b) for the major intensity earthquake.)

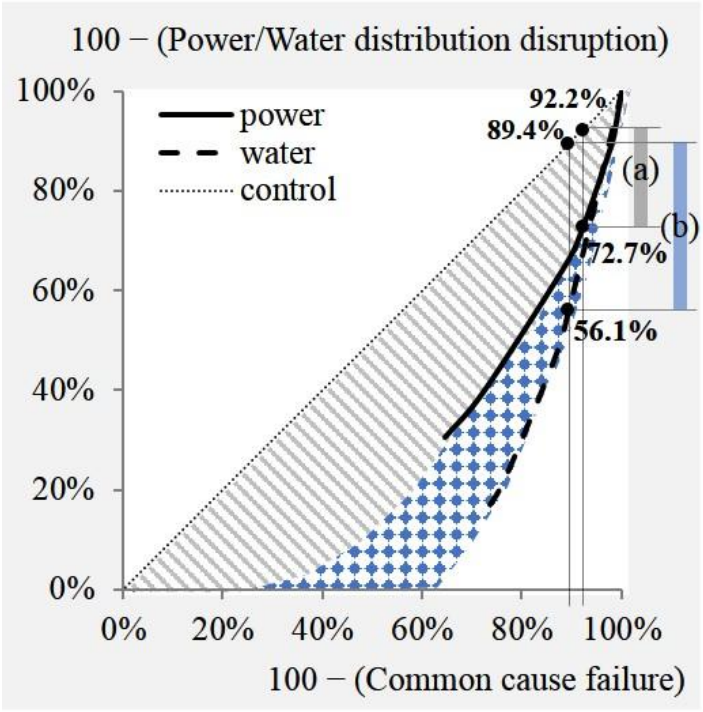

Figure 5-9. The extent of cascading failure

Impact of Demand Changes

Since the earthquake occurrence aspects are totally random, this research used an earthquake with maximum PGA (e.g., "ground shaking" in SD model) is 0.22g and recurrence period is 2400 year described on Korea Building Code (KBC 2016). Additional information for conducting case simulation is summarized as follows: (a) time step: 1 day, (b) original generation (transmission, distribution) capacity: 10,944 MW/day, (c) reliability of power plant: 1, (d) reliability of transmission substation: 0.75, (e) reliability of distribution substation: 0.86, (f) reliability of other system (water treatment plant in this case): 0.96.

(1) What kinds of failures occur during an earthquake? And how they propagate to a whole electric power system?

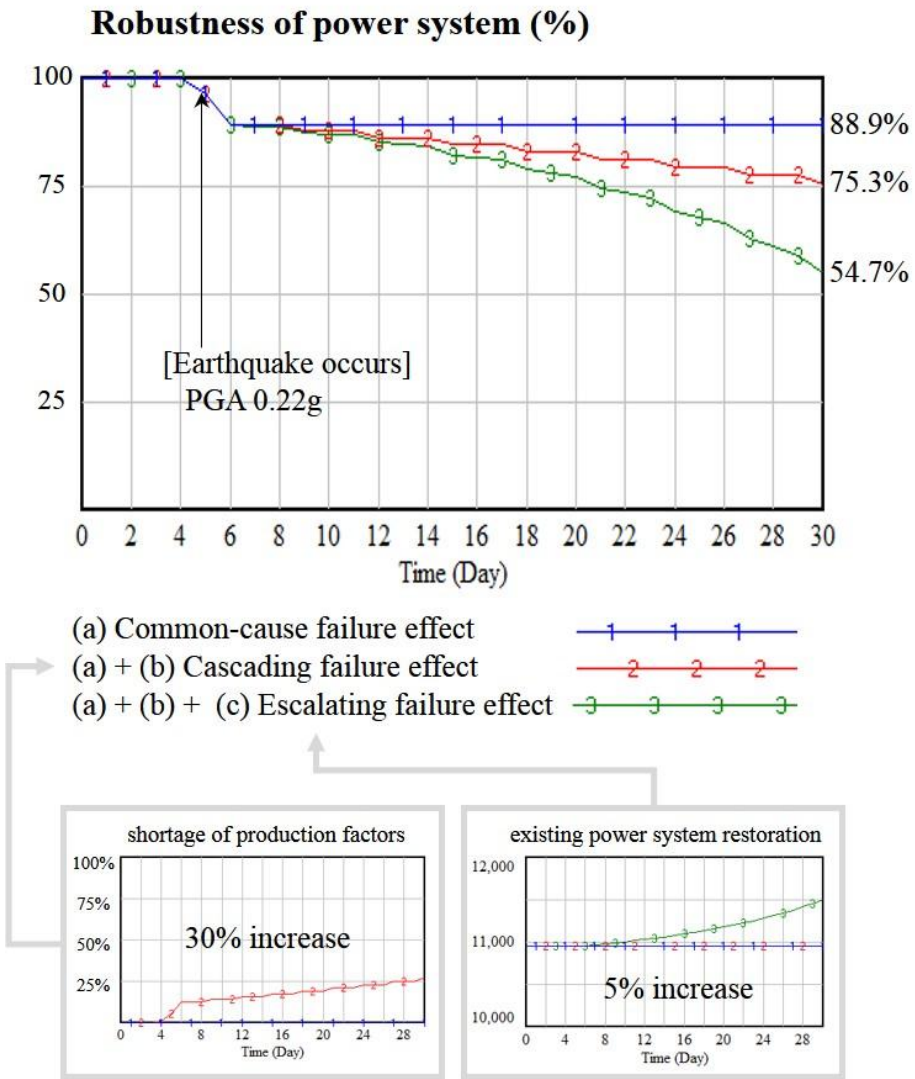

Figure 5-10. Comparison of three types of failures effects on robustness

Throughout the proposed causal loop diagrams, the authors examine the progress of failure in power system. Then, in this section, simulations are conducted under three different constraints: (a) electricity generation rate in power plant is evaluated by just reliability of power plant. In turn, there are common-cause failures only (no loop); (b) the rate is evaluated by reliability and shortage rate of production factors. In our case region, shortage of production comes from other lifeline system's degradation means water treatment plants malfunctions (R1 only); (c) the last one includes the precedence conditions and also reflects an increase of daily electricity usage (R1 and R2). Fig. 5-10 shows the comparison of such three types of failures effects on system robustness. Due to the structural destruction while earthquake, power system illustrated in Fig. 5-10 loses its function about 25%. Moreover, it is expected that 32% of the extra loss from cascading failures can arise, and if restoration works do not perform, electricity eventually has run dry.

(2) If each sub-sector reliability improves, can supply of the system meet demand? If not, how can a decision maker manage the imbalance between supply and demand?

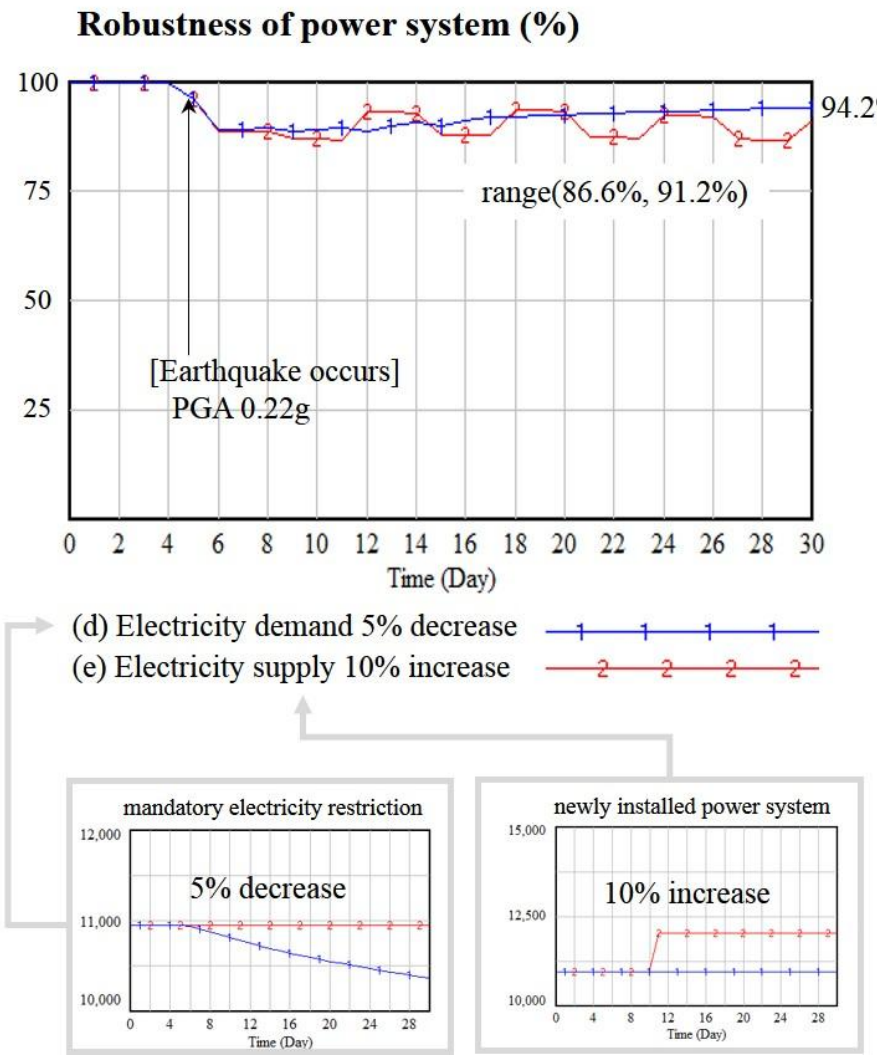

Figure 5-11. Comparison of two mitigation strategies

In order to mitigate adverse impacts from power blackout and enhance the robustness, following two strategies are discussed: (d) one is an increase of designed generation capacity; and (e) another is a decrease of daily electricity usage. More specifically, in the first case, when the level of transformed 22.9kV 30% decreases, power generation capacity increases up to 10% and it brings a result that the robustness maintains a range of 0.7 to 0.8. On the other hand, 3% of electricity usage decrease by energy saving strategies, balancing loops in the proposed model, can lead to recover the robustness gradually.

This research also conducts the sensitivity analysis with two main uncertain supply and demand-side variables, shortage of production factors and mandatory energy savings, to how their change affects the system robustness. In this analysis, each variable follows random uniform function (min= 0, max= 0.3). The simulation result in Fig. 5-12 displays that an effort for solving imbalance problems from supplier-side guarantees immediate effect in the expected range. However, it is hard to expect steady recovery without additional supply resources input. While it is confirmed that the customer-side efforts to conserve electricity usage can be significantly regarded as reinforcement of system robustness despite it tend to tend to be short-term strategies.

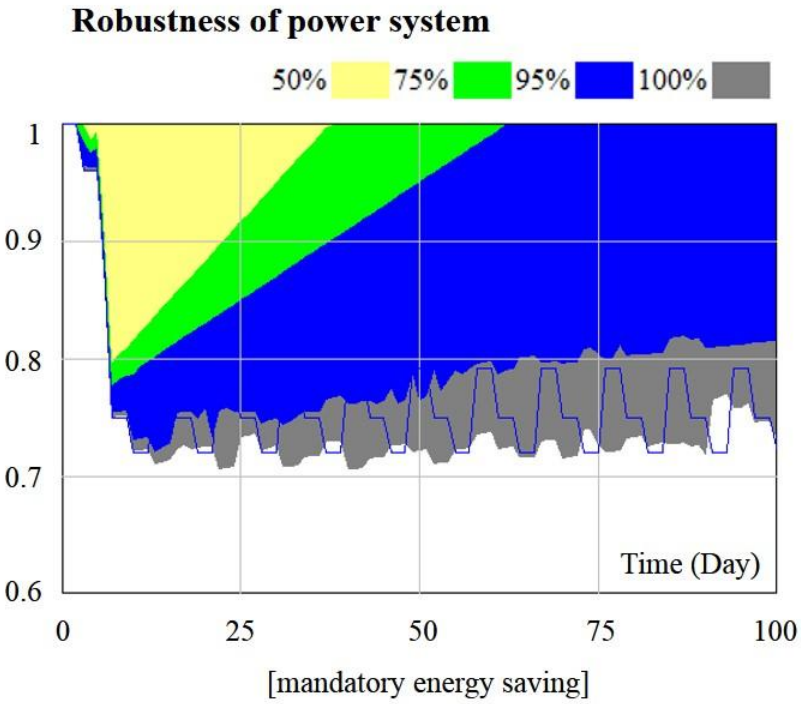
Robustness of power system
50%
75%
95%
100%
1
0.9
0.8
0.7
0.6
Time (Day)
0
25
50
75
100
[mandatory energy saving]

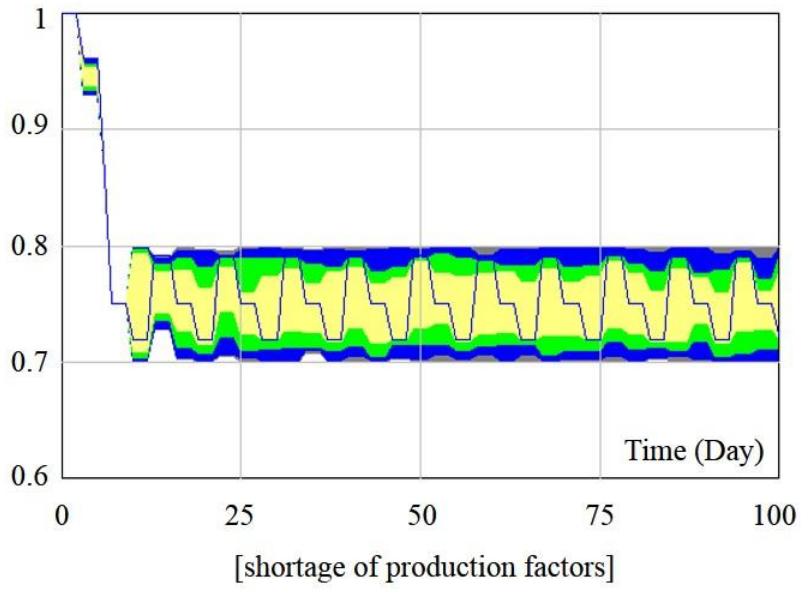
1
0.9
0.8
0.7
0.6
Time (Day)
0
25
50
75
100
[shortage of production factors]

Figure 5-12. Sensitivity analysis with customer and supplier-side

5.3 Summary

In this chapter, this research examined the degraded performance of two real-world lifeline system subjected the 2011 Tohoku earthquake and the 2016 Gyeongju earthquake respectively. Major facilities (i.e., 3 power plants and 11 substations) were considered in Tohoku case. On the other hand, since there are no power plants in Daegu, transmission substations are located near the city boundary are counted as gate stations are provided electricity from outside regions. In addition, this research assumed that only 4 water treatment plants within Daegu city depend on the electricity from the power system.

With the information of network topologies and earthquake scenario of the 2011 Tohoku case, this research firstly compared estimated simulation results and actual observed data focused on the number of power outage households to examine how well proposed IIM fits such reported data. As a result, general behavior patterns of a power outage ratio was similar to actual data patterns and this research argued that it is more appropriate representation of the real world compared the analysis that just dealt with common-cause failure. Another feature that of the model presented here was its ability to observe the demand effect on network robustness. In particular, this research considered the concept of "Setsuden" which is mandatory energy

saving movement to overcome power shortage. Through the results of this analysis, this research found that although the maximum value of damage propagation remains constant, initial points of occurrence move to the right side (i.e., reinforcement of system robustness) as the Setsuden rate increase.

In the case of the 2016 Gyeongju earthquake, there was not much seismic-damage in terms of common-cause failure. For this reason, this research considered an virtual earthquake that occurred at the right side of the case region (128.882E, 35.78N) with magnitude 6.0 (minor), 6.4 (major) and 6.8 (critical). For example, there was around 10.6% expected physical destruction in water supply system, however, the final water supply distribution disruptions incorporating cascading failures was around 43.9%. Finally, this research conducted several experiments using proposed SD model with respect to demand changes. To be specific, there were three different constraints: common-cause failures only, cascading failures occurs, and escalating failure occurs. Through the causal loop diagrams and simulation results, the progress of failure was examined with quantitative descriptions.

Table 5-9. Summary of two case studies

Attributes	Power network in Tohoku	Power and water network in Daegu
Region	• Japan – high seismicity regions	• South Korea – low and moderate seismicity region
Earthquake Information	• 14:46 on March 11, 2011 • Magnitude 9.0 • Epicenter (143.37, 38.82) • Focal depth 24km	• 20:32 on September 12, 2016 • Magnitude 5.4 • Epicenter (129.22, 35.78) • Focal depth 13km
Network Information	• 3 power plants • 11 transmission substations	• 4 transmission substations • 29 distribution substations
		• 4 water treatment plants • 15 pumping stations • 5 storage tanks
Number of customers	• 2.3 million households	• 994,000 households
Static Performance after an earthquake	• 53.9%	• 92.2%
		• 89.4%
Dynamic Performance after an earthquake	• 30.6%	• 72.7%
		• 56.1%

Chapter 6. Applications for Improved Resilience

For improved resilience against an earthquake, it is required that information to assist decision-making about which lifeline components should be the object of reinforcement. In this chapter, several applications are proposed based on the case simulation results. The first one is identifying a critical component for sustainable operation after an earthquake. In detail, this research determines the component importance in two assumptions: (a) only a node will be completely damage (performance 0%) while that of all others in normal, (b) only a node will be restored (performance 100%) while that of all others in damage. In addition, because restoration resources are generally not sufficient in reality, the second application is comparing restoration plan with different restoration standards: (a) no priority, (b) priority according to the common-cause failure, and (c) priority according to the component importance that defined in the first experiments.

6.1 Identifying a Critical Component

Regarding the term, criticality, previous research works (Nicholson et al. 2016; Whitson and Ramirez-Marquez 2009) have proposed different definitions. In this research, a component criticality is defined as a measure of how much the whole system performance will degrade by a component's failure.

Table 6-1. Correlation matrix of Tohoku electric network

$\{a_{ij}\}$	**1**	**2**	**3**	**4**	**5**	**6**	**7**	**8**	**9**	**10**	**11**	**12**	**13**	**14**
1	0	0	0	0	0	0	0	0	0	0	0	0	0	0
2	0	0	0	0	0	0	0	0	0	0	0	0	0	0
3	0	0	0	0	0	0	0	0	0	0	0	0	0	0
4	0	0	0	0	0	0	1	0	0	0	0	0	0	0
5	0	0	0	0	0	1	0	0	0	0	0	0	0	0
6	0	0	0	0	0	0	0.44	0	0.32	0	0.24	0	0	0
7	0.72	0	0	0	0	0.28	0	0	0	0	0	0	0	0
8	0.78	0	0	0	0	0	0.11	0	0	0.11	0	0	0	0
9	0	0.92	0	0	0	0	0	0	0	0	0.08	0	0	0
10	0.38	0	0	0	0	0	0	0	0	0	0.62	0	0	0
11	0	0	0.92	0	0	0	0	0	0.08	0	0	0	0	0
12	0	0	0	0	0	0	0	0	0	1	0	0	0	0
13	0	0	0	0	0	0	0	0	0	0	1	0	0	0
14	0	0	0	0	0	0	0	0	0	1	0	0	0	0

For example, in Tohoku electric network case (same as in Chapter 5.1), component-by-component coefficients of all nodes can be quantified based Eq. 7 and Eq. 10. Table 6-1 shows the results of calculations, and if $a_{ij} > 0$, it

can say that at least node *j* is critical to node *i*. In addition, if a node has a strong possibility of spreading its initial damage to the other nodes, it means that the node is an important component for the whole network resiliency. Thus a component criticality for node *j* can be measured by the value of damage propagation when assuming that only the node *j* is completely damaged (static functionality of node *j* equals 0%, while that of all others equal 100%) among its network.

Table 6-2. Damage propagation of a first node

Node Index	Dynamic Functionality (%)	Generation or Sales	
		In normal (households)	After earthquake (households)
1	0	645	0
2	100	605	820
3	100	1,085	840
4	26.2	270	63
5	84.9	150	124
6	84.9	245	203
7	26.2	165	38
8	16.2	210	24
9	99.7	210	209
10	82.6	225	181
11	99.7	115	115
12	82.6	230	185
13	99.7	265	264
14	82.6	250	202
Total		4,670	3,268

Table 6-2 describes the example of damage propagation when the first

power generator node stops producing electricity entirely. In this case, other nodes with no physical damage issues (such as node 4 to 14) may drop their supply of electricity than in the normal because they derive it from the first power generator. Consequently, the average generation and sale of electricity are about 30% lower than in the normal. In this way, this research ranks component criticality of all the 14 nodes, and these are listed in Table 6-3.

Table 6-3. Damage propagation and component criticality

Node Index	Static Functionality (%)	Dynamic Functionality (%)	Damage Propagation (%)	Criticality Rank
1	86.2	70.6	15.6	3
2	87.0	76.5	10.6	5
3	76.8	52.9	23.9	1
4	94.2	94.2	0	9
5	96.8	96.8	0	9
6	94.8	88.4	6.3	8
7	96.5	88.1	8.3	6
8	95.5	95.5	0	9
9	95.5	88.3	7.2	7
10	95.2	84.2	11.0	4
11	97.5	73.9	23.7	2
12	95.1	95.1	0	9
13	94.3	94.3	0	9
14	94.6	94.6	0	9
Average	92.9	85.2	7.7	

From the network performance-impact perspective, the most important component is third generator node that covers the most number of households.

Deliverer nodes that have several sub-deliverer nodes (indexed 11) and first generator node are also identified as a critical component to supply the electric power. On the other hand, nodes in the end of the electric path (indexed 4, 5, 12, 13, and 14) cannot spread damage to the network.

On the other hand, component importance can be determined by assuming that only the damaged node *j* will be restored (static functionality of node *j* equals 100%, while that of all others lower than 100%). In detail, several days after an earthquake, for example, some information (e.g., earthquake intensity and destruction of components) are observed and can be used as the evidence to update target estimation (i.e., power and water distribution disruption).

In this context, this research tested the Daegu case, for figure out how a recovery of damaged component impacts on whole system performance. Table 6-4 listed the posterior probability of PDD and WDD given some evidence. Scenario 0 is an original case as described in Bayesian network model (Fig.5-8), while others assumed the restoration of damaged-components. Through the scenario 1 to 5, it should be noted that even though a transmission substation is not included in the potable water system, the change on its damage state has a significant impact on the performance of water distribution. Therefore, when needed to determine restoration priorities,

damaged-transmission substation has the highest priority (scenario 1) and damaged-pumping station is the next (scenario 9) in the case of presented Daegu case networks.

Table 6-4. The posterior probability given evidence

Scenario	Evidence	PDD (%)	WDD (%)
0	-	27.3	43.9
1	P (D_{TS}=None)	7.77	28.8
2	P (D_{DS}=None)	21.6	39.5
3	P (D_{WTP}=None)	27.3	41.3
4	P (D_{ST}=None)	27.3	39.5
5	P (D_{PS}=None)	27.3	36.4
6	P (D_{TS}= None, D_{DS}=None)	0	21.6
7	P (D_{TS}= None, D_{WTP}=None)	7.77	25.5
8	P (D_{TS}= None, D_{ST}=None)	7.77	23.2
9	P (D_{TS}= None, D_{PS}=None)	7.77	19.3

Such test results can extend to component-level for identifying a component that contributes to the robustness of the system. To be specific, if the state of certain component changes, its impact can be measured in terms of a probability change in PDD and WDD. For example, P (PDD = True) increase up to 0.53 when the damage state of the first component turns “None” to “Complete”. From the graphs in Fig. 6-1, it is confirmed that the important components to be handled during an earthquake are P1, P12, and P3 for power system and W3, P2, and P22 for potable water system.

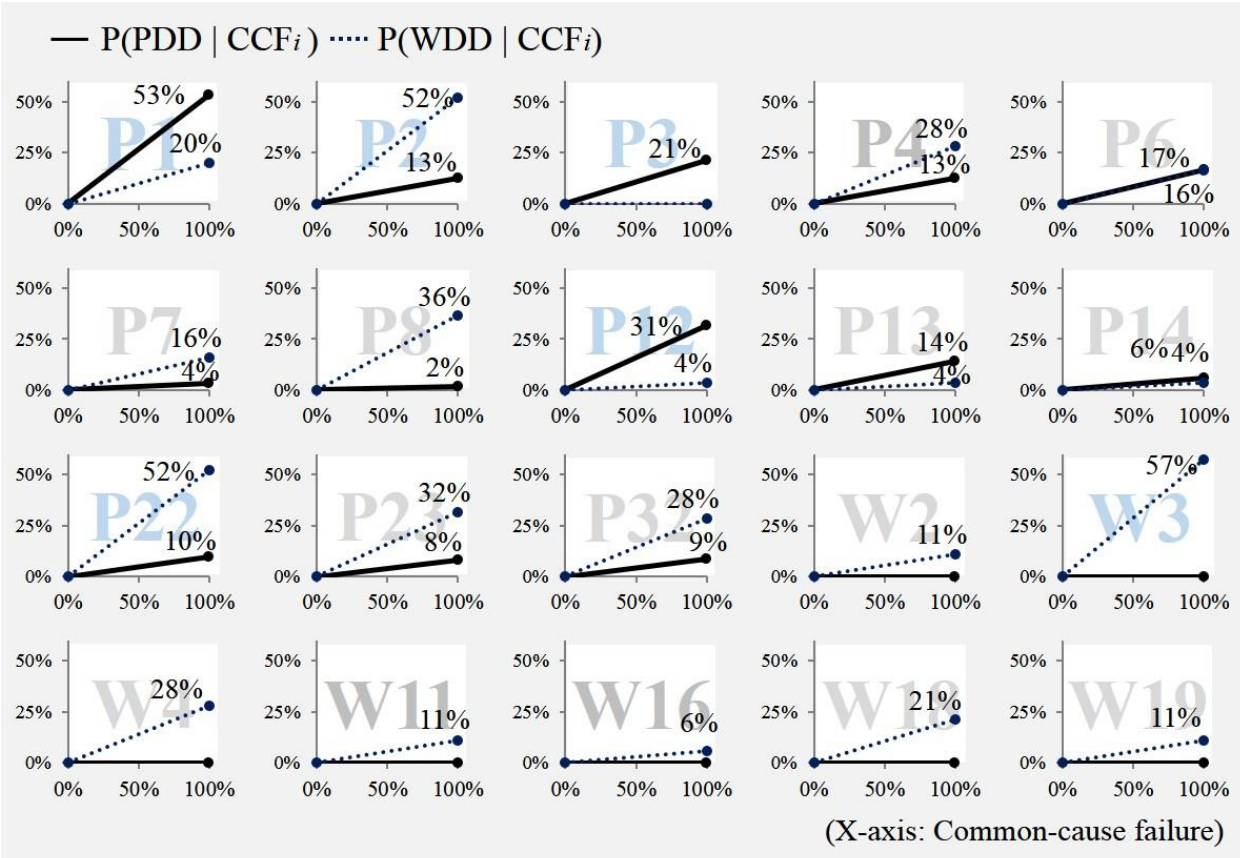

Figure 6-1. Identifying a critical component for power and water

6.2 Suggestions of Restoration Management

As mentioned above, it is important that seismic-damaged lifelines return to normal condition as soon as possible. Thus, this research discusses restoration functions that were also introduced by FEMA (2003). As presented in Table 6-5, there are two types of restoration functions: (a) linear functions with means and standard deviations of restoration days; and (b) approximate discrete functions expressed in terms of functionality. In our case, discrete functions are used because measuring a day-to-day functionality change is the main concern.

Table 6-5. Restoration functions for lifeline components

Type	Damage state	Restoration Days		Functionality (%)				
		mean	β*	after 1day	after 3days	after 7days	after 30days	after 90days
EPP3	ds2	0.5	0.1	100	100	100	100	100
	ds3	3.6	3.6	24	44	83	100	100
	ds4	22	21	16	19	24	65	100
	ds5	65	30	2	2	3	13	80
ESS1 / ESS3	ds2	1	0.5	50	100	100	100	100
	ds3	3	1.5	9	50	100	100	100
	ds4	7	3.5	4	13	50	100	100
	ds5	30	15	3	4	7	50	100

* β is the lognormal standard deviation

For example, if there are sufficient crews and resources to conduct restoration in the area, a medium voltage electric substation in "moderate" damage state will recover their function up to 44% of the declined functionality on the third day after the starting restoration, and total restoration time will be between 7 days and 30 days. As such, components' common-cause failure is continuously updated with the restoration process.

Furthermore, this research compares some restoration priorities to confirm the importance of restoration management to mitigate the damage propagation. For example, in the Tohoku case, when the restoration begins on the next day of an earthquake (March-12, 2011) and ends when the system performance recovers up to 90%. The simulation results with three different priority standards: (a) first plan is that all components are uniformly assigned restoration resource a day ("plan 1" in Fig. 6-2), (b) second plan is that resource distributed according to common-cause failure ("static functionality" in Table 5-3 and "plan 2" in Fig. 6-2), and (c) third plan is that resource distributed according to the component importance ("criticality rank" in Table 6-3 and "plan 3" in Fig. 6-2). For example, when the simulation model runs with the second restoration plan, the component with the lowest static functionality (e.g., 14 node in this case) is firstly and intensively assigned resources. Despite the fact that each plan has different resource priorities, it is noted that the total amount of resource usage during a simulation are set equal.

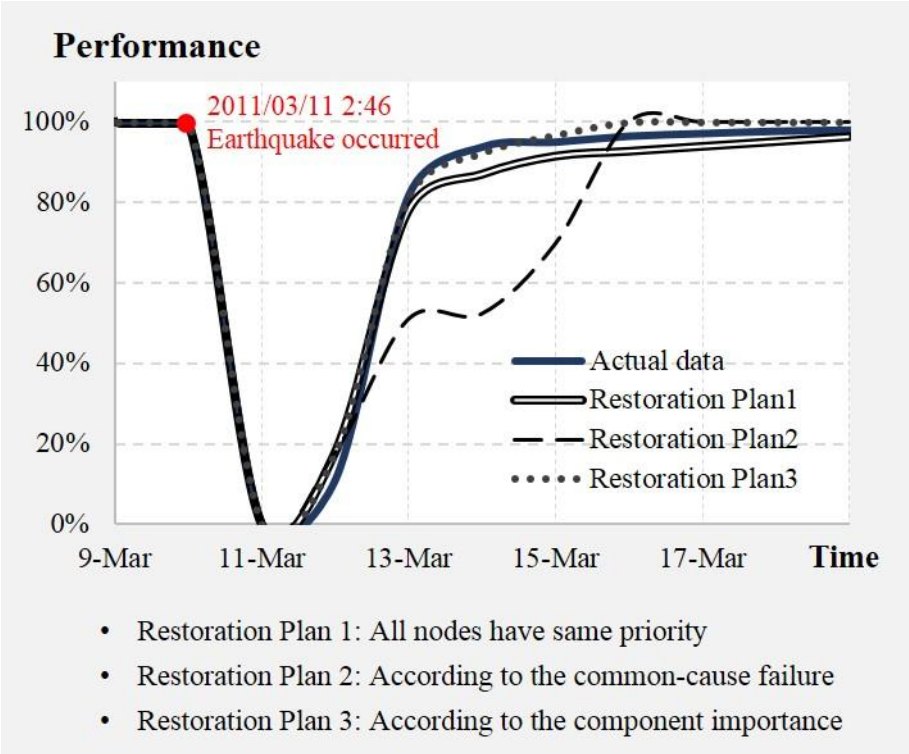

Figure 6-2. Comparison of restoration plan

Simulation results, as described in Fig. 6-2, show that the first and third plan are aligned with the actual data from Tohoku-EPCO, while the second plan is not. This is because the functional recovery of components with high resource priority in the second plan (i.e., node 14, 12, and 13) do little to improve system performance. Thus, such results show that the inefficient utilization of resources can lead to a delay in community resilience. In contrast, the third plan (resource priority is given to node 3,11, 1 and others in order) is effective in reducing the number of households in a blackout after an

earthquake; and this result demonstrates the importance of identifying critical component with a consideration of damage propagation to mitigate cascade outage effect.

In summary, two types of functionality assessment (static and dynamic) presented in this research ensure an appropriate restoration plan that helps to minimize the total restoration time.

6.3 Summary

In this chapter, this research proposed two applications for maintaining the resilience of seismic-damaged lifeline systems based on Tohoku and Daegu network case. In particular, the proposed model can be used for identifying a critical component to maintain sustainable operation. In general, with consideration of a sing lifeline, a generator that covers the most demand (e.g., node 3 in Tohoku case) and a deliverer that have several sub-deliverer (e.g., node 11 in Tohoku case) were essential to maintain the system robustness.

Furthermore, the results of this research can be extended by determining restoration priority with considerations the external interdependency. Through the experiments, it was confirmed that even though a certain component is not included in the managing target lifeline system (e.g., transmission substation and potable water supply system in Daegu case), it can be assigned the highest priority because of its significant impact on the reduction inflow of operational materials. In both cases, components at the end of the supply chain cannot elapse cascading failure to the system as expected.

Chapter 7. Conclusions

The objective of this research is to develop a comprehensive framework for the functionality assessment of the seismic-damaged lifeline systems to solve the problems: (a) destruction due to ground shaking, (b) reduction of inflow due to internal/external dependency, and (c) demand fluctuation due to environment changes. In this chapter, essential findings derived from the results of this research is described. Then, the expected contribution both in academic and in practical is discussed. Finally, the last section concludes with the limitation that will be handled in future works.

7.1 Research Results

The question addressed in this paper is how the damage of individual component would propagate and how to quantify its effect on the whole system performance. To achieve the solution, a common-cause failure, a cascading failure, and an escalating failure were firstly defined. Then, this research argued that although the reliability and the robustness seem to be similar, they are quite differently accepted since the former is a static variable; while the latter is dynamic variable. Based on such theoretical backgrounds, the functionality assessment framework for the seismic-damaged lifeline

system was proposed including – (a) a computational approach to estimate the functionality of a single component that spatially distributed and structurally specified using ground motion prediction equations and fragility functions, (b) an inoperability input-output model with a component-by-component coefficient matrix that based upon spatial path analysis to analyze the effect of internal dependency within a single lifeline system, (c) a Bayesian network model in terms of lifeline service distribution disruptions to analyze the effect of external-dependency between two lifeline systems, and (d) a system dynamics model to determine the possible factors driving uncertainty and assess the impact of demand change on the system robustness.

In addition, to demonstrate test the damage propagation effect, case simulations using the data from the 2011 Tohoku earthquake were conducted. From the simulation results, the following conclusions can be drawn:

(1) The impact of seismic damage in a network is generally underestimated when predicted without considering damage propagation due to topological and functional interdependencies between components. These findings are useful information that the person who has a concern in the electricity sector have to expect the additional functional loss.

(2) As the electricity usage decreased, the initiation of damage propagation occurred at high magnitude earthquake. It means that the demand-side efforts can be regarded as reinforcement of network robustness.

(3) When the restoration conducted in accordance with the criticality rank presented this research, it minimized the time required to ensure community resilience. It provides useful information for risk assessment and management.

On the other hand, for the functionality assessment of the 2011 Gyeongju earthquake, earthquake that occurred with magnitude 6.0 (minor), 6.4 (major) and 6.8 (critical) was considered. By setting up different state combinations of parent nodes, the posterior probability of power and potable water distribution disruption are estimated, and the major findings are:

(1) The operational state of a component is even dependent through the availability of input inflow from adjacent components rather than its physical damage.

(2) In particular, with respect to the reliability of the water system, destruction of transmission substations and the reduction of water inflow to pumping stations are key variables.

(3) Sometimes, solving the problem in different system (e.g., destruction of transmission substation in the case system) can be quite effective on improving a system reliability (e.g., potable water distribution disruption in the case system).

7.2 Research Contributions

The main academic contribution is that this research introduces two-types of functionality (e.g., static and dynamic) and allows to quantify the influence of three types of uncertainty (e.g., physical destruction, reduction inflow, and demand change) on the system performance in a probabilistic manner. Although the methodology specifically applied to the Tohoku and Gyeongju earthquake, this research assured that other disaster case can be implemented while still using the same analytical approach.

Since the actions taken immediately following an earthquake can play a significant role on the extent of cascading failures, this research can contribute to solve practical-issues for those with a concern in the community resilience maintaining. In particular, time-varying features of the functionality assessment model can be helpful for risk management organization that operates lifeline system to prioritize which components were restored first for maintaining system resilience and reducing the number of blackout households under seismic hazards.

7.3 Furutre Research

There are still a lot of uncertainty for the functionality assessment regarding on the other types of lifeline components such as transmission lines and water pipe. Generally, such lines outage can spread the following steps: (1) there is no power flow through a damaged line; (2) power grid breaking into a number of disconnected islands; and (3) some islands are heavily overloaded and more line outages trigger. In other words, cascade failure in the line is the matter of electricity load imbalance, and thus most modeling approaches have focused on line programming and grid analysis. This is one of the reasons that transmission and distribution line outages fall outside the scope of our study. And fortunately, according to disaster reports published after Chile earthquake and Tohoku earthquake, adverse impacts on the whole power system due to line outage were quite low, as shown in the table below.

Table 7-1. System failure rate caused by link outage

Historical event	Total line	Damaged line	Rate	Reference
The 2010 Chile earthquake	7,280km	1.6km	0.02%	Araneda, J. C. et al. (2010)
2011 Tohoku earthquake	14,809km	22km	0.15%	Tohoku Electric Power Company. (2011)

Another uncertainty factors such as ramp-down time due to resource delivery delay. For example, electricity output is zero when the generator in emergency shutdown or safety inspection phase. Likewise, three of power plants discussed in this research automatically stopped operation after the earthquake (PGA value of all of them is more than 0.1g but less than 0.2g). However, according to the damage report from Tohoku-EPCO, they restarted operations within a day after the event. In addition, power plants are required to carry out regular inspections and it can be conducted when part of the plant is shutdown. In this case, other power sources are ready to increase their generations and electrical paths are restructured before shutdown. Thus, scheduled maintenance is not disruptions, but the correlation matrix (conditional probability) that expresses the relationships between nodes in normal condition may be changed. On the other hand, if unscheduled maintenance means no preparations for supply reduction, it is no longer in normal, but in disasters; and system functionality at that time can be determined through this research.

Therefore, future research might be focused on coping the challenge regarding validation derived from the lack of adequately observation data in earthquake-induced damage assessment.

References

Adachi, T. and Ellingwood, B. R. (2008). "Serviceability of earthquake-damaged water systems: Effects of electrical power availability and power backup systems on system vulnerability." Reliability Engineering and System Safety, 93(1), 78 – 88.

Adachi, T. and Ellingwood, B. R. (2010). "Comparative assessment of civil infrastructure network performance under probabilistic and scenario earthquakes." Journal of Infrastructure Systems, 16(1), 1 – 10.

Albadi, M. and El-Saadany, E. (2008). "A summary of demand response in electricity markets." Electric power systems research, 78(11), 1989 – 1996.

Allan, R. and Billinton, R. (2000). "Probabilistic assessment of power systems." In Proceedings of the IEEE, 88(2), 140 – 162.

Ansal, A., Kurtulus, A. and Tönük, G. (2008). "Earthquake loss estimation tool for urban areas." Geotechnical Earthquake Engineering and Soil Dynamics Congress, May, Sacramento, California.

Araneda, J. C., Rudnick, H., Mocarquer, S. and Miquel, P. (2010). "Lessons

from the 2010 Chilean earthquake and its impact on electricity supply." IEEE International Conference on Power System Technology, October, Hangzhou, Zhejiang, China.

Asefa, T., Clayton, J., Adams, A., and Anderson, D. (2014). "Performance evaluation of a water resources system under varying climatic conditions: Reliability, Resilience, Vulnerability and beyond." Journal of Hydrology, 508, 53 – 65.

Barker, K. and Haimes, Y. Y. (2009). "Uncertainty analysis of interdependencies in dynamic infrastructure recovery: Applications in risk-based decision making." Journal of Infrastructure Systems, 15(4), 394 – 405.

Barton, D., Eidson, E., Schoenwald, D., Stamber, K. and Reinert, R. (2000). "Aspen-EE: an agent-based model of infrastructure interdependency." Sandia National Laboratories Report, SAND2000-2925.

Bensi, M. T., Der Kiureghian, A. and Straub, D. (2009). "A Bayesian network framework for post-earthquake infrastructure system performance assessment." TCLEE 2009: Lifeline Earthquake Engineering in a Multihazard Environment, 1 – 12.

Bobbio, A., Portinale, L., Minichino, M. and Ciancamerla, E. (2001).

"Improving the analysis of dependable systems by mapping FTs into bayesian networks." Reliability Engineering and System Safety, 71, 249–260.

Boore, D. M. and Atkinson, G. M. (2008). "Ground-motion prediction equations for the average horizontal component of PGA, PGV, and 5%-damped PSA at spectral periods between 0.01 s and 10.0 s." Earthquake Spectra, 24(1), 99 – 138.

Bourouni, K. (2013). "Availability assessment of a reverse osmosis plant: Comparison between reliability block diagram and fault tree analysis methods." Desalination, 313, 66 – 76.

Bruneau, M., Chang, S. E., Eguchi, R. T., Lee, G. C., O'Rourke, T. D., Reinhorn, A. M. and Von Winterfeldt, D. (2003). "A framework to quantitatively assess and enhance the seismic resilience of communities." Earthquake spectra, 19(4), 733 – 752.

Bulleit, W. M. and Drewek, M. W. (2012). "Agent-based modeling and simulation for hazard management." Construction Research Congress, May, West Lafayette, Indiana

Bush, B. et al. (2005). "Critical infrastructure protection decision support system (CIP/DSS) project overview." In Proceedings of the 23rd international

system dynamics conference, Boston, MA.

Campbell, K. W. (2003). “Prediction of strong ground motion using the hybrid empirical method and its use in the development of ground-motion (attenuation) relations in eastern North America.” Bulletin of the Seismological Society of America, 93(3), 1012 – 1033.

Castillo A. (2014) “Risk analysis and management in power outage and restoration: a literature survey.” Electric Power Systems Research, 107, 9 – 15.

Cats, O., Koppenol, G. J., and Warnier, M. (2017). “Robustness assessment of link capacity reduction for complex networks: Application for public transport systems.” Reliability Engineering and System Safety, 167, 544 – 553.

Chang, L., and Wu, Z. (2011) “Performance and reliability of electrical power grids under cascading failures.” International Journal of Electrical Power and Energy Systems, 33(8), 1410 – 1419.

Chang, S. E. et al. (2009). “Societal impacts of infrastructure failure interdependencies: building an empirical knowledge base.” Technical Council on Lifeline Earthquake Engineering, June, Oakland, California.

Cheng, J., Greiner, R., Kelly, J., Bell, D. and Liu, W. (2002). “Learning

Bayesian networks from data: an information-theory based approach. Artificial intelligence." 137(1-2), 43 – 90.

Chida, T. et al. (2015). "Analysis of Hourly Demand Data before and after the 2011 Tohoku Earthquake." Electrical Engineering in Japan, 192(3), 46 – 53.

Cimellaro, G. P., Solari, D., and Bruneau, M. (2014). "Physical infrastructure interdependency and regional resilience index after the 2011 Tohoku Earthquake in Japan." Earthquake engineering and structural Dynamics, 43(12), 1763 – 1784.

De la Llera, J. C. et al. (2017). "Data collection after the 2010 Maule earthquake in Chile." Bulletin of Earthquake Engineering, 15(2), 555 – 588.

Di Giorgio, A. and Liberati, F. (2012). "A Bayesian network-based approach to the critical infrastructure interdependencies analysis." IEEE Systems Journal, 6(3), 510 – 519.

Dialynas, E. N. et al. (1988). "An expert system methodology for determining the characteristics of power system component failures." Electric Power System Research, 14(1), 71 – 82.

Dijkstra, E. W. (1959). "A note on two problems in connexion with graphs."

Numerische Mathematik, 1(1), 269 – 271.

Dobson, I. et al. (2008). "Initial review of methods for cascading failure analysis in electric power transmission systems." IEEE PES CAMS Task Force on Understanding, Prediction, Mitigation and Restoration of Cascading Failures, 1 – 8.

Dobson, I. (2012). "Estimating the propagation and extent of cascading line outages from utility data with a branching process." IEEE Transactions on Power Systems 27(4), 2146 – 2155.

Dueñas-Osorio, L., Craig, J. and Goodno, B. (2007). "Seismic response of critical interdependent networks." Earthquake Engineering and Structural Dynamics, 36(2), 285 – 306.

Dueñas-Osorio, L. and Kwasinski, A. (2012). "Quantification of lifeline system interdependencies after the 27 February 2010 Mw 8.8 offshore Maule, Chile, earthquake." Earthquake Spectra, 28(S1), S581 – S603.

Dunn, S. and Wilkinson, S. (2012). "Identifying critical components in infrastructure networks using network topology." Journal of Infrastructure Systems, 19(2), 157 – 165.

Egawa, E., Kawamura, K., Ikuta, M., and Eguchi, T. (2013). “Use of construction machinery in earthquake recovery work.” Hitachi Review, 62(2), 136 – 141.

Emolo, A., Sharma, N., Festa, G., Zollo, A., Convertito, V., Park, J, Chi, H. and Lim, I. (2015). “Ground motion prediction equation for South Korea peninsula.” Bulletin of the Seismological Society of America, 105(5), 2625 – 2640.

Espinoza, S., Panteli, M., Mancarella, P., and Rudnick, H. (2016) “Multi-phase assessment and adaptation of power systems resilience to natural hazards.” Electric Power Systems Research, 136, 352 – 361.

Federal Emergency Management Agency. (2003). “HAZUS-MH 2.1 earthquake model technical manual.” <https://www.fema.gov/media-library-data/20130726-18 20-25045-6286/hzmh2_1_eq_tm.pdf> (Last updated: Jan., 2015)

Frangopol, D. and Saydam, D. (2011). “Performance indicators for structures and infrastructures.” In Proceedings of the Structures Congress, Las Vegas, Nevada.

Guo, Haitao, and Xianhui Yang. (2007). “A simple reliability block diagram

method for safety integrity verification." Reliability engineering and System Safety 92(9), 1267 – 1273.

Haggerty, M. S., Santos, J. R., and Haimes, Y. Y. (2008). "Transportation-based framework for deriving perturbations to the inoperability input-output model." Journal of Infrastructure Systems, 14(4), 293 – 304.

Haimes, Y. Y. and Jiang, P. (2001). "Leontief-based model of risk in complex interconnected infrastructures." Journal of Infrastructure Systems, 7(1), 1 – 12.

Haimes, Y. Y., Horowitz, B., Lambert, J., Santos, J., Lian, C. and Crowther, K. (2005). "Inoperability input-output model for interdependent infrastructure sectors. I: Theory and methodology." Journal of Infrastructure Systems, 11(2), 67 – 79.

Haimes, Y. Y. (2017) "Risk modeling of interdependent complex systems of systems: theory and practice." Risk Analysis (Advance online publication) doi:10.1111/risa.12804.

Hallegatte, S. (2008). "An adaptive regional input–output model and its application to the assessment of the economic cost of Katrina." Risk Analysis, 28(3), 779 – 799.

Hasan, S. and Foliente, G. (2015). "Modeling infrastructure system interdependencies and socioeconomic impacts of failure in extreme events: emerging R&D challenges." Natural Hazards, 78(3), 2143 – 2168.

Hernandez-Fajardo, I. and Dueñas-Osorio, L. (2013). "Probabilistic study of cascading failures in complex interdependent lifeline systems." Reliability Engineering and System Safety, 111, 260 – 272.

Holguín-Veras, J. and Jaller, M. (2011). "Immediate resource requirements after hurricane Katrina." Natural Hazards Review, 13(2), 117 – 131.

Hwang, S., Park, M., Lee, H., Lee, S., and Kim, H. (2013). "Dynamic feasibility analysis of the housing supply strategies in a recession: Korean housing market." Journal of Construction Engineering and Management, 139(2), 148 – 160.

Jo, N. and Bagg, C. (2003). "Estimation of spectrum decay parameter χ and stochastic prediction of strong ground motions in Southeastern Korea." Journal of the Earthquake Engineering Society of Korea, 7(6), 59 – 70.

Johansson, J. and Hassel, H. (2010). "An approach for modelling interdependent infrastructures in the context of vulnerability analysis." Reliability Engineering and System Safety, 95(12), 1335 – 1344.

Johansson, J., Hassel H., and Zio, E. (2013). “Reliability and vulnerability analyses of critical infrastructures: comparing two approaches in the context of power systems.” Reliability Engineering and System Safety, 120, 27 – 38.

Juarez Garcia, H. (2010). “Multi-hazard risk assessment: an interdependency approach.” (Doctoral dissertation, University of British Columbia).

Kanno, T., Narita, A., Morikawa, N., Fujiwara, H., and Fukushima, Y. (2006). “A new attenuation relation for strong ground motion in Japan based on recorded data.” Bulletin of the Seismological Society of America, 96(3), 879 – 897.

Kawakami, H. (1990). “Earthquake physical damage and functional functionality of lifeline network models.” Earthquake Engineering and Structural Dynamics, 19(8), 1153 – 1165.

Kazama, M. and Noda, T. (2012). “Damage statistics (Summary of the 2011 off the Pacific coast of Tohoku earthquake damage).” Soils and Foundations, 52(5), 780 – 792.

Khakzad, N., Khan, F. and Amyotte, P. (2011). “Safety analysis in process facilities: Comparison of fault tree and Bayesian network approaches.” Reliability Engineering and System Safety, 96(8), 925 – 932.

Kim, M., Choun, Y., Choi, I., and Oh, K. (2009). “Seismic fragility analysis of substation systems by using the fault tree method.” Journal of the Earthquake Engineering Society of Korea, 13(2), 47 – 58.

Korea Atomic Energy Research Institute (2008). “The evaluation of seismic fragility curves for electric power systems in Korea.” KAERI Research Report.

Korea Meteorological Administration. (2016) “2016 Earthquake catalog.” <http://www.kma.go.kr/download_01/earthquake/earthquake_2016.pdf> (Last updated: Apr., 2017)

Krimgold, F., Bigger, J., Willingham, M., and Mili, L. (2006). “Power systems, water, transportation and communications lifeline interdependencies.” American Lifelines Alliance.

Lai, T. et al. (2013). “Modeling railway damage due to shake, liquefaction, and tsunami for the 2011 Tohoku earthquake.” International Efforts in Lifeline Earthquake Engineering, 38, 267 – 274.

LeClaire, R. J. and O’Reilly, G. (2005). “Leveraging a high fidelity switched network model to inform system dynamics model of the telecommunications infrastructure.” In Proceedings of the 23rd International System Dynamics

Conference, Boston, MA.

Lee, C. (2017). “Earthquake engineering analysis of ground accelerations measured in the 912 Gyeongju earthquake.” Journal of the Koran society of civil Engineers, 65(4), 8 – 13.

Lee, S., Hwang, S., Park, M., and Lee, H. (2018). “Damage Propagation from Component Level to System Level in the Electricity Sector.” Journal of Infrastructure Systems, 24(3), 04018016.

Lisnianski, A. (2007). “Extended block diagram method for a multi-state system reliability assessment.” Reliability Engineering and System Safety, 92(12), 1601 – 1607.

MacKenzie, C. A., and Barker, K. (2012). “Empirical data and regression analysis for estimation of infrastructure resilience with application to electric power outages.” Journal of Infrastructure Systems, 19(1), 25 – 35.

Maes, M., Fritzson, K. and Glowienka, S. (2006). “Structural robustness in the light of risk and consequence analysis.” Structural Engineering International, 16(2), 101 – 107.

Malik, F. H. and Lehtonen M. (2016) “A review: Agents in smart grids.”

Electric Power Systems Research, 131, 71 – 79.

McDaniels, T., Chang, S., Peterson, K., Mikawoz, J. and Reed, D. (2007). "Empirical framework for characterizing infrastructure failure interdependencies." Journal of Infrastructure Systems, 13(3), 175 – 184.

Mosleh, A. (1991) "Common cause failures: an analysis methodology and examples." Reliability Engineering and System Safety, 34(3) 249 – 292.

Mori, H., and Wakiyama, T. (2012). "Changing behaviours-the Japanese Setsuden experience post-Fukushima." Institute for Global Environmental Strategies.

Nedic, D. P. et al. (2006) "Criticality in a cascading failure blackout model." International Journal of Electrical Power and Energy Systems, 28(9), 627 – 633.

Nejat, A. and Damnjanovic, I. (2012). "Modeling dynamics of post-disaster recovery." In Proceedings of the Construction Research Congress 2012: Construction Challenges in a Flat World, West Lafayette, Indiana.

Nicholson, C. D. et al. (2016). "Flow-based vulnerability measures for network component importance: Experimentation with preparedness planning."

Reliability Engineering and System Safety, 145, 62 – 73.

Nojima, N. and Sugito, M. (2000). "Simulation and evaluation of post-earthquake functional performance of transportation network." In Proceedings of the 12th World Conference on Earthquake Engineering (12WCEE), Auckland, New Zealand.

Norris, F. H. et al. (2008). "Community resilience as a metaphor, theory, set of capacities, and strategy for disaster readiness." American journal of community psychology, 41, 127 – 150.

Oliva, G., Panzieri, S., and Setola, R. (2010). "Agent-based input–output interdependency model." International Journal of Critical Infrastructure Protection, 3(2), 76 – 82.

Orabi, W., Senouci, A. B., El-Rayes, K., and Al-Derham, H. (2010). "Optimizing resource utilization during the recovery of civil infrastructure systems." Journal of Management in Engineering, 26(4), 237 – 246.

O'Rourke, T. D. (2007). "Critical infrastructure, interdependencies, and resilience." BRIDGE, Washington National Academy of Engineering, 37(1), 22 – 29.

Ouyang, M. and Dueñas-Osorio, L. (2011) “Efficient approach to compute generalized interdependent effects between infrastructure systems.” Journal of Computing in Civil Engineering, 25(5), 394 – 406.

Ouyang, M. (2014) “Review on modeling and simulation of interdependent critical infrastructure systems.” Reliability Engineering and System Safety, 121, 43 – 60.

Pant, R., Barker, K. and Zobel, C. (2014). “Static and dynamic metrics of economic resilience for interdependent infrastructure and industry sectors.” Reliability Engineering and System Safety, 125, 92 –102.

Park D., Lee, J., Bagg, C. and Kim, J. (2001). “Stochastic prediction of strong ground motions and attenuation equations in the Southeastern Korean peninsula.” Journal of the Geological Society of Korea, 37(1), 21 – 30.

Pearl, J. (1988). Probabilistic reasoning in intelligent systems: networks of plausible inference. San Francisco, CA: Morgan Kaufmann Publishers Inc. (ISBN: 0-934613-73-7)

Portante, E, Kavicky, J., Craig, B., Talaber, L. and Folga, S. (2017). “Modeling electric power and natural gas system interdependencies.” Journal of Infrastructure Systems, 23(4), 04017035.

Qi, J., Sun, K., and Mei, S. (2015) “An interaction model for simulation and mitigation of cascading failures.” IEEE Transactions on Power Systems, 30(2), 804 – 819.

Rinaldi, S. M., Peerenboom, J. P., and Kelly, T. K. (2001). “Identifying, understanding, and analyzing critical infrastructure interdependencies.” IEEE Control Systems, 21(6), 11 – 25.

Rinaldi, S. M. (2004). “Modeling and Simulating Critical Infrastructures and Their Interdependencies.” In Proceedings of the 37th Annual Hawaii International Conference on System Sciences (HICSS), Hawaii, USA.

Rose, A., Benavides, J., Chang, S. E., Szczesniak, P., and Lim, D. (1997). “The regional economic impact of an earthquake: direct and indirect effects of electricity lifeline disruptions.” Journal of Regional Science, 37(3), 437 – 458.

Rose A and Liao S. (2005) “Modeling regional economic resilience to disasters: a computable general equilibrium analysis of water service disruptions.” Journal of Regional Science, 45(1), 75 – 112.

Yang, S. N., Zhang, X. C., Ye, J. Y., and Wu, J. L. (2012). "Reliability Analysis of Highway Evacuation Network Post-Earthquake Disaster." In Sustainable Transportation Systems: Plan, Design, Build, Manage, and

Maintain 404 - 411. Chongqing, China.

Santos, J. R., and Haimes, Y. Y. (2003). "Demand-reduction input-output (IO) analysis for modeling interconnectedness." In Risk-Based Decision making in Water Resources X, 104 – 118.

Santos, J. R., Haimes, Y. Y., and Lian, C. (2007) "A framework for linking cybersecurity metrics to the modeling of macroeconomic interdependencies." Risk Analysis, 27(5), 1283 – 1297.

Santos, J. R., Orsi, M. J., and Bond, E. J. (2009) "Pandemic recovery analysis using the dynamic inoperability input–output model." Risk Analysis, 29(12), 1743 – 1758.

Saydam, D. and Dan M. F. (2011) "Time-dependent performance indicators of damaged bridge superstructures." Engineering Structures, 33(9), 2458 – 2471.

Shahjouei A. and Pezeshk S. (2016). "Alternative hybrid empirical ground motion model for central and eastern North America using hybrid simulations and NGA-West2 Models." Bulletin of the Seismological Society of America, 106(2), 734 – 754.

Sterman, J. (2000). Business dynamics: System thinking and modeling for a

complex world, McGraw-Hill, New York.

Tohoku Electric Power Company. (2011) “Annual corporate social responsibility report.” <http://www.tohoku-epco.co.jp/ir/report/pdf/ar2011.pdf> (Last updated: Jan., 13, 2014)

Tsuruta, M., Goto, Y., Shoji, Y. and Kataoka, S. (2008). “Damage propagation caused by interdependency among critical infrastructures.” In Proceedings of the 14th World Conference on Earthquake Engineering (14WCEE), Beijing, China.

VanDerHorn, E., and Mahadevan, S. (2018). “Bayesian model updating with summarized statistical and reliability data.” Reliability Engineering and System Safety, 172, 12 –24.

Volkanovski, A., Čepin, M. and Mavko, B. (2009). “Application of the fault tree analysis for assessment of power system reliability.” Reliability Engineering and System Safety, 94(6), 1116 – 1127.

Wang, L. and Yang, Z. (2018). “Bayesian network modelling and analysis of accident severity in waterborne transportation: A case study in China.” Reliability Engineering and System Safety, 180, 277 – 289.

Whitson, J. C. and Ramirez-Marquez, J. E. (2009). “Resiliency as a component importance measure in network reliability.” Reliability Engineering and System Safety, 94(10) 1685 – 1693.

Wu, B., Tang, A., and Wu, J. (2016). “Modeling cascading failures in interdependent infrastructures under terrorist attacks.” Reliability Engineering and System Safety, 147, 1 – 8.

Wu, J., Dueñas-Osorio, L. and Villagran, M. (2012). “Spatial Quantification of Lifeline System Interdependencies.” In Proceedings of the 15th world conference in earthquake engineering (15WCEE), Lisbon, Portugal.

Xie, L., Lundteigen, M. A., and Liu, Y. L. (2018). “Common cause failures and cascading failures in technical systems: Similarities, differences and barriers.” In Safety and Reliability–Safe Societies in a Changing World, CRC Press, 2401 – 2407.

Xu, W. et al. (2012). “An uncertainty assessment of interdependent infrastructure systems and infrastructure sectors with natural disasters analysis.” International Journal of System of Systems Engineering, 3(1), 60 – 75.

Yun, K., Park, D. and Park, S. (2009). “The statistical model of Fourier

acceleration spectra according to seismic intensities for earthquakes in Korea." Journal of the Earthquake Engineering Society of Korea, 13(6), 11 – 25.

Zio, E. and Piccinelli, R. (2010). "Randomized flow model and centrality measure for electrical power transmission network analysis." Reliability Engineering and System Safety, 95(4), 379 – 385.

Zio, E., and Golea, L. R. (2012). "Analyzing the topological, electrical and reliability characteristics of a power transmission system for identifying its critical elements." Reliability Engineering and System Safety, 101, 67 – 74.

國 文 抄 錄

지진으로 손상된 라이프라인 시스템의 성능을 연쇄피해를 고려하여 예측하는 방안

전력, 가스, 상하수도 등 사회기반시설 가운데 광범위한 지역에 분산된 네트워크적 특성을 갖고 있는 라이프라인 시스템(Lifeline System)의 피해 진단을 위해서는 구조물이 얼마나 무너졌는가의 물리적 손상이 아닌, 시스템이 본래 의도로 했던 서비스를 제공할 수 있는 능력(Functionality)이 얼마나 감소되었는가의 기능적 저하로의 접근이 필요하다. 이러한 배경에서 정해진 설계 기간 동안 임의의 규모를 갖는 지진에 의하여 구조물이 붕괴 방지 수준을 초과할 확률을 추정하는 개념인 지진취약도가 등장했다. 그러나 이때의 지진취약도는 구조물이 단독으로 기능을 수행한다 가정하고 있기 때문에 여러 개의 구조물(예: 발전소, 변전소 등)이 하나의 목적을 갖고 전체 시스템(예: 전력계통)의 부분으로써 역할을 하는 라이프라인 시스템의 경우 같은 네트워크 안에 있는 구조물들과의 상호의존성에 대한 고려가 필요하다. 뿐만 아니라 전력 계통이 가동 중지되는 경우 그로부터 전력을 공급받는 하위 구조물을 다수 보유한 시스템(예: 상수도시설)으로 피해가 전이될 수 있기 때문에 서로 다른 네트워크 간 상호의존성 또한 반영이 요구된다.

따라서 본 연구는 라이프라인 시스템 기능 유지 관점에서 피해를 다음의 세 가지 – (a) 공통원인피해: 지반 거동으로 인한 라이프라인 구성 요소의 물리적 파괴, (b) 연쇄피해: 라이프라인 구성요소 간 상호 의존으로 인한 서비스 흐름 감소, (c) 증폭피해: 외부 환경 변화로 인한 서비스 수요 변화 – 로 분류하고, 지진으로 손상된 라이프라인 시스템의 성능을 예측하는 방안을 제시하였다.

구체적으로 공통원인피해는 지진동 감쇠함수로써 추정되는 최대 지반가속도에 따라 단일 시설물이 각 손상단계에 위치할 확률로 제시되었으며, 이로 인해 야기되는 연쇄피해의 파급 정도를 정량화 하기 위하여 투입-산출 불능(Inoperability Input-Output) 모형과 베이지안(Bayesian) 네트워크가 적용되었다. 이를 통해 최종적으로 라이프 라인 시스템의 성능은 지진 발생 직후 특정 시점에서 서비스를 받고 있는 수요자의 함수로 표현되며, 시스템 다이나믹스(System Dynamics)를 활용하여 수요의 변화가 라이프라인 시스템 성능에 미치는 영향을 분석하였다.

더하여 제안한 모형을 2011년 동일본 대지진 사례와 2016년 경주 지진 사례에 적용하여 타당성을 검증하였으며, 시뮬레이션 분석을 바탕으로 지진 이후 지역사회의 회복탄력성(Resilience)을 높이기 위한 대책을 비교하였다. 본 연구 결과는 지진 이전에 라이프라인 시스템의 성능 저하를 예측 가능하게 함으로써 연쇄피해가 급격하게 전개되는 지진의 규모를 특정하거나, 현재 네트워크에서 가장 핵심이 되는 중요 구성요소를 식별하여 선제적으로 보완할 수 있도록 한다. 또한 지진 이후에 라이프라인 구성요소의 물리적 피해가 계측되면, 네트워크 분석을 통해 어떤 구성요소를 먼저 복구하는 것이 전체 시스템의 성능을 회복하는데 가장 효과적인지 비교할 수 있도록 지원한다.

주요어: 라이프라인 시스템; 성능; 지진; 공통원인피해; 연쇄피해; 탄력성; 견고성; 신속성.

학번: 2012-23127

감사의 글

지난 6년 반 간의 학위과정을 마치고 박사 논문을 마무리하며, 이 논문이 나오기까지 도움을 주신 많은 분들께 글을 전합니다.

우선 저를 늘 당신의 자랑이라 여기시고 응원해주신 부모님께 존경과 깊은 감사를 드립니다. 남들보다 조금 오래 공부하는 딸을 믿고 배려해주신 덕분에 지금의 순간을 맞이할 수 있었습니다. 그리고 박사학위 심사가 통과된 소식을 전했을 때 가장 먼저 축하 전화를 걸어온 오빠와, 우리 가족이 되어주어 고마운 새언니, 즐거움을 주는 시환이와 곧 만나게 될 둘째 조카에게 매일 행복이 가득하기를 바랍니다.

다음으로 건설기술연구실을 창립하여 저를 포함한 후배 연구자를 양성하신 김문한 교수님, 건설관리 분야 학문의 발전을 위해 애쓰시는 와중에도 연구원들의 안위를 걱정하시는 이현수 교수님, 지도교수로써 연구뿐만 아니라 다양한 경험과 시간을 함께 나눈 박문서 교수님께 감사의 인사를 드립니다. 교수님 분들의 가르침을 항상 마음에 새기고 올바른 연구자가 되도록 노력하겠습니다. 그리고 바쁘신 와중에도 논문심사에 응해주시고 유익한 조언을 주신 건설혁신연구실 지석호 교수님과 서울시립대학교 한상원 교수님 덕분에 조금 더 나은 논문이 될 수 있었습니다. 감사합니다.

연구실에 처음 입학하여 아무것도 모를 때도 있었습니다. 그때부터 지금까지 많은 도움을 준 황성주 선배님과 김현수 선배님, 소소한 즐거움을 함께한 신동숙 (전)행정실장님, 민지 언니, 진강이, 보경이에게 특별히 감사 드립니다. 또한 앞으로 연구실을 지켜나갈 선후배 동기님들의 안녕을 기원합니다. 그리고 인생의 절반 이상을 함께한 소중한 친구들(주연, 채민, 샛별, 소라, 혜정, 찬미)과 언제나 다음 여행을 계획하는 보고 싶은 친구들(수지, 영주, 예진)에게 고마운 마음을 전합니다.

마지막으로 새로운 길에 첫 발을 내디딘 저 자신에게도 축하를 전하며, 지금보다 다소 힘든 날들이 있을 수도 있겠지만 후회 없이 즐겁게 지내기를 바랍니다.

짧은 글로는 다 담을 수 없겠지만 감사한 마음이 모두에게 전해지기를 소원합니다.

2019년 1월 28일

이슬비 올림